Volume 13, Number 1, 2013 ISSN 1562-8353

NONLINEAR DYNAMICS AND SYSTEMS THEORY

An International Journal of Research and Surveys

Volume 13 Number 1 2013

CONTENTS

 ISSN 1562-8353 Printed in Ukraine
To receive contents and abstracts by e-mail, visit our Website at: **http://www.e-ndst.kiev.ua**

NONLINEAR DYNAMICS & SYSTEMS THEORY

Volume 13, No. 1, 2013

Nonlinear Dynamics and Systems Theory

An International Journal of Research and Surveys

InforMath Publishing Group
http://www.e-ndst.kiev.ua

Nonlinear Dynamics and Systems Theory

An International Journal of Research and Surveys

INSTRUCTIONS FOR CONTRIBUTORS

(1) General. Nonlinear Dynamics and Systems Theory (ND&ST) is an international journal devoted to publishing peer-refereed, high quality, original papers, brief notes and review articles focusing on nonlinear dynamics and systems theory and their practical applications in engineering, physical and life sciences. Submission of a manuscript is a representation that the submission has been approved by all of the authors and by the institution where the work was carried out. It also represents that the manuscript has not been previously published, has not been copyrighted, is not being submitted for publication elsewhere, and that the authors have agreed that the copyright in the article shall be assigned exclusively to InforMath Publishing Group by signing a transfer of copyright form. Before submission, the authors should visit the website:

http://www.e-ndst.kiev.ua

for information on the preparation of accepted manuscripts. Please download the archive Sample_NDST.zip containing example of article file (you can edit only the file Samplefilename.tex).

(2) Manuscript and Correspondence. Manuscripts should be in English and must meet common standards of usage and grammar. To submit a paper, send by e-mail a file in PDF format directly to

Professor A.A. Martynyuk, Institute of Mechanics,
Nesterov str.3, 03057, MSP 680, Kiev-57, Ukraine
e-mail: anmart@stability.kiev.ua; center@inmech.kiev.ua

or to one of the Regional Editors or to a member of the Editorial Board. Final version of the manuscript must typeset using LaTex program which is prepared in accordance with the style file of the Journal. Manuscript texts should contain the title of the article, name(s) of the author(s) and complete affiliations. Each article requires an abstract not exceeding 150 words. Formulas and citations should not be included in the abstract. AMS subject classifications and key words must be included in all accepted papers. Each article requires a running head (abbreviated form of the title) of no more than 30 characters. The sizes for regular papers, survey articles, brief notes, letters to editors and book reviews are: (i) 10-14 pages for regular papers, (ii) up to 24 pages for survey articles, and (iii) 2-3 pages for brief notes, letters to the editor and book reviews.

(3) Tables, Graphs and Illustrations. Each figure must be of a quality suitable for direct reproduction and must include a caption. Drawings should include all relevant details and should be drawn professionally in black ink on plain white drawing paper. In addition to a hard copy of the artwork, it is necessary to attach the electronic file of the artwork (preferably in PCX format).

(4) References. References should be listed alphabetically and numbered, typed and punctuated according to the following examples. Each entry must be cited in the text in form of author(s) together with the number of the referred article or in the form of the number of the referred article alone.

Journal: [1] Poincare, H. Title of the article. *Title of the Journal* **Vol. l** (No.l), Year, Pages. [Language]

Book: [2] Liapunov, A.M. *Title of the book.* Name of the Publishers, Town, Year.

Proceeding: [3] Bellman, R. Title of the article. In: *Title of the book.* (Eds.). Name of the Publishers, Town, Year, Pages. [Language]

(5) Proofs and Sample Copy. Proofs sent to authors should be returned to the Editorial Office with corrections within three days after receipt. The corresponding author will receive a sample copy of the issue of the Journal for which his/her paper is published.

(6) Editorial Policy. Every submission will undergo a stringent peer review process. An editor will be assigned to handle the review process of the paper. He/she will secure at least two reviewers' reports. The decision on acceptance, rejection or acceptance subject to revision will be made based on these reviewers' reports and the editor's own reading of the paper.

NONLINEAR DYNAMICS AND SYSTEMS THEORY
An International Journal of Research and Surveys
Published by InforMath Publishing Group since 2001

Volume 13 Number 1 2013

CONTENTS

Founded by A.A. Martynyuk in 2001.
Registered in Ukraine Number: KB 5267 / 04.07.2001.

NONLINEAR DYNAMICS AND SYSTEMS THEORY

An International Journal of Research and Surveys

Impact Factor from SCOPUS for 2011: SNIP – 0.84, RIP – 0.77

Nonlinear Dynamics and Systems Theory (ISSN 1562–8353 (Print), ISSN 1813–7385 (Online)) is an international journal published under the auspices of the S.P. Timoshenko Institute of Mechanics of National Academy of Sciences of Ukraine and Curtin University of Technology (Perth, Australia). It aims to publish high quality original scientific papers and surveys in areas of nonlinear dynamics and systems theory and their real world applications.

AIMS AND SCOPE

Nonlinear Dynamics and Systems Theory is a multidisciplinary journal. It publishes papers focusing on proofs of important theorems as well as papers presenting new ideas and new theory, conjectures, numerical algorithms and physical experiments in areas related to nonlinear dynamics and systems theory. Papers that deal with theoretical aspects of nonlinear dynamics and/or systems theory should contain significant mathematical results with an indication of their possible applications. Papers that emphasize applications should contain new mathematical models of real world phenomena and/or description of engineering problems. They should include rigorous analysis of data used and results obtained. Papers that integrate and interrelate ideas and methods of nonlinear dynamics and systems theory will be particularly welcomed. This journal and the individual contributions published therein are protected under the copyright by International InforMath Publishing Group.

PUBLICATION AND SUBSCRIPTION INFORMATION

Nonlinear Dynamics and Systems Theory will have 4 issues in 2013, printed in hard copy (ISSN 1562–8353) and available online (ISSN 1813–7385), by InforMath Publishing Group, Nesterov str., 3, Institute of Mechanics, Kiev, MSP 680, Ukraine, 03057. Subscription prices are available upon request from the Publisher (`mailto:anmart@stability.kiev.ua`), SWETS Information Services B.V. (`mailto:Operation-Academic@nl.swets.com`), EBSCO Information Services (`mailto:journals@ebsco.com`), or website of the Journal: `http://e-ndst.kiev.ua`. Subscriptions are accepted on a calendar year basis. Issues are sent by airmail to all countries of the world. Claims for missing issues should be made within six months of the date of dispatch.

ABSTRACTING AND INDEXING SERVICES

Papers published in this journal are indexed or abstracted in: Mathematical Reviews / MathSciNet, Zentralblatt MATH / Mathematics Abstracts, PASCAL database (INIST–CNRS) and SCOPUS.

Nonlinear Dynamics and Systems Theory, **13** (1) (2013) 1–12

Existence of Almost Periodic Solutions to Some Singular Differential Equations

M. Arienmughare and T. Diagana*

Department of Mathematics, Howard University,
2441 6th Street N.W., Washington, D.C. 20059, USA

Received: March 26, 2012;   Revised: January 20, 2013

Abstract: In this paper we make use of the well-known Drazin inverse to study and obtain the existence of almost periodic solutions to some singular systems of first- and second-order differential equations with complex coefficients in the case when the forcing term is almost periodic. In order to illustrate our abstract results, an example will be discussed at the end of the paper.

Keywords: *Drazin inverse; almost periodic; singular system of differential equation; singular system of second-order differential equation.*

Mathematics Subject Classification (2010): 34A30, 34C20.

1 Introduction

Let $\mathbb{C}^m$ be the m-dimensional complex space, which we equip with its natural Euclidean norm $|\cdot|$ and inner product $<\cdot,\cdot>$. Let $M(m,\mathbb{C})$ stand for the collection of all $m\times m$-square matrices with complex entries. If $A \in M(m,\mathbb{C})$ then its index which we will denote by $i(A)$ is the smallest nonnegative integer k such that

$$\operatorname{rank}(A^k) = \operatorname{rank}(A^{k+1}).$$

If $A \in M(m,\mathbb{C})$, then the Drazin inverse A^D of A is the matrix $X \in M(m,\mathbb{C})$ satisfying the following three properties:

$$AX = XA, \quad XAX = X, \quad XA^{k+1} = A^k,$$

where $k = i(A)$.

* Corresponding author: mailto:tdiagana@howard.edu

If we denote the zero matrix of $\mathbb{C}^m$ by O, and if we assume that the Jordan decomposition of $A \in M(m, \mathbb{C})$ is given by

$$A = T \begin{pmatrix} C & O \\ O & N \end{pmatrix} T^{-1},$$

where $C \in M(r, \mathbb{C})$ is (nonsingular) invertible and $N \in M(n-r, \mathbb{C})$ is nilpotent of order k ($N^k = O$ and $N^{k-1} \neq O$), then A^D is given by

$$A^D = T \begin{pmatrix} C^{-1} & O \\ O & O \end{pmatrix} T^{-1}.$$

It should be mentioned that if A is nilpotent, then $A^D = O$. Similarly, if A is (nonsingular) invertible, then $A^D = A^{-1}$. Now, the special case $i(A) = 1$ is equivalent to $N = O$. In this event, A^D is called the group inverse of A and is denoted by $A^{\#}$.

The Drazin inverse is a powerful tool when it comes to studying singular systems of differential equations, singular systems of difference equations, Markov Chains, see for instance Campbell [6]. For more on the Drazin inverse and related issues we refer the reader to the landmark books of Campbell [3, 4].

In this paper we make use of the Drazin inverse to study and obtain the existence of almost periodic solutions to the singular system of differential differential equation

$$Au'(t) + Bu(t) = f(t), \quad t \in \mathbb{R}, \tag{1}$$

where A, B are (possibly singular) $m \times m$-square matrices with complex entries and $f : \mathbb{R} \mapsto \mathbb{C}^m$ is $C^{(k)}$-almost periodic with $k = i(A)$ (Theorem 3.5).

Next, we make use of Theorem 3.5 and its consequences to study and obtain the existence of almost periodic solutions to some general singular systems of second-order differential equations (Corollary 3.2).

Our work will be heavily based upon that of Campbell [3, 4] on the existence of solutions to singular systems of differential equations. In particular, we will consider two important cases. We first consider the case when $AB = BA$ and $N(A) \cap N(B) = \{0\}$. The second case which will be a consequence of the first one requires the existence of a $\lambda \in \mathbb{C}$ such that $(\lambda A + B)^{-1}$ exists.

An important assumption that we will make consists of assuming that $A^D B$ (respectively, $A_z^D B_z$) is symmetric, has a spectral decomposition, and that $\sigma(A^D B) - \{0\} \neq \emptyset$ with $\Re e\, \lambda > 0$ for all $\lambda \in \sigma(A^D B) - \{0\}$. This assumption excludes in particular the case when $A^D B$ (respectively, $A_z^D B_z$) is nilpotent.

The existence of almost periodic solutions to differential equations is one of the most attractive topics in qualitative theory of differential equations due to applications [1, 8, 10, 11]. However, to the best of the authors knowledge, the existence of almost periodic solutions to singular systems of differential equations of the form (1) remains an untreated question, which is the mean motivation of this paper.

This paper is organized as follows. Section 2 will cover almost periodic and $C^{(n)}$-almost periodic functions [10]. Section 3 discusses our main results and its consequences. Section 4 will be devoted to the case of singular systems of second-order differential equations. In Section 5, we consider an illustrative example.

2 Almost Periodic and $C^{(l)}$-Almost Periodic Functions

Most of the material of this section is taken from [1, 8, 10]. Let $C(\mathbb{R}, \mathbb{C}^m)$ stand for the collection of continuous functions from $\mathbb{R}$ into $\mathbb{C}^m$. Define $C^{(l)}(\mathbb{R}, \mathbb{C}^m)$ as the collection of functions $f : \mathbb{R} \mapsto \mathbb{C}^m$ such that $f^{(k)}$ exists and belongs to $C(\mathbb{R}, \mathbb{C}^m)$ for $k = 0, 1, 2, ..., l$. (The symbol $f^{(k)}$ being the k-derivative of f with $f^{(0)}$ corresponding to the continuity of the function f.)

Define $BC^{(l)}(\mathbb{R}, \mathbb{C}^m)$ as the collection of all functions $f \in C^{(l)}(\mathbb{R}, \mathbb{C}^m)$ such that

$$\|f\|_{(l)} := \sup_{t\in\mathbb{R}} \sum_{k=0}^{l} |f^{(k)}(t)| < \infty.$$

Clearly, $(BC^{(l)}(\mathbb{R}, \mathbb{C}^m), \|\cdot\|_{(l)})$ is a Banach space.

In this paper, the symbols $f^{(0)}$, $\|\cdot\|_{(0)}$, $C^{(0)}(\mathbb{R}, \mathbb{C}^m)$, $BC^{(0)}(\mathbb{R}, \mathbb{C}^m)$, and $AP^{(0)}(\mathbb{C}^m)$ stand respectively for f, $\|\cdot\|_\infty$, $C(\mathbb{R}, \mathbb{C}^m)$, $BC(\mathbb{R}, \mathbb{C}^m)$, and $AP(\mathbb{C}^m)$.

2.1 Almost periodic functions

Definition 2.1 [1, 8] (Bor) A function $f \in C(\mathbb{R}, \mathbb{C}^m)$ is called almost periodic if for each $\varepsilon > 0$ there exists $l(\varepsilon) > 0$ such that every interval of length $l(\varepsilon)$ contains a number τ with the property that $|f(t + \tau) - f(t)| < \varepsilon$ for all $t \in \mathbb{R}$. The collection of those functions is denoted by $AP(\mathbb{C}^m)$.

Definition 2.2 [1, 8] (Bochner) A continuous function $f : \mathbb{R} \to \mathbb{C}^m$ is said to be Bochner almost periodic if for every sequence of real numbers $(\sigma'_n)_{n\in\mathbb{N}}$ has a subsequence $(\sigma_n)_{n\in\mathbb{N}}$ such that $\{f(\sigma_n + t)\}$ converges uniformly in $t \in \mathbb{R}$.

It is well-known that Definition 2.1 and Definition 2.2 are equivalent (see Corduneanu [8]). In what follows we give another equivalent definition using trigonometric polynomials.

Basic properties of almost periodic functions include the following:

Theorem 2.1 *If $f : \mathbb{R} \to \mathbb{C}^m$ is almost periodic, then f is uniformly continuous in $t \in \mathbb{R}$. Moreover, the range $R(f) = \Big\{f(t) : t \in \mathbb{R}\Big\}$ is precompact in $\mathbb{C}^m$.*

Corollary 2.1 *Any almost periodic function is bounded on $\mathbb{R}$.*

Theorem 2.2 *If $f, g \in AP(\mathbb{C}^m)$ and $\mu \in \mathbb{C}$, then*

(i) μf *and* $f \pm g$ *belong to* $AP(\mathbb{C}^m)$.

(ii) *If* f, g *are* $\mathbb{C}$*-valued, then* $fg \in AP(\mathbb{C})$.

(iii) *If* $g \in AP(\mathbb{C})$ *and* $\inf_{t\in\mathbb{R}} |g(t)| = m > 0$, *then* $\dfrac{f}{g} \in AP(\mathbb{C}^m)$.

(iv) *If* $h \in L^1(\mathbb{C})$, *then* $(h * f)$, *the convolution between* h *and* f *defined by*

$$(h * f)(t) = \int_{-\infty}^{+\infty} h(s)f(t - s)\, ds$$

belongs to $AP(\mathbb{C}^m)$.

Theorem 2.3 *The space $AP(\mathbb{C}^m)$ equipped with the supnorm $\|\cdot\|_\infty$ is a Banach space.*

2.2 $C^{(n)}$-almost periodic functions

Definition 2.3 A function $f \in C^{(l)}(\mathbb{R}, \mathbb{C}^m)$ is said to be $C^{(l)}$-almost periodic if $f^{(k)} \in AP(\mathbb{C}^m)$ for $k = 0, 1, ..., l$. The collection of $C^{(l)}$-almost periodic functions is denoted by $AP^{(l)}(\mathbb{C}^m)$, which turns out to be a Banach space when equipped with the norm $\| \cdot \|_{(l)}$.

Clearly, the following inclusions hold

$$... \hookrightarrow AP^{(l+2)}(\mathbb{C}^m) \hookrightarrow AP^{(l+1)}(\mathbb{C}^m) \hookrightarrow AP^{(l)}(\mathbb{C}^m) \hookrightarrow ... \hookrightarrow AP^{(1)}(\mathbb{C}^m) \hookrightarrow AP(\mathbb{C}^m).$$

Theorem 2.4 *[10] The space $AP^{(l)}(\mathbb{C}^m)$ equipped with the norm $\left\| \cdot \right\|_{(l)}$ is a Banach space.*

Theorem 2.5 *[10] If $f \in AP^{(l)}(\mathbb{C}^m)$ and if $g \in L^1(\mathbb{C})$, then their convolution $f * g \in AP^{(l)}(\mathbb{C}^m)$.*

Proposition 2.1 *[10] If $(f_n)_{n\in\mathbb{N}} \subset AP(\mathbb{C}^m)$ converges uniformly to f on $\mathbb{R}$, then $f \in AP(\mathbb{C}^m)$.*

Theorem 2.6 *[10] If $f \in AP^{(l)}(\mathbb{C}^m)$ such that $f^{(l+1)}$ is uniformly continuous, then $f \in AP^{(l+1)}(\mathbb{C}^m)$.*

3 Existence of Almost Periodic Solutions

In this paper if $C \in M(m, \mathbb{C})$, we then denote the collection of its eigenvalues $\lambda_1, \lambda_2, ..., \lambda_m$ by $\sigma(C)$.

In this section we first recall some of the results obtained by Campbell [5] on the existence of solutions to Eq. (1). We then make extensive use of those results to study the existence of almost periodic solutions to Eq. (1) in the case when $f \in AP^{(k)}(\mathbb{C}^m)$. We next use the results for Eq. (1) to study the existence of almost periodic solutions to some general singular second-order differential equations formulated through Eq. (10).

It is well-known that real symmetric matrices can be diagonalized. That is not always the case for complex symmetric matrices [9].

Definition 3.1 A symmetric matrix $C \in M(m, \mathbb{C})$ with r distinct eigenvalues λ_j is said to have a spectral decomposition if there exist matrices P_j for $j = 1, 2, ..., r$ such that

$$C = \sum_{j=1}^{r} \lambda_j P_j = \sum_{j=1, \lambda_j \neq 0}^{r} \lambda_j P_j, \tag{2}$$

where $P_i P_j = 0$ if $i \neq j$, and $P_j^2 = P_j$ for all $i, j = 1, ..., r$, and $I = \displaystyle\sum_{j=1}^{r} P_j$.

This setting requires the following assumptions: let f, $A, B \in M(m, \mathbb{C})$ satisfy the following assumptions:

(H.1) $AB = BA$.

(H.2) $N(A) \cap N(B) = \{0\}$.

(H.3) $f \in AP^{(k)}(\mathbb{C}^m)$ where $k = i(A)$.

(H.4) $\sigma^*(A^D B) := \sigma(A^D B) - \{0\} \neq \emptyset$ with $\Re e\lambda > 0$ for all $\lambda \in \sigma^*(A^D B)$.

(H.5) $A^D B$ is symmetric and has a spectral decomposition.

Remark 3.1 The case when A is non-singular will not be considered here as this is well-understood. Indeed, if A^{-1} exists, then Eq. (1) can be written as follows

$$u' + B_1 u = f_1, \tag{3}$$

where $B_1 = A^{-1}B$, and $f_1 = A^{-1}f$.

In the rest of the paper, we associate with Eq. (1), its homogeneous equation given by

$$Au' + Bu = 0. \tag{4}$$

Theorem 3.1 *[5] Under assumption* (H.1), $u = e^{-A^D Bt} AA^D \xi$ *is a solution to Eq. (4) where* ξ *is an arbitrary vector in* $\mathbb{C}^m$.

Proof. Indeed, $Au' = -AA^D Be^{-A^D Bt} AA^D \xi = -Be^{-A^D Bt} AA^D \xi = -Bu$. The proof is complete.

Corollary 3.1 *[5] If assumption* (H.1) *holds and if* $A^D Af = f$, *then*

$$u = e^{-A^D Bt} \int e^{-A^D Bt} f(t)\, dt$$

is a particular solution to Eq. (1).

Lemma 3.1 *[5] If assumptions* (H.1)–(H.2) *hold, then* $(I - AA^D)BB^D = (I - AA^D)$.

Theorem 3.2 *[5] If assumptions* (H.1)–(H.2) *hold, then* $u = e^{-A^D Bt} AA^D \xi$ *where* $\xi \in \mathbb{C}^m$, *is the general solution to Eq. (4).*

Theorem 3.3 *[5] Suppose* (H.1)–(H.2) *hold and let* $k = Ind(A)$. *If* f *is of class* C^k *and* $\mathbb{C}^m$*-valued, then Eq. (1) is consistent and a particular solution of it is given*

$$u = A^D e^{-A^D Bt} \int_a^t e^{A^D Bs} f(s)\, ds + (I - AA^D) \sum_{l=0}^{k-1} (-1)^l (AB^D)^l B^D f^{(l)},$$

where $a \in \mathbb{R}$ *is arbitrary.*

Theorem 3.4 *[5] Suppose* (H.1)–(H.2) *hold and let* $k = Ind(A)$. *If* f *is of class* C^k *and* $\mathbb{C}^m$*-valued, then the general solution to Eq. (1) is explicitly given by*

$$u = e^{-A^D Bt} A^D A\xi + A^D e^{-A^D Bt} \int_a^t e^{A^D Bs} f(s)\, ds + (I - AA^D) \sum_{l=0}^{k-1} (-1)^l (AB^D)^l B^D f^{(l)},$$

where ξ *is arbitrary constant vector, and* $a \in \mathbb{R}$ *is arbitrary.*

Lemma 3.2 *If $C \in M(n,\mathbb{C})$ is symmetric, has a spectral decomposition, and $\sigma^*(C) \neq \emptyset$ with $\Re e\lambda > 0$ for all $\lambda \in \sigma^*(C)$, then there exist $M > 0$ and $\omega > 0$ such that*

$$\|e^{-tC}\| \leq Me^{-\omega t}$$

for $t \geq 0$.

Proof. Using Definition 3.1, one can write $C = \sum_{j=1}^{r} \lambda_j P_j = \sum_{j=1,\ \lambda_j \neq 0}^{r} \lambda_j P_j$ and hence

$$e^{-tC} = \sum_{j=1,\ \lambda_j \in \sigma^*(C)}^{r} e^{-\lambda_j t} P_j, \quad t \geq 0.$$

Now

$$\begin{aligned} \|e^{-tC}\| &= \|\sum_{j=1,\ \lambda_j \in \sigma^*(C)}^{r} e^{-\lambda_j t} P_j\| \leq \sum_{j=1,\ \lambda_j \in \sigma^*(C)}^{r} e^{-\Re e\,\lambda_j t}\|P_j\| \\ &\leq \sum_{j=1,\ \lambda_j \in \sigma^*(C)}^{r} e^{-\omega t}\|P_j\| \leq Me^{-\omega t} \end{aligned}$$

for $t \geq 0$, where $\omega = \min\{\Re e\lambda_j : \lambda_j \neq 0, \quad j = 1, 2, ..., r\}$ and $M = \sum_{j=1}^{r} \|P_j\| < \infty$.

Lemma 3.3 *Suppose* (H.1)–(H.2) *hold. Then all the solutions to Eq. (4) on the real number line $\mathbb{R}$ are of the form*

$$w_0(t) = e^{-A^D B(t-s)} w_0(s) \ \ \text{for all} \ \ t, s \in \mathbb{R}, \quad t \geq s. \tag{5}$$

Proof. Let w be an arbitrary solution to Eq. (4). Now from Theorem 3.2, it follows that the solution w can be written as $w(t) = e^{-A^D Bt} AA^D \xi$ where $\xi \in \mathbb{C}^n$ is an arbitrary vector. Similarly, $w(s) = e^{-A^D Bs} AA^D \xi$. Thus for $t \geq s$,

$$e^{-A^D B(t-s)} w(s) = e^{-A^D B(t-s)} e^{-A^D Bs} AA^D \xi = e^{-A^D Bt} AA^D \xi = w(t).$$

Theorem 3.5 *Under assumptions* (H.1)–(H.2)–(H.3)–(H.4)–(H.5)*, Eq. (1) has a unique almost periodic solution which is explicitly given by*

$$u_0(t) = A^D \int_{-\infty}^{t} e^{-A^D B(t-s)} f(s)\mathrm{d}s + (I - AA^D) \sum_{l=0}^{k-1} (-1)^l (AB^D)^l B^D f^{(l)}(t) \tag{6}$$

for all $t \in \mathbb{R}$.

Proof. We first show that the function u_0 given by

$$u_0(t) = A^D \int_{-\infty}^{t} e^{-A^D B(t-s)} f(s)\mathrm{d}s + (I - AA^D) \sum_{l=0}^{k-1} (-1)^l (AB^D)^l B^D f^{(l)}(t), \quad t \in \mathbb{R},$$

is a solution to Eq. (1). Indeed,

$$
\begin{aligned}
Au_0'(t) &= -AA^DA^DB\int_{-\infty}^{t} e^{-A^DB(t-s)}f(s)\mathrm{d}s + AA^De^{-A^DBt}e^{A^DBt}f(t)\\
&+ A(I-AA^D)\sum_{l=0}^{k-1}(-1)^l(AB^D)^lB^Df^{(l+1)}(t)\\
&= -AA^DA^DB\int_{-\infty}^{t} e^{-A^DB(t-s)}f(s)\mathrm{d}s + AA^Df(t)\\
&+ (I-AA^D)\sum_{l=0}^{k-1}(-1)^l(AB^D)^{l+1}f^{(l+1)}(t)\\
&= -B(A^DAA^D)\int_{-\infty}^{t} e^{-A^DB(t-s)}f(s)\mathrm{d}s + AA^Df(t)\\
&+ (I-AA^D)[\sum_{l=0}^{k-2}(-1)^l(AB^D)^{l+1}f^{(l+1)}(t) + (-1)^{k-1}(AB^D)^{k-1+1}f^{(k-1+1)}(t)]\\
&= -BA^D\int_{-\infty}^{t} e^{-A^DB(t-s)}f(s)\mathrm{d}s + AA^Df(t)\\
&+ (I-AA^D)[\sum_{l=0}^{k-2}(-1)^l(AB^D)^{l+1}f^{(l+1)}(t) + 0]\\
&= -BA^D\int_{-\infty}^{t} e^{-A^DB(t-s)}f(s)\mathrm{d}s + AA^Df(t)\\
&- (I-AA^D)\sum_{l=0}^{k-2}(-1)^{l+1}(AB^D)^{l+1}f^{(l+1)}(t)\\
&= -BA^D\int_{-\infty}^{t} e^{-A^DB(t-s)}f(s)\mathrm{d}s\\
&- (I-AA^D)\sum_{j=1}^{k-1}(-1)^j(AB^D)^jf^{(j)}(t) + AA^Df(t)\\
&= -BA^D\int_{-\infty}^{t} e^{-A^DB(t-s)}f(s)\mathrm{d}s\\
&- (I-AA^D)[\sum_{j=0}^{k-1}(-1)^j(AB^D)^jf^{(j)}(t) - f(t)] + AA^Df(t)\\
&= -BA^D\int_{-\infty}^{t} e^{-A^DB(t-s)}f(s)\mathrm{d}s\\
&- (I-AA^D)\sum_{j=0}^{k-1}(-1)^j(AB^D)^jf^{(j)}(t) + (I-AA^D)f(t) + AA^Df(t)\\
&= -BA^D\int_{-\infty}^{t} e^{-A^DB(t-s)}f(s)\mathrm{d}s - (I-AA^D)\sum_{l=0}^{k-1}(-1)^l(AB^D)^lf^{(l)}(t) + f(t)
\end{aligned}
\tag{7}
$$

$$
\begin{aligned}
&= -BA^D \int_{-\infty}^{t} e^{-A^D B(t-s)} f(s)\mathrm{d}s \\
&- (I - AA^D) \sum_{l=0}^{k-1} (-1)^l (AB^D BB^D)^l f^{(l)}(t) + f(t) \\
&= -BA^D \int_{-\infty}^{t} e^{-A^D B(t-s)} f(s)\mathrm{d}s \\
&- (I - AA^D) \sum_{l=0}^{k-1} (-1)^l (AB^D)^l (BB^D)^l f^{(j)}(t) + f(t) \\
&= -BA^D \int_{-\infty}^{t} e^{-A^D B(t-s)} f(s)\mathrm{d}s \\
&- (I - AA^D) \sum_{l=0}^{k-1} (-1)^l (AB^D)^l (BB^D) f^{(l)}(t) + f(t) \\
&= -B[A^D \int_{-\infty}^{t} e^{-A^D B(t-s)} f(s)\mathrm{d}s \\
&- (I - AA^D) \sum_{l=0}^{k-1} (-1)^l (AB^D)^l B^D f^{(l)}(t)] + f(t) = -Bu_0(t) + f(t),
\end{aligned}
$$

and hence $u_0(t)$ is a solution to Eq. (1).

We next show that u_0 given above is bounded. Indeed, since by assumption $Re\lambda > 0$ for all $\lambda \in \sigma(A^D B) - \{0\}$, then using Lemma 3.2 it follows that there exist $M > 0$ and $\omega > 0$ such that

$$\|e^{-tA^D B}\| \le Me^{-\omega t}, \quad t \ge 0.$$

First of all, note that

$$\left|(I - AA^D) \sum_{l=0}^{k-1} (-1)^l (AB^D)^l B^D f^{(l)}(t)\right| \le \big(1 + \|AA^D\|\big) \|f\|_{(k)} \sum_{l=0}^{k-1} \|AB^D\|^l \|B^D\| < \infty,$$

where $\|f\|_{(k)} = \sup_{t\in\mathbb{R}} \sum_{l=0}^{k} |f^{(l)}(t)| < \infty$ as $f \in AP^{(k)}(\mathbb{C}^m)$. Similarly,

$$
\begin{aligned}
\left|A^D \int_{-\infty}^{t} e^{-A^D B(t-s)} f(s) ds\right| &\le ||A^D|| \int_{-\infty}^{t} ||e^{-A^D B(t-s)}|| \cdot |f(s)| ds \\
&\le ||A^D|| \cdot ||f||_\infty \int_{-\infty}^{t} Me^{-\omega(t-s)} ds \\
&= M||A^D|| \cdot ||f||_\infty \omega^{-1} < \infty
\end{aligned}
$$

and hence $u_0 \in BC(\mathbb{R}, \mathbb{C}^m)$.

The next step consists of showing that the function u_0 given above is the unique (bounded) solution to Eq. (1). Indeed, suppose $u_1, u_2 \in BC(\mathbb{R}, \mathbb{C}^m)$ are two solutions to Eq. (1). Thus $w = u_1 - u_2 \in BC(\mathbb{R}, \mathbb{C}^m)$ is a solution to Eq. (4). Using Lemma 3.3 it follows that $w(t) = e^{-A^D B(t-s)} w(s)$ for $t \ge s$.

Now

$$\begin{aligned} |w(t)| &= |e^{-A^D B(t-s)} w(s)| \\ &\leq Me^{-\omega(t-s)} \cdot |w(s)| \\ &\leq Me^{-\omega(t-s)} \cdot \|w\|_\infty \quad \text{for all} \quad t \geq s. \end{aligned}$$

Now let $(s_l)_{l\in\mathbb{N}}$ be a sequence of real numbers such that $s_l \to -\infty$ as $l \to \infty$. Clearly, for any fixed $t \in \mathbb{R}$, there exists a subsequence $(s_{l_p})_{p\in\mathbb{N}}$ of $(s_l)_{l\in\mathbb{N}}$ such that $s_{l_p} < t$ for all $p \in \mathbb{N}$. In view of the above, letting $p \to \infty$ yields $w(t) = 0$ for all $t \in \mathbb{R}$. Therefore, $u_1 = u_2$.

We next show that the function u_0 given above is almost periodic. Indeed, since $f \in AP^{(k)}(\mathbb{C}^m)$ and all the operators involved in the sum

$$\varphi(t) := (I - AA^D) \sum_{l=0}^{k-1} (-1)^l (AB^D)^l B^D f^{(l)}(t)$$

are matrices (hence are bounded linear operators), it follows that $t \mapsto \varphi(t) \in AP^{(k)}(\mathbb{C}^n) \subset AP(\mathbb{C}^m)$.

Now since $f \in AP(\mathbb{C}^m)$, it follows that for all $\varepsilon > 0$ there exists $l(\varepsilon) > 0$ such that every interval of length $l(\varepsilon) > 0$ contains a τ with the property

$$|f(t+\tau) - f(t)| \leq \frac{\varepsilon\omega}{M\|A^D\|}$$

for all $t \in \mathbb{R}$.

Now setting $\psi(t) := A^D \int_{-\infty}^{t} e^{-A^D B(t-s)} f(s)ds$ it follows that

$$\begin{aligned} |\psi(t+\tau) - \psi(t)| &\leq \|A^D\| \cdot |\int_{-\infty}^{t+\tau} e^{-A^D B(t+\tau-s)} f(s)ds - \int_{-\infty}^{t} e^{-A^D B(t-s)} f(s)ds| \\ &= \|A^D\| \cdot |\int_{-\infty}^{t} e^{-A^D B(t-s)} \left(f(s+\tau) - f(s)\right) ds| \\ &\leq \|A^D\| \cdot \frac{\varepsilon\omega}{M\|A^D\|} \int_{-\infty}^{t} \|e^{-A^D B(t-s)}\| ds \\ &\leq \frac{\varepsilon\omega}{M} M \int_{-\infty}^{t} e^{-\omega(t-s)} ds \\ &= \varepsilon \end{aligned}$$

and hence $\psi \in AP(\mathbb{C}^m)$ which yields $u_0 = \varphi + \psi \in AP(\mathbb{C}^m)$.

We now consider the case when A and B may or may not commute. Moreover, both A and B can be taken nonsingular. In what follows, we set

$$\rho_{A,B} = \{\lambda \in \mathbb{C} : (\lambda A + B)^{-1} \ \text{ exists}\}.$$

If $\lambda \in \rho_{A,B}$, we also set

$$A_\lambda = (\lambda A + B)^{-1} A, \quad B_\lambda = (\lambda A + B)^{-1} B, \quad \text{and} \quad f_\lambda = (\lambda A + B)^{-1} f.$$

Consider

$$A_z u' + B_z u = f_z, \quad t \in \mathbb{R}. \tag{8}$$

Corollary 3.2 *Suppose $\rho_{A,B} \neq \emptyset$. Let $z \in \rho_{A,B}$ such that $A_z^D B_z$ is symmetric, has a spectral decomposition, $\sigma^*(A_z^D B_z) \neq \emptyset$ with $Re\lambda > 0$ for all $\lambda \in \sigma^*(A_z^D B_z)$. Moreover, we suppose that $f \in AP^{(k)}(\mathbb{C}^m)$ with $i(A_z) = k$. Then Eq. (8) has a unique almost periodic solution which is explicitly given by*

$$u_z(t) = A_z^D \int_{-\infty}^t e^{-A_z^D B_z (t-s)} f_z(s) \mathrm{d}s + (I - A_z A_z^D) \sum_{l=0}^{k-1} (-1)^l (A_z B_z^D)^l B_z^D f_z^{(l)}(t) \tag{9}$$

for all $t \in \mathbb{R}$.

Therefore, Eq. (1) has a unique almost periodic solution.

Proof. Since $\rho_{A,B} \neq \emptyset$, suppose $\rho_{A,B}$ contains a $z \in \mathbb{C}$. To complete the proof we have to show that Eq. (8) has a unique almost periodic solution. For that, we have to show that assumptions (H.1)–(H.2)—(H.3) are fulfilled when A is replaced with A_z, B with B_z, and f with f_z.

Let us first show that A_z and B_z commute. This is based upon the fact $zA_z + B_z = I$, which yields $B_z = I - zA_z$.

Now

$$A_z B_z = A_z(I - zA_z) = A_z - zA_z^2 \text{ and } B_z A_z = (I - zA_z)A_z = A_z - zA_z^2.$$

We next show that $N(A_z) \cap N(B_z) = \{0\}$. First of all, note that

$$N(A_z) \cap N(B_z) = N(A) \cap N(B).$$

Now, if $u \in N(A) \cap N(B)$, then $(zA + B)u = 0$, which yields $(zA + B)^{-1}(zA + B)u = u = 0$. Therefore, $N(A) \cap N(B) = \{0\}$.

Since $f \in AP^{(k)}(\mathbb{C}^m)$, it easy follows that $f_z \in AP^{(k)}(\mathbb{C}^m)$.

To complete the proof it suffices to apply Theorem 3.5 to the case when A replaced by A_z, B with B_z, and f with f_z. Doing so yields the existence and uniqueness of an almost periodic solution to Eq. (8), which is explicitly given by

$$u_z(t) = A_z^D \int_{-\infty}^t e^{-A_z^D B_z (t-s)} f_z(s) \mathrm{d}s + (I - A_z A_z^D) \sum_{m=0}^{k-1} (-1)^m (A_z B_z^D)^m B_z^D f_z^{(m)}(t), \ \ t \in \mathbb{R}.$$

Therefore, Eq. (1) has a unique almost periodic solution.

4 Second-Order Singular Differential Equations

In this Section we study and obtain the existence of almost periodic solutions to the singular system of second-order differential differential equations given by

$$Au''(t) + Bu'(t) + Cu(t) = f(t), \quad t \in \mathbb{R}, \tag{10}$$

where A, B, C (possibly singular) are $m \times m$-square matrices with complex entries and $f : \mathbb{R} \mapsto \mathbb{C}^m$ is $C^{(k)}$-almost periodic with $k = i(\mathcal{A})$. For that, our strategy consists of following the work of Campbell [3, p. 161] and rewriting Eq. (10) as a first-order singular differential equation and making extensive use of the results of the previous Section to establish the existence and uniqueness of an almost periodic solution to Eq. (10). Indeed, assuming that $u : \mathbb{R} \mapsto \mathbb{C}^m$ is twice differentiable and setting

$$w := \begin{pmatrix} u \\ u' \end{pmatrix},$$

then Eq. (10) can be rewritten on $\mathbb{C}^m \times \mathbb{C}^m$ in the following form

$$\mathcal{A}w'(t) + \mathcal{B}w = \mathcal{F}(t),\ t \in \mathbb{R}, \tag{11}$$

where $\mathcal{A}$, $\mathcal{B}$, and $\mathcal{F}$ are defined by

$$\mathcal{A} = \begin{pmatrix} B & A \\ I & 0 \end{pmatrix},\quad \mathcal{B} = \begin{pmatrix} C & O \\ O & -I \end{pmatrix},\quad \text{and}\quad \mathcal{F} = \begin{pmatrix} f \\ O \end{pmatrix}.$$

Let $\rho_{\mathcal{A},\mathcal{B}} = \{\lambda \in \mathbb{C} : (\lambda\mathcal{A} + \mathcal{B})^{-1}\ \text{ exists}\}$. If $\lambda \in \rho_{\mathcal{A},\mathcal{B}}$, we then set

$$\mathcal{A}_\lambda = (\lambda\mathcal{A} + \mathcal{B})^{-1}\mathcal{A},\quad \mathcal{B}_\lambda = (\lambda\mathcal{A} + \mathcal{B})^{-1}\mathcal{B},\quad \text{and}\quad \mathcal{F}_\lambda = (\lambda\mathcal{A} + \mathcal{B})^{-1}\mathcal{F}.$$

Consider

$$\mathcal{A}_z w' + \mathcal{B}_z w = \mathcal{F}_z,\quad t \in \mathbb{R}. \tag{12}$$

Corollary 4.1 *Suppose $\rho_{\mathcal{A},\mathcal{B}} \neq \emptyset$. Let $z \in \rho_{\mathcal{A},\mathcal{B}}$ such that $\mathcal{A}_z^D\mathcal{B}_z$ is symmetric, has a spectral decomposition, and $\sigma^*(\mathcal{A}_z^D\mathcal{B}_z) \neq \emptyset$ such that $Re\lambda > 0$ for all $\lambda \in \sigma^*(\mathcal{A}_z^D\mathcal{B}_z)$. Moreover, we suppose $\mathcal{F} \in AP^{(k)}(\mathbb{C}^m \times \mathbb{C}^m)$ with $k = i(\mathcal{A})$. Then Eq. (12) has a unique almost periodic solution which is explicitly given by*

$$w_z(t) = \mathcal{A}_z^D \int_{-\infty}^{t} e^{-\mathcal{A}_z^D\mathcal{B}_z(t-s)}\mathcal{F}_z(s)\mathrm{d}s + (I - \mathcal{A}_z\mathcal{A}_z^D)\sum_{l=0}^{k-1}(-1)^l(\mathcal{A}_z\mathcal{B}_z^D)^l\mathcal{B}_z^D\mathcal{F}_z^{(l)}(t) \tag{13}$$

for all $t \in \mathbb{R}$.

Therefore, Eq. (10) has a unique almost periodic solution u. Moreover, since $u, u' \in AP(\mathbb{C}^m)$, it follows that $u \in AP^{(1)}(\mathbb{C}^m)$.

The proof of Corollary 4.1 follows along the same lines as that of Corollary 3.2 and hence is omitted.

5 Example

In this section we give an example to illustrate Theorem 3.5. For that, let $m = 3$ and fix $\alpha, \beta, \gamma \in \mathbb{C}$ such that $\Re e\,\alpha > 0$, $\Re e\,\beta > 0$, and $\Re e\,\gamma > 0$.

Consider the singular system of differential equations given by

$$\begin{cases} \alpha u'(t) + \beta v'(t) + \alpha u(t) + \beta v(t) = \sin t + i \sin\sqrt{2}t, \\ \alpha v'(t) + \alpha v(t) = \cos t + i\cos\pi t, \\ \gamma w(t) = \cos t + i \sin\sqrt{3}t, \end{cases} \tag{14}$$

for all $t \in \mathbb{R}$.

Clearly the matrices $A, B \in M(3,\mathbb{C})$ and $f : \mathbb{R} \mapsto \mathbb{C}^3$ associated with the system Eq. (14) are given by

$$A = \begin{pmatrix} \alpha & \beta & 0 \\ 0 & \alpha & 0 \\ 0 & 0 & 0 \end{pmatrix}, \quad B = \begin{pmatrix} \alpha & \beta & 0 \\ 0 & \alpha & 0 \\ 0 & 0 & \gamma \end{pmatrix}, \quad \text{and} \quad f(t) = \begin{pmatrix} \sin t + i \sin \sqrt{2}t \\ \cos t + i \cos \pi t \\ \cos t + i \sin \sqrt{3}t \end{pmatrix}.$$

Moreover, assumptions (H.1)–(H.2), (H.4)–(H.5) hold as

$$A^D = \begin{pmatrix} \frac{1}{\alpha} & -\frac{\beta}{\alpha^2} & 0 \\ 0 & \frac{1}{\alpha} & 0 \\ 0 & 0 & 0 \end{pmatrix}, \quad \text{and} \quad A^D B = \begin{pmatrix} 1 & 0 & 0 \\ 0 & 1 & 0 \\ 0 & 0 & 0 \end{pmatrix} \quad \text{is symmetric with} \quad \sigma^*(A^D B) = \{1\}.$$

Furthermore, $i(A) = 1$ and $f \in AP^{(1)}(\mathbb{C}^3)$. Therefore, from Theorem 3.5 the singular system of first-order differential equation

$$Az'(t) + Bz(t) = f(t), \quad t \in \mathbb{R},$$

has a unique almost periodic solution, that is,

$$z_{\alpha,\beta,\gamma}(t) = \begin{pmatrix} u(t) \\ v(t) \\ w(t) \end{pmatrix} \in AP(\mathbb{C}^3).$$

References

[1] Bezandry, P.H. and Diagana, T. *Almost periodic stochastic processes,* Springer, New York, 2011.

[2] Bochner, S. A new approach to almost periodicity. *Proc. Nat. Acad.* **48** (1962), 2039–2043.

[3] Campbell, S.L. *Singular systems of differential equations.* Research Notes in Mathematics, Pitman, London, 1980, 5–9.

[4] Campbell, S. L. *Singular systems of differential equations II.* Research Notes in Mathematics, Pitman, London, 1982.

[5] Campbell, S. L. Applications of the drazin inverse to linear systems of differential equations with singular constant coefficients. *SIAM J. Appl. Math.* **31**(3) (1976) 411–425.

[6] Campbell, S. L. and Meyer, C. D. *Generalized inverses of linear transformations.* Corrected reprint of the 1979 original. Dover Publications, Inc., New York, 1991.

[7] Campbell, S. L. and Meyer, C. D. Generalized inverses of linear transformations. Surveys and Reference Works in Mathematics, 4. Pitman (Advanced Publishing Program). Boston, Mass.-London, 1979.

[8] Corduneanu, C. *Almost periodic functions,* Second Edition. Chealsea – New York, 1989.

[9] Craven, B. D. Complex symmetric matrices. *J. Austral. Math. Soc.* **10** (1969) 341–354.

[10] Diagana, T. and Nelson, V. $C^{(n)}$-Pseudo almost automorphy and its applications to some higher-order differential equations. *Nonlinear Studies.* **19**(3) (2012) 443–455.

[11] Mishra, I., Bahuguna, D. and Abbas, S. Existence of Almost Automorphic Solutions of Neutral Functional Differential Equation. *Nonlinear Dynamics and Systems Theory* **11**(2) (2011) 165–172.

Nonlinear Dynamics and Systems Theory, **13** (1) (2013) 13–23

Nonlinear Dynamic Inequalities and Stability of Quasilinear Systems on Time Scales

S.V. Babenko [1*] and A.A. Martynyuk [2]

[1] *National Bohdan Khmelnytsky University of Cherkasy, Shevchenko Blvd., 81, Cherkasy, 18031, Ukraine*
[2] *S.P. Timoshenko Institute of Mechanics of NAS of Ukraine, Nesterov str., 3, Kyiv, 03057, Ukraine*

Received: November 19, 2012; Revised: January 25, 2013

Abstract: In this paper a novel nonlinear integral inequality on time scale is proposed. This inequality is applied to analyze stability of zero solution of quasilinear dynamic equations on time scale. Also, stability conditions are established for a wide class of nonlinearities in the system of dynamic equations.

Keywords: *dynamic equations on time scales; nonlinear inequalities; stability; asymptotic stability.*

Mathematics Subject Classification (2010): 34A34, 34A40, 34D20, 39A13, 39A11.

1 Introduction

The method of integral inequalities of motion stability theory (see [8,9] and bibliography therein) has been developed in terms of linear and nonlinear integral inequalities treated in numerous papers (see [2,14] and bibliography therein). Appearance of dynamic equations on time scale [6] gave an impetus to the investigations in the theory of dynamic integral inequalities (see [3] and bibliography therein). The inequalities of Gronwall - Bellman type established by now and some types of nonlinear inequalities (see [4]) have been applied in the stability analysis of solutions to dynamic equations on time scale. It is of interest to further generalize nonlinear dynamic inequality of Stakhursky type (see [4, 10, 13]) for dynamic equations in the case of arbitrary real nonlinearity exponent larger than one. Such generalization makes possible the analysis of various types of stability of zero solution for a new class of quasilinear dynamic equations.

* Corresponding author: mailto:sofuslee@rambler.ru

In the present paper a new nonlinear dynamic integral inequality is obtained in view of the results of [10]. The new inequality is applied to establish sufficient conditions for stability, uniform stability and asymptotic stability of trivial solutions to a class of quasilinear dynamic equations. All the necessary information from the mathematical analysis on time scale can be found in monographs [3, 7] or paper [4] and so is omitted here.

2 Statement of the Problem

Consider a quasilinear dynamic equation of the type

$$x^{\Delta} = A(t)x + f(t,x), \quad f(t,0) = 0, \tag{1}$$

where $x \in \mathbb{R}^n$, $t \in \mathbb{T}$, and the matrix-valued function $A : \mathbb{T} \to \mathbb{R}^{n\times n}$ and the vector-function $f : \mathbb{T} \times \mathbb{R}^n \to \mathbb{R}^n$ satisfy the following hypotheses:

(H_1) functions $A(t)$ and $f(t,x)$ are rd-continuous and $A \in \mathcal{R}(\mathbb{T}, \mathbb{R}^{n\times n})$;

(H_2) function $f(t,x)$ satisfies Lipschitz condition with respect to spatial variable in $\mathbb{R}^n$, i.e. there exists $L > 0$ such that

$$\|f(t,x_1) - f(t,x_2)\| \le L\|x_1 - x_2\|, \quad \text{for all} \quad (t,x_1),(t,x_2) \in \mathbb{T}\times\mathbb{R}^n; \tag{2}$$

(H_3) there exist functions $\alpha(t), \varphi(t), \psi(t) \in \mathbb{C}_{rd}(\mathbb{T}, \mathbb{R}_+)$ and a constant $m > 1$ such that:

(a) $\|f(t,x)\| \le \alpha(t)\|x\|^m$;

(b) $\|e_A(t,t_0)\| \le \varphi(t)\psi(t_0)$,

for all $t \ge t_0$, belonging to $\mathbb{T}$, and $x \in \mathbb{R}^n$, where $e_A(t,t_0)$ denotes the matrix exponential function [3] of the linear dynamic equation: $x^{\Delta} = A(t)x$.

It should be noted that the conditions of hypotheses (H_1) and (H_2) ensure existence and uniqueness of solution for the dynamic equation with given initial conditions. Further, under hypotheses (H_1) — (H_3), we investigate the problem on stability, uniform stability and asymptotic stability of zero solution for dynamic equation (1). For quasilinear systems of ordinary differential equations of (1) type the conditions similar to condition (a) for integer nonlinearity exponents have been considered in a number of papers (see [5], p.266-270, [7], [12] and bibliography therein).

3 Generalized Nonlinear Dynamic Inequality

Nonlinear dynamic inequality has been a subject of investigation in paper [4] for the integer nonlinearity exponents larger than one. Here we deal with a more general situation.

Let $\mu(t)$ be a graininess function on the time scale $\mathbb{T}$. The following assertion holds.

Lemma 3.1 *Assume that the functions $a(t), b(t)$ are positive rd-continuous on $\mathbb{T}$, the function $h(t)$ is nonnegative rd-continuous on $\mathbb{T}$ and $m > 1$ is a real number. If the function $\frac{a(t)}{b(t)}$ is non-decreasing on $\mathbb{T}$, for any function $u(t)$, satisfying the inequality*

$$u(t) \le a(t) + b(t)\int_{t_0}^{t} h(s)u^m(s)\Delta s, \quad t \ge t_0, \tag{3}$$

the estimate

$$u(t) \le \frac{a(t)}{\left[1 + \int\limits_{t_0}^{t} \frac{a^{m-1}(\sigma(s)) - (a(\sigma(s)) + \mu(s)b(\sigma(s))a^m(s)h(s))^{m-1}}{\mu(s)(a(\sigma(s)) + \mu(s)b(\sigma(s))a^m(s)h(s))^{m-1}} \Delta s\right]^{\frac{1}{m-1}}} \tag{4}$$

is valid on the interval $[t_0, \widetilde{t})$*, where* $\widetilde{t}$ *is the first point from the interval* $[t_0, +\infty) \cap \mathbb{T}$*, at which the denominator base number in the right-hand part of inequality* (4) *becomes non-positive.*

Proof. Assume that the function $u(t)$ satisfies inequality (3) which is written as

$$u(t) \le a(t)\Big(1 + \frac{b(t)}{a(t)} \int\limits_{t_0}^{t} h(s)u^m(s)\Delta s\Big) = a(t)w(t), \quad \text{for all} \quad t \ge t_0.$$

According to the rule of Δ-differentiation of a product of two functions, we have for $w(t)$:

$$w^\Delta(t) = \Big(\frac{b(t)}{a(t)}\Big)^\Delta \int\limits_{t_0}^{t} h(s)u^m(s)\Delta s + \Big(\frac{b(t)}{a(t)}\Big)^\sigma h(t)u^m(t) \le \frac{b(\sigma(t))}{a(\sigma(t))} h(t)u^m(t),$$

due to the function $b(t)/a(t)$ decreasing. Further

$$w^\Delta(t) \le \frac{b(\sigma(t))}{a(\sigma(t))} h(t)u^m(t) \le \frac{b(\sigma(t))}{a(\sigma(t))} h(t)a^m(t)w^m(t) = r(t)w^m(t),$$

for all $t \ge t_0$. Consider the dynamic comparison equation

$$v^\Delta(t) = r(t)v^m(t) \tag{5}$$

and study the behavior of its solution starting from the point $v(t_0) = 1 + \varepsilon$, where $\varepsilon > 0$ is a sufficiently small number. To this end in (5) we make the change of variable $\xi(t) = v^{1-m}(t)$, and by definition of Δ-derivative of a function obtain

$$\begin{aligned} \xi^\Delta(t) &= \frac{\xi(\sigma(t)) - \xi(t)}{\mu(t)} = \frac{v^{1-m}(\sigma(t)) - v^{1-m}(t)}{\mu(t)} = \\ &= \frac{(v(t) + \mu(t)v^\Delta(t))^{1-m} - v^{1-m}(t)}{\mu(t)} = \frac{v^{1-m}(t)}{\mu(t)}\Big(\Big(1 + \mu(t)\frac{v^\Delta(t)}{v(t)}\Big)^{1-m} - 1\Big) = \\ &= \frac{v^{1-m}(t)}{\mu(t)}\Big((1 + \mu(t)r(t)v^{1-m}(t))^{1-m} - 1\Big) = \frac{\xi(t)}{\mu(t)}\Big(\Big(1 + \frac{\mu(t)r(t)}{\xi(t)}\Big)^{1-m} - 1\Big) \equiv \\ &\equiv F(t, \xi), \quad \xi(t_0) = (1 + \varepsilon)^{1-m}. \end{aligned}$$

Besides, it is assumed that the expression $\frac{\xi(\sigma(t)) - \xi(t)}{\mu(t)}$ in the case $\mu(t) = 0$ is equal to the limit $\lim\limits_{\tau \to 0} \frac{\xi(t+\tau) - \xi(t)}{\tau}$. Further we find that

$$\frac{\partial F(t, \xi)}{\partial \xi} = \frac{1}{\mu(t)}\left(\frac{1 + \frac{m\mu(t)r(t)}{\xi} - \Big(1 + \frac{\mu(t)r(t)}{\xi}\Big)^m}{\Big(1 + \frac{\mu(t)r(t)}{\xi}\Big)^m}\right) \le 0,$$

for all $t \in [t_0, +\infty)$, i.e. the function $F(t, \cdot)$ does not increase on the set $(0, +\infty)$. Since $\xi(t) \in (0, 1)$ for all $t \in [t_0, +\infty)$ (due to connection with the function $v(t)$), for the indicated values of t the chain of inequalities holds true

$$F(t, 0) \geq F(t, \xi(t)) \geq F(t, 1) > F(t, \infty). \tag{6}$$

We find that $F(t, 1) = \frac{(1+\mu(t)r(t))^{1-m}-1}{\mu(t)}$. It is easy to verify that the function $F(t, \xi)$ satisfies all conditions of the theorem on existence and uniqueness of solution to Cauchy problem for dynamic equation on time scale (see [6]). Therefore, the Cauchy problem

$$\xi^{\Delta}(t) = F(t, \xi(t)), \quad \xi(t_0) = (1 + \varepsilon)^{1-m}$$

possesses the only solution $\xi(t)$, which can be presented in the integral form

$$\xi(t) = (1 + \varepsilon)^{1-m} + \int_{t_0}^{t} F(s, \xi(s))\Delta s. \tag{7}$$

Further, using formula (7) and inequalities (6) we arrive at the estimate

$$\begin{aligned} \xi(t) = (1 + \varepsilon)^{1-m} + \int_{t_0}^{t} F(s, \xi(s))\Delta s \geq (1 + \varepsilon)^{1-m} + \int_{t_0}^{t} F(s, 1)\Delta s = \\ = (1 + \varepsilon)^{1-m} + \int_{t_0}^{t} \frac{(1 + \mu(s)r(s))^{1-m} - 1}{\mu(s)}\Delta s, \end{aligned} \tag{8}$$

which is valid for all $t \in [t_0, \widetilde{t})$. For the values of t from the scale $\mathbb{T}$ the expression in the right-hand part of inequality (8) is positive by Lemma 3.1, and therefore, inequality (8) is equivalent to the inequality

$$v(t) = v(t; t_0, 1 + \varepsilon) \leq \left((1 + \varepsilon)^{1-m} + \int_{t_0}^{t} \frac{(1 + \mu(s)r(s))^{1-m} - 1}{\mu(s)}\Delta s \right)^{\frac{1}{1-m}},$$

for all $t \in [t_0, \widetilde{t})$.

In view of the comparison principle [6] and the passage to the limit for $\varepsilon \to 0$ we get inequality (4). Lemma 3.1 is proved. $\square$

Designate $h(t) = \psi(\sigma(t))\varphi^m(t)\alpha(t)$,

$$D(t, a, \rho) = \int_{a}^{t} \frac{1}{\mu(s)} \left(1 - \frac{1}{(1 + \mu(s)h(s)\psi^{m-1}(a)\rho^{m-1})^{m-1}} \right) \Delta s.$$

The following lemma provides estimate of solution to equation (1) by means of inequality (4).

Lemma 3.2 *For equation* (1) *let hypotheses* (H_1) — (H_3) *be satisfied. Then for arbitrary* $t_0 \in \mathbb{T}$ *and* $x_0 \in \mathbb{R}^n$ *the following estimate of solution* $x(t; t_0, x_0)$ *to equation* (1) *holds*

$$\|x(t; t_0, x_0)\| \leq \varphi(t)\psi(t_0)\|x_0\| \Big[1 - D(t, t_0, \|x_0\|) \Big]^{1/1-m}, \tag{9}$$

for all $t \in [t_0, +\infty) \cap \mathbb{T}$, *for which* $D(t, t_0, \|x_0\|) < 1$.

Proof. As noted, hypotheses (H_1) — (H_2) ensure the existence and uniqueness of solution $x(t; t_0, x_0)$ to equation (1) found by the Cauchy formula [6]:

$$x(t; t_0, x_0) = e_A(t, t_0)x_0 + \int_{t_0}^{t} e_A(t, \sigma(s))f(s, x(s; t_0, x_0))\Delta s, \tag{10}$$

where the integration is made on the scale $\mathbb{T}$ within the limits from t_0 to t. From (10) and hypothesis (H_3) we have the estimate of the norm $x(t; t_0, x_0)$ (further denoted as $x(t)$)

$$\|x(t)\| \le \varphi(t)\psi(t_0)\|x_0\| + \int_{t_0}^{t} \varphi(t)\psi(\sigma(s))\alpha(s)\|x(s)\|^m \Delta s.$$

Having designated $u(t) = \frac{\|x(t)\|}{\varphi(t)}$, $a(t) = \psi(t_0)\|x_0\|$, we get the inequality

$$u(t) \le a(t) + \int_{t_0}^{t} h(s)u^m(s)\Delta s, \quad t \ge t_0.$$

Since the functions in this inequality satisfy all conditions of Lemma 3.1, we get the estimate

$$u(t) \le a(t)\Big(1 - D(t, t_0, \|x_0\|)\Big)^{1/1-m},$$

which is valid for all t, such that $D(t, t_0, \|x_0\|) < 1$. Lemma 3.2 is proved. □

4 Stability Analysis of Quasilinear System.

In this section sufficient conditions of stability, uniform stability and asymptotic stability of zero solution to dynamic equations of (1) type are established in terms of generalized nonlinear dynamic inequality.

Theorem 4.1 *If for equation* (1) *for all $s \ge t_0$ there exists $K(s)$ such that $\varphi(t) \le K(s)$ for all $t \ge s \ge t_0$ and*

$$\widetilde{D}(t_0, \rho) = \lim_{t\to\infty} D(t, t_0, \rho) < \infty, \tag{11}$$

for all $t_0 \in \mathbb{T}$ and $\rho > 0$, the solution $x = 0$ of equation (1) *is stable.*

Proof. We study properties of the function $D(t, a, \rho)$, defined above. Direct computation gives that the function $D(t, a, \cdot)$ increases on the set $\mathbb{R}_+$, uniformly in t and a. Consequently, the function $\widetilde{D}(a, \cdot)$ from (11) does not decrease on $\mathbb{R}_+$, uniformly in a, and, moreover, $\widetilde{D}(a, 0) = 0$. Then, for some $\lambda \in (0, 1)$ the equation $\widetilde{D}(a, \rho) = \lambda$ possesses the largest solution $\rho = \rho_\lambda(a)$ for all $a \in \mathbb{T}$. We consider λ_1 to be the largest of the mentioned ones.

Then consider the function $G(t, a, \rho) = \rho\Big(1 - D(t, a, \rho)\Big)^{\frac{1}{1-m}}$. We find that

$$\frac{\partial G}{\partial \rho} = \Big(1 - D\Big)^{\frac{m}{m-1}}\Big(1 - D + \frac{\rho}{m-1} \cdot \frac{\partial D}{\partial \rho}\Big) = \Big(1 - D\Big)^{\frac{m}{m-1}}(1 - G_1), \tag{12}$$

where $G_1(t,a,\rho) = D(t,a,\rho) - \frac{\rho}{m-1}\cdot\frac{\partial D(t,a,\rho)}{\partial\rho}$. Having computed the derivative $\frac{\partial G_1}{\partial\rho}$, we make sure that the function $G_1(t,a,\cdot)$ does not decrease on $\mathbb{R}_+$, uniformly in t and a as well.

It can be easily seen that the function $\widetilde{G}_1(a,\rho) = \widetilde{D}(a,\rho) - \frac{\rho}{m-1}\cdot\frac{\partial\widetilde{D}(a,\rho)}{\partial\rho}$ does not decrease in the second argument on the set $\mathbb{R}_+$, uniformly in a, and $\widetilde{G}_1(a,0) = 0$. Then, there exists the largest value ω_1 of the parameter ω from the interval $(0,1]$, such that the equation $\widetilde{G}_1(a,\rho) = \omega$ possesses the largest solution $\rho = \rho_\omega(a)$ for all $a \in \mathbb{T}$.

Also, for the derivative $\frac{\partial\widetilde{G}}{\partial\rho}$ of the function $\widetilde{G}(a,\rho) = \rho\Big(1-\widetilde{D}(a,\rho)\Big)^{\frac{1}{1-m}}$ make sure that an equality similar to (12) takes place

$$\frac{\partial\widetilde{G}}{\partial\rho} = \Big(1-\widetilde{D}\Big)^{\frac{m}{m-1}}\Big(1-\widetilde{D}+\frac{\rho}{m-1}\cdot\frac{\partial\widetilde{D}}{\partial\rho}\Big) = \Big(1-\widetilde{D}\Big)^{\frac{m}{m-1}}(1-\widetilde{G}_1). \tag{13}$$

Proceeding from the above arguments we find that on the set $\rho \in (0,\rho_{\omega_1}(a)]$ the derivative $\frac{\partial\widetilde{G}}{\partial\rho}$ is nonnegative for all $a \in \mathbb{T}$, and hence, the function $\widetilde{G}(a,\cdot)$ is nondecreasing.

Now let us choose some $\varepsilon > 0$ and $t_0 \in \mathbb{T}$. Designate by ξ_1 the largest value of the parameter ξ from the interval $(0,\varepsilon/\psi(t_0)K(t_0))$, such that the equation $\widetilde{G}(a,\rho) = \xi$ possesses the largest solution $\rho = \rho_\xi(a)$, not larger than $\rho_{\omega_1}(a)$ for all $a \in \mathbb{T}$. Set $\delta = \min\{\rho_{\lambda_1}(t_0), \rho_{\xi_1}(t_0)\}$ and show that if $\|x_0\| < \delta$, then $\|x(t,t_0,x_0)\| < \varepsilon$, for all $t \geq t_0$.

By the condition of the theorem for all $t \geq t_0$ from the scale we have

$$D(t,t_0,\|x_0\|) \leq \lim_{t\to\infty} D(t,t_0,\|x_0\|) = \widetilde{D}(t_0,\|x_0\|). \tag{14}$$

Since it is proved that the function $\widetilde{D}(a,\cdot)$ does not decrease on $\mathbb{R}_+$, inequalities (14) can be continued as

$$D(t,t_0,\|x_0\|) \leq \widetilde{D}(t_0,\delta) \leq \widetilde{D}(t_0,\rho_{\lambda_1}(t_0)) = \lambda_1 < 1. \tag{15}$$

From (15) we conclude that by Lemma 3.2 for all $t \geq t_0$ from the scale estimate (9) is valid. Using (9), the established properties of functions D, $\widetilde{D}$, $\widetilde{G}$ and the method of choosing of δ, we arrive at the estimates

$$\begin{gathered}
\|x(t;t_0,x_0)\| \leq \varphi(t)\psi(t_0)\|x_0\|\Big[1-D(t,t_0,\|x_0\|)\Big]^{1/1-m} \leq \\
\leq K(t_0)\psi(t_0)\|x_0\|\Big[1-D(t,t_0,\|x_0\|)\Big]^{1/1-m} \leq \\
\leq K(t_0)\psi(t_0)\|x_0\|\Big[1-\widetilde{D}(t_0,\|x_0\|)\Big]^{1/1-m} = K(t_0)\psi(t_0)\widetilde{G}(t_0,\|x_0\|) \leq \\
\leq K(t_0)\psi(t_0)\widetilde{G}(t_0,\delta) \leq K(t_0)\psi(t_0)\widetilde{G}(t_0,\rho_{\xi_1}(t_0)) = K(t_0)\psi(t_0)\xi_1 \leq \\
\leq K(t_0)\psi(t_0)\xi < K(t_0)\psi(t_0)\frac{\varepsilon}{K(t_0)\psi(t_0)} = \varepsilon,
\end{gathered}$$

which are valid for all $t \geq t_0$ from the scale. This completes the proof. □

Theorem 4.2 *If for equation* (1) *there exist a positive constant K_1 and a continuous nondecreasing function $K_2(\rho)$ such that $\varphi(t)\psi(s) \leq K_1$ for all $t \geq s \geq t_0$ and*

$$\widetilde{D}(s,\rho) = \lim_{t\to\infty} D(t,s,\rho) \leq K_2(\rho),$$

for all $s \geq t_0$ $\rho > 0$, then solution $x = 0$ of equation (1) *is uniformly stable.*

Proof. Let $\varepsilon > 0$, $t_0 \in \mathbb{T}$. Due to the properties of function $K_2(\rho)$ there exists a value of the parameter η from the interval $(0, \frac{1}{2}]$ such that the equation $K_2(\rho) = \eta$ possesses the largest solution $\rho(\eta)$. Designate by η_1 the largest of the mentioned values of parameter η. We set $\delta = \min\{\rho(\eta_1), \varepsilon(2^{\frac{1}{m-1}} k_1)^{-1}\}$ and show that if $\|x_0\| < \delta$, then $\|x(t; t_0, x_0)\| < \varepsilon$, for all $t \geq t_0$.

By the condition of the theorem, for all $t \geq t_0$ from the time scale we have

$$D(t, t_0, \|x_0\|) \leq \lim_{t\to\infty} D(t, t_0, \|x_0\|) \leq K_2(\|x_0\|) < k_2(\delta) << K_2(\rho(\eta_1)) = \eta_1 \leq \frac{1}{2} < 1. \tag{16}$$

From (16) we conclude that estimate (9) is fulfilled for all $t \geq t_0$ from the time scale. Therefore,

$$\|x(t; t_0, x_0)\| \leq \varphi(t)\psi(t_0)\|x_0\| \Big[1 - D(t, t_0, \|x_0\|)\Big]^{1/1-m} \leq$$
$$\leq K_1\|x_0\| \Big[1 - D(t, t_0, \|x_0\|)\Big]^{1/1-m} \leq K_1\|x_0\| \Big[1 - \widetilde{D}(t_0, \|x_0\|)\Big]^{1/1-m} \leq$$
$$\leq K_1\|x_0\| \Big(1 - K_2(\|x_0\|)\Big)^{1/1-m} < K_1 \delta 2^{\frac{1}{m-1}} \leq \varepsilon,$$

for all $t \geq t_0$ from the scale. The theorem is proved. $\square$

Theorem 4.3 *If for equation* (1) *the conditions*

$$\widetilde{D}(s, \rho) = \lim_{t\to\infty} D(t, s, \rho) < \infty,$$

are satisfied for all $s \geq t_0$ *and* $\rho > 0$, *and* $\lim_{t\to\infty} \varphi(t) = 0$, *then the solution* $x = 0$ *of equation* (1) *is asymptotically stable. Besides, the domain of attraction of solution* $x = 0$ *contains a sphere* $B(0, \rho_\lambda(t_0))$, *where* $\rho_\lambda(t_0)$ *is the largest solution of the equation* $\widetilde{D}(t_0, \rho) = \lambda$, $\lambda \in (0, 1)$.

Proof. Let $\varepsilon > 0$, $t_0 \in \mathbb{T}$. Since the value of function $\varphi(t)$ vanishes for $t \to \infty$, the function is bounded. Then, by Theorem 4.2 the solution $x = 0$ of equation (1) is stable. Let us show that there exists a $\delta_0 > 0$ such that if $\|x_0\| < \delta_0$, then the limit equality $\lim_{t\to+\infty} \|x(t; t_0, x_0)\| = 0$ holds true. It can be easily verified that the function $D(t, s, \rho)$ increases in the last variable on $\mathbb{R}_+$. Therefore, the function $\widetilde{D}(s, \rho)$ does not decrease in ρ on $\mathbb{R}_+$. Then, there exists a $\lambda \in (0, 1)$, for which the equation $\widetilde{D}(a, \rho) = \lambda$ possesses the largest solution designated by $\rho_\lambda(a)$. We set $\delta_0 = \rho_\lambda(t_0)$, then for all $t \geq t_0$ and $\|x_0\| < \delta_0$ the following inequalities hold true

$$D(t, t_0, \|x_0\|) \leq \widetilde{D}(t_0, \|x_0\|) \leq \widetilde{D}(t_0, \delta_0) = \lambda < 1.$$

By Lemma 3.2 for solution $x(t; t_0, x_0)$ of equation (1) estimate (9) is valid. Using the above inequality and inequality (9) we get

$$\|x(t; t_0, x_0)\| \leq \varphi(t)\psi(t_0)\|x_0\| \Big[1 - D(t, t_0, \|x_0\|)\Big]^{1/1-m} \leq$$
$$\leq \varphi(t)\psi(t_0)\|x_0\| \Big[1 - \widetilde{D}(t_0, \|x_0\|)\Big]^{1/1-m} <$$
$$< \varphi(t)\psi(t_0)\delta_0 \Big[1 - \widetilde{D}(t_0, \delta_0)\Big]^{1/1-m} \to 0,$$

whenever $t \to \infty$.

Thus, the neighborhood of the point $x = 0$ with the radius $\rho_\lambda(t_0)$ is contained in the domain of attraction of the solution $x = 0$ of equation (1). □

5 Applications

Consider system of dynamic equations (1) on time scale, satisfying hypotheses (H_1) — (H_3) for any real $m > 1$, for the following values of functions $\varphi(t)$, $\psi(t)$, $\alpha(t)$:

$$\varphi(t) = Me_\lambda(t,0), \quad \psi(t) = e_\lambda(0,t), \quad \alpha(t) = Ae_\gamma(t,0). \tag{17}$$

Here A and M are positive constants and the real numbers λ and γ satisfy positive regressivity conditions [3]

$$1 + \mu(t)\lambda > 0, \quad 1 + \mu(t)\gamma > 0, \quad \text{for all} \quad t \in \mathbb{T}. \tag{18}$$

Assume that the scale $\mathbb{T}$ has a bounded graininess function $\mu(t)$ (i.e. there exists $\mu^* \geq 0$ v $\mu(t) \leq \mu^*$ for all $t \in \mathbb{T}$) and for arbitrary integrable function $f(t)$ and any scale segment $\langle a, b\rangle$ the representation

$$\int_a^b f(t)\Delta t = \sum_i \int_{a_i}^{b_i} f(t)dt + \sum_k f(t_k)\mu(t_k), \tag{19}$$

is valid, where the segments $\langle a_i, b_i\rangle$ and the points t_k belong to $\langle a, b\rangle$.

Applying Theorem 4.3 one can easily establish additional conditions, which the constants λ and γ must satisfy to, so that the solution $x = 0$ of equation (1) be asymptotically stable under assumptions (17) and (18). Such result is contained in Corollary 5.1. Recall that for any function $F = F(\mu(t))$ under consideration it is assumed that $F(0) = \lim\limits_{\mu\to 0} F(\mu)$ if the value $F(0)$ is not defined.

Corollary 5.1 *Let equation* (1) *satisfy assumptions (H_1) — (H_3), and the functions $\varphi(t)$, $\psi(t)$ and $\alpha(t)$ from these assumptions, in their turn, satisfy assumptions* (17) *and* (18). *Then, if there exist positive constants $\delta_1, \delta_2, \delta_3$ such that for all $t \in \mathbb{T}$ the following conditions are fulfilled:*

1) $\ln(1 + \mu(t)\lambda)^{\frac{1}{\mu(t)}} \leq -\delta_1$;

2) $\ln\Big((1 + \mu(t)\lambda)^{m-1}(1 + \mu(t)\gamma)\Big)^{\frac{1}{\mu(t)}} \leq -\delta_2$;

3) $1 + \mu(t)\lambda \geq \delta_3$,

then the solution $x = 0$ of equation (1) *is asymptotically stable.*

Proof. Since by the definition of an exponential function $\varphi(t) = Me_\lambda(t,0) = Mexp\Big\{\int\limits_0^t \frac{Log(1+\mu(s)\lambda)}{\mu(s)}\Delta s\Big\}$, where Log is the main logarithmic function (if $\mu(s) = 0$, then the integrand equals to λ by definition), due to (18) we have $\varphi(t) = Me_\lambda(t,0) = Mexp\Big\{\int\limits_0^t \frac{\ln(1+\mu(s)\lambda)}{\mu(s)}\Delta s\Big\}$. According to condition 1) of Corollary 5.1 we find that

$\varphi(t) \leq Me^{-t\delta_1} \to 0$, for $t \to \infty$. Consider further the integrand $R(t,a,\rho) = \frac{1}{\mu(t)}\Big(1 - \frac{1}{(1+\mu(t)h(t)\psi^{m-1}(a)\rho^{m-1})^{m-1}}\Big)$ of the integral in the expression for $D(t,a,\rho)$. If the inequality $\mu(t)h(t)\psi^{m-1}(a)\rho^{m-1} < 1$ is fulfilled, then the function $R(t,a,\rho)$ can be presented in the form of a sum of the convergent series

$$\begin{gathered} R(t,a,\rho) = \frac{1}{\mu(t)}\Big(1 - \sum_{k=0}^{\infty} \frac{(1-m)(-m)\cdot\ldots\cdot(2-m-k)}{k!}\times \\ \times\Big(\mu(t)h(t)\psi^{m-1}(a)\rho^{m-1}\Big)^k\Big) = -\sum_{k=1}^{\infty} \frac{(1-m)(-m)\cdot\ldots\cdot(2-m-k)}{k!}\times \\ \times\mu^{k-1}(t)(h(t)\psi^{m-1}(a)\rho^{m-1})^k = \sum_{k=1}^{\infty} r_k(t). \end{gathered} \tag{20}$$

We shall establish conditions under which the series in (20) converges uniformly in t. To this end we find a convergent numerical series majorizing the series in (20). In view of assumptions (17) and (18) and the properties of exponential functions we find that

$$\begin{gathered} |\mu^{k-1}(t)h^k(t)| = |\mu^{k-1}(t)\psi^k(\sigma(t))\varphi^{km}(t)\alpha^k(t)| = \\ = A^k M^{km}\mu^{k-1}(t)e^k_\lambda(0,\sigma(t))e^{km}_\lambda(t,0)e^k_\gamma(t,0) = A^k M^{km}\mu^{k-1}(t)\times \\ \times\frac{e^{km}_\lambda(t,0)e^k_\gamma(t,0)}{e^k_\lambda(t,0)e^k_\lambda(\sigma(t),t)} = A^k M^{km}\frac{\mu^{k-1}(t)e_\beta(t,0)}{(1+\mu(t)\lambda)^k}, \end{gathered}$$

where $\beta(t) = \frac{1}{\mu(t)}\Big((1+\mu(t)\lambda)^{k(m-1)}(1+\mu(t)\gamma)^k - 1\Big)$. We estimate the expression obtained for $|\mu^{k-1}(t)h^k(t)|$ in view of conditions 1) – 2) of Corollary 5.1:

$$\begin{gathered} |\mu^{k-1}(t)h^k(t)| \leq A^k M^{km}\frac{\mu^{k-1}(t)}{(1+\mu(t)\lambda)^k}\times \\ \times exp\Big\{\int_0^t \frac{\ln(1+\mu(s)\lambda)^{k(m-1)}(1+\mu(s)\gamma)^k}{\mu(s)}\Delta s\Big\} \leq \\ \leq A^k M^{km}\frac{(\mu^*)^{k-1}}{\delta_3^k} exp\Big\{\int_0^t -k\delta_2\Delta s\Big\} = \frac{A^k M^{km}(\mu^*)^{k-1}}{\delta_3^k}e^{-kt\delta_2}, \end{gathered}$$

for all $t \in \mathbb{T}$. The obtained estimate implies that when choosing the values of the parameter ρ from sufficiently small neighborhood of zero, the series in (20) is uniformly convergent in t, therefore, by the theorem from [11] the series for $R(t,a,\rho)$ allows the term-by-term integration. As a result, we have

$$D(t,a,\rho) = \int_a^t R(s,a,\rho)\Delta s = \int_a^t \sum_{k=1}^{\infty} r_k(s)\Delta s = \sum_{k=1}^{\infty}\int_a^t r_k(s)\Delta s.$$

$$\Big|\int\limits_a^t r_k(s)\Delta s\Big| \leq \frac{1}{\delta_3^k k!}A^k M^{km}|(1-m)(-m)\cdot\ldots\cdot(2-m-k)|\times$$

$$\times(\psi^{m-1}(a)\rho^{m-1})^k\int\limits_a^t exp\Big\{k\int\limits_0^s\frac{\ln(1+\mu(\tau)\lambda)^{k(m-1)}(1+\mu(\tau)\gamma)^k}{\mu(s)}\Delta\tau\Big\}\Delta s\leq$$

$$\leq\widetilde{r}_k\int\limits_a^t\mu^{k-1}(s)e^{-ks\delta_2}\Delta s.$$

The integral $I_k=\int\limits_a^t\mu^{k-1}(s)e^{-ks\delta_2}\Delta s$ is bounded with respect to t. Really, by virtue of (19)

$$I_k=\sum_i\int\limits_{a_i}^{b_i}\mu^{k-1}(s)e^{-ks\delta_2}ds+\sum_j\mu^{k-1}(t_j)e^{-kt_j\delta_2}\mu(t_j),$$

where $(a_i,b_i)\subset(a,t)$, $t_j\in(a,t)$. Further,

$$I_k=\sum_j\mu^{k-1}(t_j)e^{-kt_j\delta_2}\mu(t_j)\leq(\mu^*)^{k-1}\sum_j e^{-kt_j\delta_2}\mu(t_j)=$$

$$=(\mu^*)^{k-1}e^{k\mu^*\delta_2}\sum_j e^{-k\delta_2(t_j+\mu^*)}\mu(t_j)\leq(\mu^*)^{k-1}e^{k\mu^*\delta_2}\sum_j e^{-k\delta_2(t_j+\mu(t_j))}\mu(t_j)=$$

$$=(\mu^*)^{k-1}e^{k\mu^*\delta_2}\sum_j e^{-k\delta_2\sigma(t_j)}\mu(t_j)\leq(\mu^*)^{k-1}e^{k\mu^*\delta_2}\int\limits_0^t e^{-ks\delta_2}ds=$$

$$=\frac{(\mu^*)^{k-1}e^{k\mu^*\delta_2}}{k\delta_2}\Big(e^{-ka\delta_2}-e^{-kt\delta_2}\Big).$$

It can be easily seen that for sufficiently small ρ the series for $D(t,a,\rho)$ is uniformly convergent in t and it can be estimated by a function of a and ρ. Thus, when conditions of Corollary 5.1 are fulfilled, all hypotheses of Theorem 4.3 are fulfilled too, and therefore, the solution $x=0$ of equation (1) is asymptotically stable. □

Note, that the conditions of asymptotic stability obtained in Corollary 5.1 for zero solution of dynamic equation of certain type cover some known results for $\mathbb{T}=\mathbb{R}$.

6 Conclusion

The results of this paper together with those of paper [4] represent a solution to stability problem of quasilinear equations on time scale via the method of dynamic integral inequalities. In the case when the fundamental matrix of solutions of linear approximation of system (1) can be determined in the explicit form the established sufficient conditions of various types of stability may be of interest for applications. Some results of the development of the method of integral inequalities for dynamic equations of (1) type were the subject of paper [1].

References

[1] Babenko, S.V. *Motion stability of continuous-discrete large-scale mechanical systems under structure perturbations.* PhD thesis, Institute of Mechanics NAS Of Ukraine, Kiev, 2011. (Manuscript) [Russian]

[2] Beesack, P.R. Gronwall Inequalities. *Cavleton Math. Lecture Notes.* (11) (1975), 123 p.

[3] Bohner, M. and Peterson, A. *Dynamic Equations on Time Scales. An Introduction with Applications.* Birkhaser, Boston–Basel–Berlin, 2001.

[4] Bohner, M. and Martynyuk, A.A. Elements of stability theory by A.M.Lyapunov for dynamic equations on time scales. *Nonlinear Dynamics and Systems Theory* **7** (3) (2007) 225–251.

[5] Demidovich, B.P. *Lectures on Mathematical Stability Theory.* Moscow: Nauka, 1967. [Russian]

[6] Hilger, S. Analysis on measure chains: a unified approach to continuous and discrete calculus. *Res. in Mathematics* (18) (1990) 18–56.

[7] Martynyuk, A.A. *Stability Theory of Solutions of Dynamic Equations on Time Scales.* Kiev: Phoenix, 2012. [Russian]

[8] Martynyuk, A.A. and Gutowski, R. *Integral Inequalities and Stability of Motion.* Kiev: Naukova Dumka, 1979. [Russian]

[9] Martynyuk, A.A., Lakshmikantham, V. and Leela, S. *Stability of Motion: Method of Integral Inequalities.* Kiev: Naukova Dumka, 1989. [Russian]

[10] Martynyuk, A.A. and Slyn'ko, V.I. On nonlinear inequalities on time scales. *Diff. Equations.* **44** (10) (2008) 1420–1426. [Russian]

[11] Mozyrska, D. and Pawluszvicz, E. Functional series on time scales. *International Journal of Mathematics and Statistics.* **2** (S08) (2008) 94-105.

[12] Oziraner, A.S. On the stability of motion by first approximation. *Prikl. Math. and Mekh.* **41** (3) (1977) 413–421. [Russian]

[13] Stachurska, B. On a nonlinear integral inequality. *Zeszyty Nauk. Uniw. Jagiellon. Prace Mat.* (15) (1971) 151–157.

[14] Walter, W. *Differential and Integral Inequalities.* Berlin–New York: Springer, 1970.

Nonlinear Dynamics and Systems Theory, **13** (1) (2013) 25–46

Asymptotic Robot Manipulator Generalized Inverse Dynamics

A.H. Bajodah *

Aeronautical Engineering Department, P.O. Box 80204
King Abdulaziz University
Jeddah 21589, Saudi Arabia

Received: January 16, 2012; Revised: January 19, 2013

Abstract: The generalized inverse dynamics methodology is improved to yield asymptotic tracking control of robot manipulator's generalized coordinate trajectories. A scalar kinematic norm measure function of generalized coordinates deviations from their desired trajectories is defined, and a servo-constraint on robot kinematics is prescribed by zeroing the deviation function. A stable linear second-order differential equation in the deviation function is evaluated along trajectory solutions of manipulator's state space model equations, resulting in an algebraic relation that is linear in the control vector. The control law is designed by generalized inversion of the controls coefficient in the algebraic relation using a modified version of the Greville formula. The generalized inverse in the particular part of the modified formula is scaled by a dynamic factor that uniformly decays as steady state response approaches. This yields a uniform convergence of the particular part to its projection on the range space of controls coefficient's generalized inverse, and in asymptotically stable generalized coordinates trajectory tracking. Null-control vector in the auxiliary part of the formula is taken to be linear in manipulator's generalized velocities, and is constructed by means of a positive semidefinite control Lyapunov function that involves controls coefficient's nullprojector, providing asymptotic internal manipulator stability over a predetermined domain of attraction.

Keywords: *generalized inversion control; generalized inverse dynamics; asymptotic tracking; semidefinite Lyapunov function; null-control vector.*

Mathematics Subject Classification (2010): 93D15, 93D20, 93D30.

* Corresponding author: mailto:abajodah@kau.edu.sa

1 Introduction

Generalized inverse dynamics (GID) [1, 2] is an evolving control design paradigm that aims to benefit from non-square inversion in solving the inverse dynamics control problem. In fulfilling that purpose, GID utilizes the nullspace parametrization feature of the generalized inversion-based Greville formula [3, 4]. Nullspace parametrization is the means by which the Greville formula captures solution nonuniqueness of linear algebraic system equations, and it forms the backbone of GID control.

The GID control design methodologies are based on the fact that a prescribed dynamics on a controllable dynamical system can be enforced by infinite number of strategies. Accordingly, a unique robot manipulator's inner loop design in a conventional inverse dynamics solution is quite restrictive. By removing that restriction from the inverse dynamics philosophy, the GID control design reveals the inherent redundancy in the control process [5].

A GID robot control design procedure begins by a coordinate transformation that reduces the size of joint space generalized coordinates error vector to a single dimension. The scalar variable in the transformed coordinate system is named the kinematic deviation function, and it is taken to be the squared Euclidean norm of the joint space error vector. Nullifying the kinematic deviation function is equivalent to bringing manipulator's generalized coordinates to their desired values.

The methodology proceeds by forming a stable second-order time-invariant linear differential equation in the kinematic deviation function. The differential equation is a servo-constraint dynamics that is to be realized by manipulator's control system. Convergence of the differential equation's solution to its steady state zero value implies satisfying the control objective. The differential equation is transformed to an algebraic equation by evaluating the first two time derivatives of the kinematic deviation function along trajectory solutions of the manipulator's state space mathematical model.

The resulting algebraic equation is linear in the control vector. The Greville formula can therefore be utilized to solve the equation for the control variables required to realize the desired servo-constraint dynamics. The solution involves the Moore-Penrose generalized inverse (MPGI) [6, 7] of the row vector formed by the coefficients of control variables in the linear algebraic equation, abbreviated as the controls coefficient [8]. The Greville formula solution is composed of particular and auxiliary parts. The particular part maps to the range space of the controls coefficient's transpose, and it works to realize desired servo-constraint dynamics. The auxiliary part maps to the orthogonal complement nullspace of the controls coefficient, and it works to provide internal manipulator stability [5].

Nevertheless, the Greville formula suffers from the undesirable characteristic of MPGI singularity [9] that hinders the particular part of the formula. The MPGI singularity occurs whenever the generalized-inverted matrix changes rank, causing divergence of the MPGI elements to infinite values. In the present application, MPGI singularity takes place when steady state response approaches as the controls coefficient converges to the zero vector. A technique of MPGI singularity avoidance is presented in Ref. [5], made by replacing the MPGI in the Greville formula by a damped generalized inverse, resulting in a globally uniformly ultimately bounded robot manipulator's generalized coordinate trajectory tracking.

This paper introduces a modified version of the Greville formula. The MPGI in the particular part of the formula is scaled by a dynamic factor that vanishes as closed loop response approaches steady state. The scaling factor is capable of overcoming the MPGI singularity. Simultaneously, the dynamically scaled generalized inverse (DSGI) uniformly converges to the standard MPGI as the dynamic scaling factor decays, resulting in asymptotic realization of desired servo-constraint dynamics, and in a uniformly asymptotically stable tracking of desired robot generalized coordinates.

The auxiliary part of the Greville formula is affine in a free null-vector that is projected onto nullspace of the controls coefficient. Therefore, the null-vector design does not affect realization of the linear algebraic relation, but it affects the manner in which the relation is realized, i.e., it affects how individual state variables evolve in time. In particular, the null-vector affects closed loop internal manipulator's stability. The null-vector in the present context is named the null-control vector, and its design is a crucial step of the GID methodology

Moreover, the design freedom of the null-control vector can be utilized to achieve further requirements, e.g., perturbed feedback linearization of internal closed loop dynamics [5]. The null-control vector is constructed in this work to be linear in manipulator's joint velocity variables. The state dependent proportionality gain matrix is designed via novel positive semidefinite control Lyapunov function and controls coefficient nullprojected Lyapunov equations, resulting in locally asymptotically stable generalized coordinate trajectory tracking. The analysis provides an explicit estimate of the corresponding domain of attraction.

The GID methodology unifies the treatments of inverse kinematics [10] and inverse dynamics by transforming the inverse dynamics problem to an underdetermined problem and utilizing generalized inversion to solve it, overcoming the restrictions of dimensionality and rank that limit the applications of regular inversion.

The contribution of this article is twofold. First, a new GID design element is introduced to robot control applications, namely the dynamically scaled generalized inverse, improving the recently developed GID methodology to yield asymptotic tracking control. Second, a new GID control design methodology is presented. The null-control vector is designed by means of a novel type of control Lyapunov functions and Lyapunov equations.

2 Mathematical Model for Robot Manipulator

The mathematical model of an n degrees of freedom robot manipulator is given by the following system of differential equations

$$M(q,t)\ddot{q} + C(q,\dot{q},t) + G(q,t) = \mathcal{F}, \quad q(t_0) = q_0,\ \dot{q}(t_0) = \dot{q}_0, \tag{1}$$

where $q, \dot{q}, \ddot{q} \in \mathbb{R}^n$ are vectors of manipulator generalized coordinates, velocities, and accelerations, respectively. The vector valued function $C(q,\dot{q},t) : \mathbb{R}^n \times \mathbb{R}^n \times [t_0,\infty) \to \mathbb{R}^n$ contains centrifugal and coriolis forces, the vector valued function $G(q,t) : \mathbb{R}^n \times [t_0,\infty) \to \mathbb{R}^n$ contains gravitational forces, and $\mathcal{F} \in \mathbb{R}^n$ is the vector of control forces acting on the manipulator. The inertia matrix valued function $M(q,t) : \mathbb{R}^n \times [t_0,\infty) \to \mathbb{R}^{n\times n}$ is assumed to be symmetric positive definite for all $q \in \mathbb{R}^n$. Equation (1) can be put in the following state space system of $2n$ kinematical and dynamical differential equations

$$\dot{q} = u, \quad q(t_0) = q_0, \tag{2}$$

$$\dot{u} = -M^{-1}(q,t)[C(q,u,t) + G(q,t)] + \tau, \quad u(t_0) = u_0, \tag{3}$$

where $\tau \in \mathbb{R}^n$ is given by

$$\tau = M^{-1}(q,t)\mathcal{F}. \tag{4}$$

3 Generalized Coordinate Deviation Norm Measure Dynamics

Let $q_r(t) \in \mathbb{R}^n$ be a prescribed desired robot manipulator generalized coordinates vector such that $q_r(t)$ is twice continuously differentiable in t. The manipulator generalized coordinates error vector from $q_r(t)$ is defined as

$$e_q(q,t) := q - q_r(t). \tag{5}$$

Consequently, a scalar positive definite configuration deviation norm measure function $\phi : \mathbb{R}^n \times [t_0,\infty) \to \mathbb{R}$ is defined to be the squared Euclidean norm of $e_q(q,t)$

$$\phi = \| e_q(q,t) \|^2 = \| q - q_r(t) \|^2 . \tag{6}$$

Therefore, the manipulator is at its desired configuration if and only if the servo-constraint

$$\phi \equiv 0 \tag{7}$$

is realized. The first two time derivatives of ϕ along the manipulator trajectories given by the solution of (2) and (3) are

$$\dot{\phi} = 2e_q^T(q,t)\,[u - \dot{q}_r(t)] \tag{8}$$

and

$$\ddot{\phi} = 2[u - \dot{q}_r(t)]^T[u - \dot{q}_r(t)] + 2e^T(q,t)\Big[\tau - M^{-1}(q,t)[C(q,u,t) + G(q,t)] - \ddot{q}_r(t)\Big]. \tag{9}$$

A desired stable second-order dynamics of ϕ is specified to be of the form

$$\ddot{\phi} + a_1\dot{\phi} + a_2\phi = 0, \quad a_1, a_2 > 0. \tag{10}$$

With ϕ, $\dot{\phi}$, and $\ddot{\phi}$ given by (6), (8), and (9), it is possible to write (10) in the pointwise-linear form

$$\mathcal{A}(q,t)\tau = \mathcal{B}(q,u,t), \tag{11}$$

where the row vector-valued controls coefficient function $\mathcal{A}(q,t) : \mathbb{R}^n \times [t_0,\infty) \to \mathbb{R}^{1\times n}$ is given by

$$\mathcal{A}(q,t) = 2e_q^T(q,t) \tag{12}$$

and the scalar-valued controls load function $\mathcal{B}(q,u,t) : \mathbb{R}^n \times \mathbb{R}^n \times [t_0,\infty) \to \mathbb{R}$ is given by

$$\begin{aligned}\mathcal{B}(q,u,t) = {} & -2[u - \dot{q}_r(t)]^T[u - \dot{q}_r(t)] \\ & + 2e_q^T(q,t)\left[M^{-1}(q,t)[C(q,u,t) + G(q,t)] + \ddot{q}_r(t)\right] \\ & - 2a_1 e_q^T(q,t)[u - \dot{q}_r(t)] - a_2 \| e_q(q,t) \|^2 .\end{aligned} \tag{13}$$

4 Generalized Inverse Dynamics

The infinite set of all manipulator control laws τ realizing the servo-constraint given by (7) via the linear dynamics given by (10) is parameterizable by the Greville formula [3] as [1]

$$\tau(q,u,y,t) = \mathcal{A}^{+}(q,t)\mathcal{B}(q,u,t) + \mathcal{P}(q,t)y, \tag{14}$$

where $\mathcal{A}^{+}(q,t) : \mathbb{R}^n \times [0,\infty) \to \mathbb{R}^n$ is the controls coefficient Moore-Penrose generalized inverse (CCGI) given by

$$\mathcal{A}^{+}(q,t) = \begin{cases} \frac{\mathcal{A}^T(q,t)}{\|\mathcal{A}(q,t)\|^2}, & \mathcal{A}(q,t) \neq \mathbf{0}_{1\times n} \\ \\ \mathbf{0}_{n\times 1}, & \mathcal{A}(q,t) = \mathbf{0}_{1\times n} \end{cases} \tag{15}$$

and $\mathcal{P}(q,t) : \mathbb{R}^n \times [0,\infty) \to \mathbb{R}^{n\times n}$ is the corresponding controls coefficient nullprojector (CCNP) given by

$$\mathcal{P}(q,t) = I_{n\times n} - \mathcal{A}^{+}(q,t)\mathcal{A}(q,t) \tag{16}$$

and $y \in \mathbb{R}^n$ is an arbitrary null-control vector.

Substituting the control laws expressions given by (14) in manipulator's equations of motion (3) yields the following parametrization of the infinite set of manipulator closed loop system equations that realize the servo-constraint dynamics given by (10)

$$\dot{q} = u \tag{17}$$

$$\begin{aligned} \dot{u} = & -M^{-1}(q,t)[C(q,u,t) + G(q,t)] \\ & + \mathcal{A}^{+}(q,t)\mathcal{B}(q,u,t) + \mathcal{P}(q,t)y. \end{aligned} \tag{18}$$

Different choices of the null-control vector y in the control laws expression given by (14) yield different solutions to (11), and every solution results in closed loop system trajectory solutions for (17) and (18) that satisfy the linear servo-constraint dynamics given by (10). Nevertheless, designing y is a critical issue, because y substantially affects manipulator's internal dynamics given by (3), and an inadequate design of y can destabilize that dynamics [1].

5 Generalized Inversion Singularity

Satisfying the servo-constraint dynamics given by (10) implies from the definition of ϕ given by (6) and the expression of $\mathcal{A}(q,t)$ given by (12) that

$$\lim_{\phi\to 0} \mathcal{A}(q,t) = \mathbf{0}_{1\times 3}. \tag{19}$$

Since the expression of $\mathcal{A}(q,t)$ is continuous in q and t, the definition of $\mathcal{A}^{+}(q,t)$ given by (15) implies that if the initial manipulator configuration condition is such that $\mathcal{A}(q_0,t_0) \neq \mathbf{0}_{1\times n}$, then [5]

$$\lim_{\mathcal{A}(q,t)\to\mathbf{0}_{1\times n}} \|\mathcal{A}^{+}(q,t)\| = \lim_{\mathcal{A}(q,t)\to\mathbf{0}_{1\times n}} \frac{1}{\|\mathcal{A}^T(q,t)\|} = \infty_{n\times 1} \tag{20}$$

causing the particular part in the expression of the control law $\tau(q,u,y,t)$ given by (14) to go unbounded, and driving the closed loop dynamical subsystem given by (18) unstable.

Instability due to generalized inversion singularity is well-known in MPGI applications. A remedy of the problem in the context of generalized inverse control is made by deactivating the particular part of the Greville formula in the vicinity of singularity, resulting in discontinuous control laws [11]. Another remedy is made by modifying the definition of the MPGI by means of a damping factor, resulting in uniformly ultimately bounded control and a tradeoff between generalized inversion stability and closed loop system performance [5]. The concept of dynamically scaled generalized inversion [12] is used in this paper for the purpose of avoiding instability due to CCGI singularity and to guarantee asymptotic generalized coordinate trajectory tracking.

6 Dynamically Scaled Generalized Inverse

A reference (desired) internal dynamics is defined based on the system equations given by (17) and (18) as

$$\dot{u}_r = -M^{-1}(q,t)[C(q,u_r,t)+G(q,t)]+\mathcal{A}^+(q,t)\mathcal{B}(q,u_r,t)+\mathcal{P}(q,t)y_r,\ q(t_0)=q_0, \quad (21)$$

where $u_r, \dot{u}_r \in \mathbb{R}^n$ are reference (desired) velocity and acceleration vectors, and $y_r \in \mathbb{R}^n$ is a reference null-control vector. The reference internal dynamics is obtained by replacing u and y by u_r and y_r in the dynamical subsystem given by (18), and the reference acceleration vector $\dot{u}_r$ is equal to the acceleration vector $\dot{u}$ for all $t \geq t_0$ if $y = y_r$ for all $t \geq t_0$ and $u_r(t_0) = u(t_0)$.

The dynamically scaled generalized inverse (DSGI) of the controls coefficient $\mathcal{A}(q,t)$ is introduced next.

Definition 6.1 [Dynamically scaled controls coefficient generalized inverse] The DSGI $\mathcal{A}_s^+(q,u,t) : \mathbb{R}^n \times \mathbb{R}^n \times [0,\infty) \to \mathbb{R}^{n\times 1}$ is given by

$$\mathcal{A}_s^+(q,u,t) = \frac{\mathcal{A}^T(q,t)}{\mathcal{A}(q,t)\mathcal{A}^T(q,t) + \|e_u(u,u_r)\|_p^p} \quad (22)$$

for some vector p norm, where

$$e_u(u,u_r) = u - u_r. \quad (23)$$

Properties of the DSGI

The following properties can be verified by direct evaluation of the CCGI $\mathcal{A}^+(q,t)$ given by (15) and its dynamic scaling $\mathcal{A}_s^+(q,u,t)$ given by (22):

1. $\mathcal{A}_s^+(q,u,t)\mathcal{A}(q,t)\mathcal{A}^+(q,t) = \mathcal{A}_s^+(q,u,t)$;
2. $\mathcal{A}^+(q,t)\mathcal{A}(q,t)\mathcal{A}_s^+(q,u,t) = \mathcal{A}_s^+(q,u,t)$;
3. $(\mathcal{A}_s^+(q,u,t)\mathcal{A}(q,t))^T = \mathcal{A}_s^+(q,u,t)\mathcal{A}(q,t)$;
4. $\lim_{\|u-u_r\|_p\to 0} \mathcal{A}_s^+(q,u,t) = \mathcal{A}^+(q,t)$.

7 Perturbed Controls Coefficient Nullprojector

Similar to other projective operators, a fundamental property of the CCNP $\mathcal{P}(q,t)$ is that it is rank deficient. A singular perturbation that disencumber rank deficiency of $\mathcal{P}(q,t)$ is provided by the perturbed controls coefficient nullprojector (PCCN) $\widetilde{\mathcal{P}}(q,\delta,t)$ [8].

Definition 7.1 [Perturbed controls coefficient nullprojector] The perturbed CCNP $\widetilde{\mathcal{P}}(q,\delta,t) : \mathbb{R}^n \times \mathbb{R}^{1\times 1} \times [0,\infty) \to \mathbb{R}^{n\times n}$ is defined as

$$\widetilde{\mathcal{P}}(q,\delta,t) := I_{3\times 3} - h(\delta)\mathcal{A}^+(q,t)\mathcal{A}(q,t), \tag{24}$$

where $h(\delta) : \mathbb{R}^{1\times 1} \to \mathbb{R}^{1\times 1}$ is any continuous function such that

$$h(\delta) = 1, \quad \text{if and only if} \quad \delta = 0.$$

The perturbed CCNP $\widetilde{\mathcal{P}}(q,\delta,t)$ is of full rank for all $\delta \neq 0$. Additionally, the CCNP $\mathcal{P}(q,t)$ commutes with its perturbation $\widetilde{\mathcal{P}}(q,\delta,t)$ and inverted perturbation $\widetilde{\mathcal{P}}^{-1}(q,\delta,t)$ for all $\delta \neq 0$. Furthermore, their matrix multiplication yields the CCNP itself [8], i.e.,

$$\widetilde{\mathcal{P}}(q,\delta,t)\mathcal{P}(q,t) = \mathcal{P}(q,t)\widetilde{\mathcal{P}}(q,\delta,t) = \mathcal{P}(q,t) \tag{25}$$

and

$$\widetilde{\mathcal{P}}^{-1}(q,\delta,t)\mathcal{P}(q,t) = \mathcal{P}(q,t)\widetilde{\mathcal{P}}^{-1}(q,\delta,t) = \mathcal{P}(q,t). \tag{26}$$

8 Asymptotic Generalized Inverse Dynamics

The dynamically scaled generalized inverse control law is constructed by replacing the CCGI $\mathcal{A}^+(q,t)$ in (14) by the DSGI $\mathcal{A}_s^+(q,t)$ given by (22), resulting in

$$\tau_s(q,u,y,t) = \mathcal{A}_s^+(q,u,t)\mathcal{B}(q,u,t) + \mathcal{P}(q,t)y. \tag{27}$$

The corresponding closed loop system equations of (2) and (3) become

$$\begin{aligned} \dot{q} &= u & (28)\\ \dot{u} &= -M^{-1}(q,t)[C(q,u,t) + G(q,t)] \\ &\quad + \mathcal{A}_s^+(q,u,t)\mathcal{B}(q,u,t) + \mathcal{P}(q,t)y. & (29) \end{aligned}$$

Null-Control Vector Design

This section presents a design of the null-control vector to guarantee asymptotic tracking of desired robot manipulator generalized coordinate trajectories while maintaining asymptotic stability of the closed loop system over a prescribed domain of the joint space.

Proposition 8.1 *If the null-control vector y in the control law expression given by (27) is chosen such that the angular velocity vector u of the closed loop system given by (28) and (29) satisfies*

$$\|e_u(u,u_r)\| < \infty \;\; \forall\, t \geq t_0, \tag{30}$$

then the resulting closed loop attitude trajectory error vector $e_q(q,t)$ remains bounded

$$\|e_q(q,t)\| < \infty \;\; \forall\, t \geq t_0, \tag{31}$$

and the controls coefficient $\mathcal{A}(q,t)$ also remains bounded

$$\|\mathcal{A}(q,t)\| < \infty \;\; \forall\, t \geq t_0. \tag{32}$$

Proof. It is evident from the expression of the controls coefficient $\mathcal{A}(q,t)$ given by (12) that $\mathcal{A}(q,t)$ is bounded if and only if $e_q(q,t)$ is bounded. Therefore, assuming on the contrary that there exists a matrix gain K that causes the closed loop angular velocity vector u to satisfy (30) such that

$$\lim_{t\to\infty} \|e_q(q,t)\| = \infty, \tag{33}$$

then it follows that

$$\lim_{t\to\infty} \|\mathcal{A}(q,t)\| = \infty \tag{34}$$

which implies from (22) and (30) that

$$\lim_{t\to\infty} \mathcal{A}_s^+(q,u,t) = \mathcal{A}^+(q,t). \tag{35}$$

It accordingly follows from the expression of $\tau_s(q,u,y,t)$ given by (27) that

$$\lim_{t\to\infty} \tau_s(q,u,y,t) = \tau(q,u,y,t), \tag{36}$$

where $\tau(q,u,y,t)$ is given by (14), causing the closed loop system trajectories to asymptotically satisfy the stable servo-constraint dynamics given by (10), and resulting in

$$\lim_{t\to\infty} \phi = 0 \tag{37}$$

which contradicts (33). Therefore, the control law $\tau_s(q,u,y,t)$ given by (27) must yield bounded elements of $e_q(q,t)$ and bounded elements of $\mathcal{A}(q,t)$. Let the null-control vector y be chosen as

$$y = Ku, \tag{38}$$

where $K \in \mathbb{R}^{n\times n}$ is a matrix gain that is to be determined. Hence, a control law that realizes the servo-constraint given by (7) via the dynamics given by (10) is obtained by substituting this choice of y in (29), resulting in the closed loop dynamical subsystem

$$\dot{u} = -M^{-1}(q,t)[C(q,u,t) + G(q,t)] + \mathcal{A}_s^+(q,u,t)\mathcal{B}(q,u,t) + \mathcal{P}(q,t)Ku. \tag{39}$$

Also, let the reference null-control vector be defined as

$$y_r = Ku_r. \tag{40}$$

Then the reference internal dynamics given by (21) becomes

$$\dot{u}_r = -M^{-1}(q,t)[C(q,u_r,t) + G(q,t)] + \mathcal{A}^+(q,t)\mathcal{B}(q,u_r,t) + \mathcal{P}(q,t)Ku_r, \;\; q(t_0) = q_0. \tag{41}$$

The derivative of the generalized velocity error vector e_u is

$$\dot{e}_u = \dot{u} - \dot{u}_r \tag{42}$$

and therefore a generalized velocity error dynamics is obtained by subtracting (41) from (39), resulting in

$$\dot{e}_u = -M^{-1}(q,t)C(q,u,t) - \left[-M^{-1}(q,t)C(q,u_r,t)\right] + \mathcal{A}_s^+(q,u,t)\mathcal{B}(q,u,t) - \mathcal{A}^+(q,t)\mathcal{B}(q,u_r,t) + \mathcal{P}(q,t)Ke_u. \quad (43)$$

Asymptotic stability of the above written error dynamics is analyzed by considering the following positive-semidefinite Lyapunov function candidate

$$V(q,e_u,t) = e_u^T\mathcal{P}(q,t)e_u. \quad (44)$$

A gain matrix K that renders $\dot{V}(q,u,e_u,t)$ negative-semidefinite over a domain $\mathcal{D} \subseteq \mathbb{R}^n \times \mathbb{R}^n \times [t_0,\infty)$ guarantees Lyapunov stability of $e_u = \mathbf{0}_{n\times 1}$ over $\mathcal{D}$ if it asymptotically stabilizes $e_u = \mathbf{0}_{n\times 1}$ over the invariant set $\mathcal{D}_{V=0} \subset \mathcal{D}$ on which $V(q,e_u,t) = 0$. Moreover, the same gain matrix asymptotically stabilizes $e_u = \mathbf{0}_{n\times 1}$ over $\mathcal{D}$ if and only if it asymptotically stabilizes $e_u = \mathbf{0}_{n\times 1}$ over the largest invariant set $\mathcal{D}_{\dot{V}=0} \subset \mathcal{D}$ on which $\dot{V}(q,u,e_u,t) = 0$ [13].

Proposition 8.2 *Let $K = K(q,u,t)$ be a full-rank normal matrix gain, i.e., $KK^T = K^TK$ for all $t \geq 0$. Then the equilibrium point $e_u = \mathbf{0}_{n\times 1}$ of the closed loop error dynamics given by (43) is asymptotically stable over the invariant set $\mathcal{D}_{V=0}$.*

Proof. Since the matrix $\mathcal{P}(q,t)$ is idempotent, the function $V(q,e_u,t)$ can be rewritten as

$$V(q,e_u,t) = e_u^T\mathcal{P}(q,t)e_u = e_u^T\mathcal{P}(q,t)\mathcal{P}(q,t)e_u \quad (45)$$

which implies that

$$V(q,e_u,t) = 0 \Leftrightarrow \mathcal{P}(q,t)e_u = \mathbf{0}_{n\times 1}. \quad (46)$$

Therefore,

$$V(q,e_u,t) = 0 \Leftrightarrow e_u \in \mathcal{N}(\mathcal{P}(q,t)), \quad (47)$$

where $\mathcal{N}(\cdot)$ refers to matrix nullspace. Since the matrix $K(q,u,t)$ is normal and of full-rank, it preserves matrix range space and nullspace under multiplication. Accordingly,

$$\mathcal{N}(\mathcal{P}(q,t)) = \mathcal{N}(\mathcal{P}(q,t)K(q,u,t)) \quad (48)$$

which implies from (46) that

$$V(q,e_u,t) = 0 \Leftrightarrow \mathcal{P}(q,t)K(q,u,t)e_u = \mathbf{0}_{n\times 1}. \quad (49)$$

Therefore, the last term in the closed loop error dynamics given by (43) is the zero vector, and the closed loop error dynamics becomes

$$\dot{e}_u = -M^{-1}(q,t)C(q,u,t) - \left[-M^{-1}(q,t)C(q,u_r,t)\right] + \mathcal{A}_s^+(q,u,t)\mathcal{B}(q,u,t) - \mathcal{A}^+(q,t)\mathcal{B}(q,u_r(t),t). \quad (50)$$

On the other hand, since [14]

$$\mathcal{N}(\mathcal{P}(q,t)) = \mathcal{R}(\mathcal{A}^T(q,t)), \quad (51)$$

it follows from (47) that

$$V(q,e_u,t) = 0 \Leftrightarrow e_u \in \mathcal{R}(\mathcal{A}^T(q,t)). \quad (52)$$

Accordingly, $V(q,e_u,t)=0$ if and only if there exists a continuously bounded scalar function $a(t),\ t\geq 0$ such that

$$e_u = a(t)\mathcal{A}^T(q,t), \ \ a(t)\neq 0. \tag{53}$$

Therefore, assuming that e_u goes unbounded, then $\mathcal{A}^T(q,t)$ must also go unbounded, both expressions of $\mathcal{A}^+(q,t)$ and $\mathcal{A}_s^+(q,u,t)$ given by (15) and (22) must go to zero, and the closed loop error dynamics given by (50) approaches the Lyapunov-stable uncontrolled dynamics

$$\begin{aligned}\dot{e}_u &= -M^{-1}(q,t)C(q,u,t) - \left[-M^{-1}(q,t)C(q,u_r,t)\right] && (54)\\ &= -M^{-1}(q,t)\left[C(q,u,t) - C(q,u_r,t)\right] && (55)\end{aligned}$$

implying boundedness of e_u, in contradiction with the original argument. Therefore, the trajectory of e_u must remain in a finite region. Since a trajectory of the error dynamical system given by (55) does not experience an isolated periodic motion (limit cycle), it follows from the Poincare-Bendixson theorem [15] that the trajectory must go to the equilibrium point $e_u = \mathbf{0}_{n\times 1}$.

Theorem 8.1 *Let the controls coefficient nullprojected gain matrix be given by*

$$\mathcal{P}(q,t)K = -vec^{-1}\Big\{\Big[\widetilde{\mathcal{P}}(q,\delta,t)\oplus\widetilde{\mathcal{P}}(q,\delta,t)\Big]^{-1} vec\Big[\dot{\mathcal{P}}(q,u,t)+\mathcal{P}(q,t)Q - 4\mathcal{P}(q,t)M^{-1}(q,t)C_m(q,u_r,t)\Big]\Big\}, \tag{56}$$

where $\oplus$ denotes the kronecker sum of matrices, "vec" and "vec^{-1}" denote the matrix vectorizing and inverse vectorizing operators, $Q\in\mathbb{R}^{n\times n}$ is an arbitrary positive definite constant matrix, and

$$C_m(q,u,t) = \frac{1}{2}\frac{\partial C(q,u,t)}{\partial u}. \tag{57}$$

Then the equilibrium point $e_u=\mathbf{0}_{n\times1}$ of the closed loop error dynamics given by (43) is asymptotically stable.

Proof. Since the Coriolis centrifugal forces vector $C(q,u,t)$ is continuously differentiable in the vector u, then expanding the Coriolis centrifugal forces error vector about $e_u=\mathbf{0}_{n\times1}$ using Taylor series yields

$$C(q,u,t)-C(q,u_r,t) = 2C_m(q,u_r,t)e_u + g(q,u,t), \tag{58}$$

where the following holds true for sufficiently small error vector norms $\|e_u\|$

$$\|g(q,u,t)\| < \|2C_m(q,u_r,t)e_u\| \tag{59}$$

and such that $g(q,u,t)$ satisfies

$$\lim_{\|e_u\|\to\mathbf{0}_{n\times1}}\frac{\|g(q,u,t)\|}{\|e_u\|} = 0. \tag{60}$$

Therefore, linearizing the first difference in the error dynamics given by (43) about $e_u=\mathbf{0}_{n\times1}$ yields

$$\dot{e}_{u_l} = -2M^{-1}(q,t)C_m(q,u_r,t)e_u + \mathcal{A}_s^+(q,u,t)\mathcal{B}(q,u,t) - \mathcal{A}^+(q,t)\mathcal{B}(q,u_r,t) + \mathcal{P}(q,t)Ke_u. \tag{61}$$

Evaluating the time derivative of V along solution trajectories of the partially linearized error system given by (61) yields

$$\begin{aligned}\dot{V}_l(q,u,e_u,t) &= 2e_u^T\mathcal{P}(q,t)\left[-2M^{-1}(q,t)C_m(q,u_r,t)e_u\right]\\&\quad+2e_u^T\mathcal{P}(q,t)\left[\mathcal{A}_s^+(q,u,t)\mathcal{B}(q,u,t)-\mathcal{A}^+(q,t)\mathcal{B}(q,u_r,t)\right]\\&\quad+2e_u^T\mathcal{P}(q,t)\left[\mathcal{P}(q,t)Ke_u\right]+e_u^T\dot{\mathcal{P}}(q,u,t)e_u. \qquad (62)\end{aligned}$$

The second property of $\mathcal{A}_s^+(q,u,t)$ and the nullprojection property of $\mathcal{P}(q,t)$ simplify the above expression to

$$\begin{aligned}&\dot{V}_l(q,u,e_u,t)=\\&\qquad e_u^T\Big[-4\mathcal{P}(q,t)M^{-1}(q,t)C_m(q,u_r,t)+2\mathcal{P}(q,t)K+\dot{\mathcal{P}}(q,u,t)\Big]e_u. \qquad (63)\end{aligned}$$

Since V is only positive-semi definite, it is impossible to design a gain matrix K that renders $\dot{V}_l$ negative definite. Nevertheless, K can be designed to yield $\dot{V}_l$ negative semidefinite by inquiring the existence of a positive semi-definite matrix $\mathcal{Q}(q,u,t)$: $\mathbb{R}^n\times\mathbb{R}^n\times[t_0,\infty)\rightarrow\mathbb{R}^{n\times n}$ that satisfies

$$\dot{V}_l(q,u,e_u,t)=-e_u^T\mathcal{Q}(q,u,t)e_u. \qquad (64)$$

Equating (63) and (64) yields the controls coefficient null-projected Lyapunov equation

$$\begin{aligned}&-4\mathcal{P}(q,t)M^{-1}(q,t)C_m(q,u_r,t)+\mathcal{P}(q,t)K\\&\qquad+K^T\mathcal{P}(q,t)+\dot{\mathcal{P}}(q,u,t)+\mathcal{Q}(q,u,t)=\mathbf{0}_{n\times n}. \qquad (65)\end{aligned}$$

The above equation is consistent if every term maps into the range space of $\mathcal{P}(q,t)$. The range space of $\dot{\mathcal{P}}(q,u,t)$ can be shown to be a subset of the range space of $\mathcal{P}(q,t)$ by writing

$$\mathcal{P}(q,t)=\mathcal{P}(q,t)\mathcal{P}(q,t)\Rightarrow\dot{\mathcal{P}}(q,u,t)=2\mathcal{P}(q,t)\dot{\mathcal{P}}(q,u,t) \qquad (66)$$

so that

$$\mathcal{R}[\dot{\mathcal{P}}(q,u,t)]=\mathcal{R}[\mathcal{P}(q,t)\dot{\mathcal{P}}(q,u,t)]\subseteq\mathcal{R}[\mathcal{P}(q,t)] \qquad (67)$$

where $\mathcal{R}(\cdot)$ refers to matrix range space. Since $\mathcal{Q}(q,u,t)$ is arbitrary positive semi definite, then restricting $\mathcal{Q}(q,u,t)$ to map into the range space of $\mathcal{P}(q,t)$ implies that there is no loss of generality in specifying an arbitrary constant positive definite matrix Q such that a polar decomposition of $\mathcal{Q}(q,u,t)$ is given by

$$\mathcal{Q}(q,u,t)=\mathcal{Q}(q,t)=\mathcal{P}(q,t)Q. \qquad (68)$$

Accordingly, (65) can be written with the aid of the relation given by (25) as

$$\begin{aligned}&-4\mathcal{P}(q,t)M^{-1}(q,t)C_m(q,u_r,t)+\widetilde{\mathcal{P}}(q,\delta,t)\mathcal{P}(q,t)K\\&\qquad+K^T\mathcal{P}(q,t)\widetilde{\mathcal{P}}(q,\delta,t)+\dot{\mathcal{P}}(q,u,t)+\mathcal{P}(q,t)Q=\mathbf{0}_{n\times n}. \qquad (69)\end{aligned}$$

By requiring the gain matrix K to be symmetric and of full rank, the unique solution of (69) for $\mathcal{P}(q,t)K$ is given by [14]

$$\begin{aligned}\mathcal{P}(q,t)K=-\mathrm{vec}^{-1}\bigg\{&\Big[I_{3\times3}\otimes\widetilde{\mathcal{P}}(q,\delta,t)+\widetilde{\mathcal{P}}(q,\delta,t)\otimes I_{3\times3}\Big]^{-1}\\&\mathrm{vec}\Big[\dot{\mathcal{P}}(q,u,t)+\mathcal{P}(q,t)Q-4\mathcal{P}(q,t)M^{-1}(q,t)C_m(q,u_r,t)\Big]\bigg\}, \qquad (70)\end{aligned}$$

where $\otimes$ denotes the kronecker product of matrices. Equation (70) can be written in the compact form of (56), and $\dot{V}_l(q,u,e_u,t)$ is guaranteed to be globally negative semidefinite. Moreover, since the gain matrix K is symmetric and of full rank, then asymptotic stability of the equilibrium point $e_u = \mathbf{0}_{n\times 1}$ of the error dynamical system given by (43) over the invariant set $\mathcal{D}_{V=0}$ follows from Proposition 8.2. Radial unboundedness of $V(q,e_u,t)$ in e_u together with global negative semidefiniteness of $\dot{V}_l(q,u,e_u,t)$ and asymptotic stability over $\mathcal{D}_{V=0}$ imply that the equilibrium point $e_u = \mathbf{0}_{n\times 1}$ of the partially linearized error dynamics system given by (61) is globally stable in the sense of Lyapunov. Nevertheless, it is evident from the expression of $\dot{V}_l$ given by (63) that $\dot{V}_l = 0$ if and only if $\mathcal{P}(q,t)e_u = \mathbf{0}_{n\times 1}$. Therefore, $\mathcal{D}_{V=0} = \mathcal{D}_{\dot{V}=0}$, and the equilibrium point $e_u = \mathbf{0}_{n\times 1}$ of the system given by (61) is globally asymptotically stable [13]. From Lyapunov's indirect method, asymptotic stability of the system given by (61) implies local stability of the fully nonlinear error system given by (43) [16]. The matrix $\mathcal{Q}(q,t)$ (and the corresponding nullprojected Lyapunov matrix Q) can be designed for guarantee asymptotic stability of $e_u = \mathbf{0}_{n\times 1}$ over a prescribed domain $\mathcal{D}$ of asymptotic stability, as stated by the following theorem.

Theorem 8.2 *Let the controls coefficient nullprojected matrix gain be given by (56), where $Q \in \mathbb{R}^{n\times n}$ is positive definite and satisfying (68). For every prescribed neighborhood $\mathcal{D} \subset \mathbb{R}^n$ of the origin $e_u = \mathbf{0}_{n\times 1}$ there exists a real number $\gamma > 0$ such that if the minimum nonzero eigenvalue of $\mathcal{Q}(q,t)$ denoted by $\bar{\lambda}_{min}(\mathcal{Q}(q,t))$ satisfies*

$$\bar{\lambda}_{min}(\mathcal{Q}(q,t)) > \frac{2\gamma}{\lambda_{min}(M(q,t))} \quad \forall\, t \geq t_0, \tag{71}$$

then the equilibrium point $e_u = \mathbf{0}_{n\times 1}$ of the closed loop error dynamics given by (43) is asymptotically stable over $\mathcal{D}$.

Proof. Evaluating the time derivative of $V(q,u,t)$ along solution trajectories of the fully nonlinear error system given by (43) with the aid of the expansion given by (58) yields

$$\begin{aligned}
\dot{V}(q,u,t) &= \dot{V}_l(q,u,t) - 2e_u^T\mathcal{P}(q,t)M^{-1}(q,t)g(q,u,t) && (72)\\
&= -e_u^T\mathcal{Q}(q,t)e_u - 2e_u^T\mathcal{P}(q,t)M^{-1}(q,t)g(q,u,t). && (73)
\end{aligned}$$

Additionally, (60) implies that for every real scalar $\gamma > 0$ there exists a vector $e_{u_\gamma} \in \mathbb{R}^n$ such that the following inequality holds [16]

$$\|g(q,u,t)\| < \gamma\|e_u\| \quad \forall\, \|e_u\| < \|e_{u_\gamma}\|. \tag{74}$$

Accordingly, if $\dot{V}_l(q,u,t) \neq 0$ then an upper bound on $\dot{V}$ is obtained from (73) as

$$\begin{aligned}
\dot{V}(q,u,t) &\leq -\bar{\lambda}_{min}(\mathcal{Q}(q,t))\|e_u\|^2 \\
&\quad +2\|e_u\|\lambda_{\max}(M^{-1}(q,t))\|g(q,u,t)\| && (75)\\
&\leq -\bar{\lambda}_{min}(\mathcal{Q}(q,t))\|e_u\|^2 + \frac{2\gamma}{\lambda_{min}(M(q,t))}\|e_u\|^2 && (76)\\
&= \left[-\bar{\lambda}_{min}(\mathcal{Q}(q,t)) + \frac{2\gamma}{\lambda_{min}(M(q,t))}\right]\|e_u\|^2 \\
&\qquad \forall\, \|e_u\| < \|e_{u_\gamma}\|. && (77)
\end{aligned}$$

Therefore, given a real scalar $\gamma > 0$ and a corresponding vector e_{u_γ}, if $\mathcal{D}$ is defined as the set of all vectors $e_u \in \mathbb{R}^n$ satisfying

$$\|e_u\| < \|e_{u_\gamma}\| \tag{78}$$

and $\mathcal{Q}(q,t)$ is chosen such that $\bar{\lambda}_{min}(\mathcal{Q}(q,t))$ satisfies (71) then $\dot{V}$ is guaranteed to remain negative along solution trajectories of the fully nonlinear error system given by (43) initiated at $e_u(t_0) \in \mathcal{D}_{\dot{V}\neq 0}$ along which

$$\dot{V}_l(q,u,t) \neq 0 \quad \forall\, t \geq t_0. \tag{79}$$

The above mentioned argument together with the arguments of Proposition 8.2 and Theorem 8.1 on global asymptotic stability of $e_u = \mathbf{0}_{n\times 1}$ with respect to trajectories initiated within $\mathcal{D}_{\dot{V}=0}$ prove asymptotic stability of $e_u = \mathbf{0}_{n\times 1}$ over $\mathcal{D}$. A corresponding necessary condition on Q for asymptotic stability of $e_u = \mathbf{0}_{n\times 1}$ can be derived also. Since

$$\bar{\lambda}_{min}(\mathcal{Q}(q,t)) = \lambda_{min}(\mathcal{P}(q,t)Q) \leq \lambda_{\max}(\mathcal{P}(q,t))\lambda_{min}(Q) = \lambda_{min}(Q), \tag{80}$$

the condition given by (71) for asymptotic stability implies that

$$\lambda_{min}(Q) > \frac{2\gamma}{\lambda_{min}(M(q,t))} \quad \forall\, t \geq t_0, \tag{81}$$

provided that

$$e_u(t_0) \in \mathcal{D}. \tag{82}$$

Corollary 8.1 *Let γ be a positive scalar that satisfies*

$$\gamma > 2\sup_{q,t}(\sigma_{\max}(C_m(q,u_r,t))), \tag{83}$$

where $\sup_{q,t}$ denotes the supremum over all admissible values of robot generalized coordinates and over all $t \geq 0$. If $\mathcal{Q}(q,t) : \mathbb{R}^n \times [t_0,\infty) \to \mathbb{R}^{n\times n}$ is positive semidefinite and satisfies the condition given by (71), $Q \in \mathbb{R}^{n\times n}$ is positive definite and satisfies (68), and the controls coefficient nullprojected gain matrix is given by (56), then the equilibrium point $e_u = \mathbf{0}_{n\times 1}$ of the closed loop error dynamics given by (43) is asymptotically stable over a domain of attraction $\mathcal{D} \subset \mathbb{R}^n$ that is given by all vectors $e_u \in \mathbb{R}^n$ satisfying

$$\|e_u\| < \|e_{u_\gamma}\|, \tag{84}$$

where

$$\|e_{u_\gamma}\| = \frac{\|C(q_0,u_0,t_0) - C(q_0,u_r(t_0),t_0) - 2C_m(q_0,u_r(t_0),t_0)e_u(t_0)\|}{2\sup_{q,t}(\sigma_{\max}(C_m(q,u_r,t)))}. \tag{85}$$

Proof. The fact on $g(q,u,t)$ given by (59) implies that for sufficiently small values of $\|e_u\|$, the following inequality holds true

$$\|g(q,u,t)\| < 2\sigma_{\max}(C_m(q,u_r,t))\|e_u\|. \tag{86}$$

Therefore, a particular choice of γ that holds inequality (74) true is found by setting

$$2\sigma_{\max}(C_m(q,u_r,t))\|e_u\| < \gamma\|e_u\| \tag{87}$$

resulting in the expression given by (83) for a lower bound estimate of γ that ensures satisfaction of (74) for sufficiently small values of $\|e_u\|$. To obtain the corresponding estimate of $\|e_{u\gamma}\|$, the two sides of (74) are equated and the above written estimate of γ is substituted in the resulting equation, yielding

$$\|g(q,u,t)\| = 2\sup_{q,t}(\sigma_{\max}(C_m(q,u_r,t)))\|e_u\|. \tag{88}$$

The value of $\|e_u\|$ in the above equation is an estimate of the smallest vector norm $\|e_u\|$ that causes inequality (74) to be violated, i.e., it is an estimate of $\|e_{u_\gamma}\|$. Accordingly, evaluating $g(q,u,t)$ at t_0 and replacing e_u by e_{u_γ} yields

$$\|e_{u_\gamma}\| = \frac{\|g(q_0,u_0,t_0)\|}{2\sup_{q,t}(\sigma_{\max}(C_m(q,u_r,t)))}. \tag{89}$$

Evaluating $g(q_0,u_0,t_0)$ using (58) yields the expression of $\|e_{u_\gamma}\|$ given by (85).

9 Outer (Kinematic) Closed Loop Stability

Let ϕ_s be a norm measure function of the attitude deviation obtained by applying the control law $\tau_s(q,u,y,t)$ given by (27) to the manipulator's equations of motion (2) and (3) in place of τ, and let $\dot{\phi}_s$, $\ddot{\phi}_s$ be its first two time derivatives. Therefore,

$$\begin{aligned}
\phi_s &:= \phi_s(q,t) = \phi(q,t) && (90)\\
\dot{\phi}_s &:= \dot{\phi}_s(q,u,t) = \dot{\phi}(q,u,t) && (91)\\
\ddot{\phi}_s &:= \ddot{\phi}_s(q,u,\tau_s,t) = \ddot{\phi}(q,u,\tau,t) + \mathcal{A}(q,t)\tau_s(q,u,y,t)\\
&\quad -\mathcal{A}(q,t)\tau(q,u,y,t), && (92)
\end{aligned}$$

where $\tau(q,u,y,t)$ is given by (14). Adding $c_1\dot{\phi}_s + c_2\phi_s$ to both sides of (92) yields

$$\begin{aligned}
\ddot{\phi}_s + c_1\dot{\phi}_s + c_2\phi_s &= \ddot{\phi} + c_1\dot{\phi} + c_2\phi + \mathcal{A}(q,t)\tau_s(q,u,y,t)\\
&\quad -\mathcal{A}(q,t)\tau(q,u,y,t) && (93)\\
&= \mathcal{A}(q,t)[\tau_s(q,u,y,t) - \tau(q,u,y,t)]. && (94)
\end{aligned}$$

With the controls coefficient nullprojected matrix gain be given by (56), the generalized inversion feedback control law given by (27) yields asymptotically stable generalized coordinate trajectory tracking, as stated by the following theorem.

Theorem 9.1 *Let the controls coefficient nullprojected matrix gain $\mathcal{P}(q,t)K$ be given by (56), and the matrix $\mathcal{Q}(q,t)$ satisfies (71) for some real number $\gamma > 0$ and a corresponding domain of asymptotic stability $\mathcal{D} \subset \mathbb{R}^n$. Then the closed loop generalized coordinate deviation dynamics given by (94) is asymptotically stable.*

Proof. Multiplying both sides of the control law $\tau_s(q,u,y,t)$ given by (27) by $\mathcal{A}(q,t)$ yields

$$\mathcal{A}(q,t)\tau_s(q,u,y,t) = \mathcal{A}(q,t)\mathcal{A}_s^+(q,u,t)\mathcal{B}(q,u,t), \tag{95}$$

where

$$\mathcal{A}(q,t)\mathcal{A}_s^+(q,u,t) = \frac{\mathcal{A}(q,t)\mathcal{A}^T(q,t)}{\mathcal{A}(q,t)\mathcal{A}^T(q,t) + \|e_u(u,u_r)\|_p^p}. \tag{96}$$

Therefore, if $\mathcal{A}(q,t) \neq \mathbf{0}_{1\times n}$ then it follows from (96) that

$$0 < \mathcal{A}(q,t)\mathcal{A}_s^+(q,u,t) \leq 1. \tag{97}$$

Dividing (95) by $\mathcal{A}(q,t)\mathcal{A}_s^+(q,u,t)$ yields

$$\mathcal{A}(q,t)\bar{\tau}(q,u,y,t) = \mathcal{B}(q,u,t), \tag{98}$$

where $\mathcal{A}(q,t)$ and $\mathcal{B}(q,u,t)$ are the same controls coefficient and controls load in (11), and

$$\bar{\tau}(q,u,y,t) = \frac{\tau_s(q,u,y,t)}{\mathcal{A}(q,t)\mathcal{A}_s^+(q,u,t)}. \tag{99}$$

Therefore, the algebraic system given by (98) recovers the algebraic system given by (11) via the control law $\bar{\tau}(q,u,y,t)$ for all $\mathcal{A}(q,t) \neq \mathbf{0}_{1\times n}$. Equivalently, the effective control law $\bar{\tau}(q,u,y,t)$ enforces the asymptotically stable second-order system given by (10) on the robot manipulator system given by (2) and (3) whenever $\mathcal{A}(q,t) \neq \mathbf{0}_{1\times n}$. Nevertheless, it is noticed from (6) and (12) that $\mathcal{A}(q,t) = \mathbf{0}_{1\times n}$ if and only if $\phi = \phi_s = 0$. This in addition to the local asymptotic stability of $e_u = \mathbf{0}_{n\times 1}$ concluded from Theorem (8.1) imply that the second order generalized coordinate deviation dynamics given by (94) is asymptotically stable over the domain $\mathcal{D}$. Theorem 9.1 states that employing the DSGI $\mathcal{A}_s^+(q,u,t)$ in the generalized inversion attitude control law yields the same asymptotic attitude tracking property that is obtained by employing the CCGI $\mathcal{A}^+(q,t)$, provided that manipulator's internal asymptotic stability is achieved by a proper design of the null-control vector y.

Remark 9.1 The second order generalized coordinate deviation dynamics given by (94) can be put in the state space form by defining the state vector $\Phi \in \mathbb{R}^2$ as

$$\Phi = \begin{bmatrix}\Phi_1 & \Phi_2\end{bmatrix}^T = \begin{bmatrix}\phi_s & \dot{\phi}_s\end{bmatrix}^T. \tag{100}$$

The two state equations become

$$\dot{\Phi}_1 = \Phi_2 \tag{101}$$

$$\dot{\Phi}_2 = -c_1\Phi_2 - c_2\Phi_1 + \mathcal{A}(q,t)[\tau_s(q,u,y,t) - \tau(q,u,y,t)]. \tag{102}$$

Asymptotic stability of $e_u = \mathbf{0}_{n\times 1}$ over the domain $\mathcal{D}$ inferred from Theorem 8.1 in addition to boundedness of $\mathcal{A}(q,t)$ over the same domain inferred from Proposition 8.1 imply that the limit of the forcing term in (102) as $t \to \infty$ is

$$\lim_{t\to\infty}\Big[\mathcal{A}(q,t)[\tau_s(q,u,y,t) - \tau(q,u,y,t)]\Big] = 0 \tag{103}$$

so that $\dot{\Phi}$ converges to the asymptotically stable canonical part of the dynamics given by (101) and (102), and results in

$$\lim_{t\to\infty}\phi_s = \lim_{t\to\infty}\dot{\phi}_s = 0 \tag{104}$$

over the domain $\mathcal{D}$, verifying the attraction property of $\Phi = \mathbf{0}_{2\times 1}$, i.e.,

$$\lim_{t\to\infty} q = q_r(t) \tag{105}$$

and

$$\lim_{t\to\infty}\dot{q} = \dot{q}_r(t). \tag{106}$$

Remark 9.2 Inequalities (97) imply that

$$\lim_{e_u(u,u_r)\to \mathbf{0}_{n\times 1}} \mathcal{A}(q,t)\mathcal{A}_s^{+}(q,u,t) = 1. \tag{107}$$

Hence, (99) yields

$$\lim_{e_u(u,u_r)\to \mathbf{0}_{n\times 1}} \bar{\tau}(q,u,y,t) = \lim_{e_u(u,u_r)\to \mathbf{0}_{n\times 1}} \tau_s(q,u,y,t) = \tau(q,u,y,t). \tag{108}$$

10 Damped Controls Coefficient Nullprojector

The damped CCNP is a modified controls coefficient nullprojector with vanishing dependency on steady state kinematic state vector q.

Definition 10.1 [Damped controls coefficient nullprojector] The damped CCNP $\mathcal{P}_d(q,\beta,t)$ is defined as

$$\mathcal{P}_d(q,\beta,t) = \begin{cases} \mathcal{P}(q,t) & : \ \|\mathcal{A}(q,t)\| \geq \beta, \\ I_{n\times n} - \frac{\mathcal{A}^T(q,t)\mathcal{A}(q,t)}{\beta^2} & : \ \|\mathcal{A}(q,t)\| < \beta. \end{cases} \tag{109}$$

The above definition implies that

$$\lim_{e_q(q,t)\to \mathbf{0}_{n\times 1}} \mathcal{P}_d(q,\beta,t) = I_{n\times n}. \tag{110}$$

11 Control System Design Procedure

Starting from the standard mathematical model given by (1) for a rigid robot manipulator, the procedure of asymptotic generalized inverse dynamics for tracking a twice continuously differentiable reference trajectory vector $q_r(t)$ is summarized in the following steps.

1. The robot manipulator mathematical model given by (1) is written in its equivalent state space model form given by (2) and (3).

2. The coefficients a_1 and a_2 in the servo-constraint dynamics equation (10) are chosen such that the dynamics of ϕ is asymptotically stable. This implies that both a_1 and a_2 are strictly positive. To avoid oscillatory closed loop transient response induced by underdamped servo-constraint dynamics, the coefficient a_1 is chosen sufficiently large compared to a_2 such that the linear second-order servo-constraint dynamics given by Equation (10) is overdamped.

3. The expressions given by (12) and (13) for $\mathcal{A}(q,t)$ and $\mathcal{B}(q,u,t)$ are obtained, where $e_q(q,t)$ is given by (5).

4. The expression given by (83) is solved for the positive scalar γ, where $C_m(q,u,t)$ is given by (57).

5. The positive semidefinite matrix $\mathcal{Q}(q,t)$ is obtained from (71), and is used to solve (68) for a positive definite constant matrix Q, where $\mathcal{P}(q,t)$ is given by (16).

6. The control law τ_s is given by

$$\tau_s(q,u,y,t) = \mathcal{A}_s^+(q,u,t)\mathcal{B}(q,u,t) + \mathcal{P}(q,t)Ku. \tag{111}$$

   The dynamically scaled controls coefficient generalized inverse $\mathcal{A}_s^+(q,u,t)$ in the above written control law is given by (22) for some vector p norm, where $e_u(u,u_r)$ is given by (23). The controls coefficient nullprojected gain matrix $\mathcal{P}(q,t)K$ in the above written control law is given by (56), where the perturbed controls coefficient nullprojection matrix $\widetilde{\mathcal{P}}(q,\delta,t)$ is given by (24), $C_m(q,u,t)$ is given by (57), and $\dot{\mathcal{P}}(q,u,t)$ is obtained by time differentiating $\mathcal{P}(q,t)$ along solution trajectories of the system equations given by (2).

7. The control law τ_s is used in (2) and (3) in place of τ, and the two sets of equations are integrated to obtain the trajectories of $q(t)$ and $u(t)$. If the initial state vector u_0 is such that $\|e_u(t_0)\| < \|e_{u_\gamma}\|$ where $\|e_{u_\gamma}\|$ is given by (85), then the closed loop robot manipulator control system is asymptotically stable, the resulting trajectory tracking error vectors $e_q(q,t)$ and $e_u(q,u,t)$ are asymptotically decaying to the zero vectors, and the generalized coordinates vector q asymptotically tracks $q_r(t)$.

12 Example: RP Robot Manipulator

The RP robot manipulator shown in Fig. 1 consists of two rigid arms A_1 and A_2 having masses m_1 and m_2, respectively. The two arms are constrained to move in the vertical plane, and A_1 is attached to an inertial reference frame at point O. The body moments of inertia of A_1 and A_2 about the axes normal to their plane of rotation and passing through their mass centers c_1 and c_2 are I_{zz1} and I_{zz2}, respectively. The manipulator is equipped with a revolute joint at point O and a prismatic joint along the longitudinal axis L_c. The revolute joint is actuated by a motor that generates a torque $\mathbf{M}$, and the prismatic joint is actuated by a motor that generates a force $\mathbf{F}$. It is required to design $\mathbf{M}$ and $\mathbf{F}$ such that A_1 oscillates about the left part of the horizontal line passing through O at a frequency of $\pi/6$ Hz according to the harmonic relation

$$\theta = \pi \sin\left(\frac{\pi}{6}t\right). \tag{112}$$

Based on the orientation of A_1, A_2 is required to translate simultaneously along L_c according to

$$d = 2l(1 - 0.5\cos\theta). \tag{113}$$

Choosing the generalized coordinates to be $q_1 = \theta$ and $q_2 = d$, the desired generalized coordinates $q_{r_1}(t)$ and $q_{r_1}(t)$ are given by

$$q_{r_1}(t) = \pi \sin\left(\frac{\pi}{6}t\right) \tag{114}$$

and

$$q_{r_2}(t) = 2l(1 - 0.5\cos q_{r_1}(t)) = 2l\left(1 - 0.5\cos\left(\pi\sin\left(\frac{\pi}{6}t\right)\right)\right). \tag{115}$$

The matrices forming the manipulator state space mathematical model given by (2) and (3) are

$$M(q,t) = \begin{bmatrix} m_1 l_1^2 + I_{zz1} + I_{zz2} + m_2 q_2^2 & 0 \\ 0 & m_2 \end{bmatrix}, \quad (116)$$

$$C(q,u,t) = \begin{bmatrix} 2m_2 q_2 u_1 u_2 \\ -m_2 q_2 u_1^2 \end{bmatrix}, \quad (117)$$

$$G(q,t) = \begin{bmatrix} (m_1 l_1 + m_2 q_2) g \cos q_1 \\ m_2 g \sin q_1 \end{bmatrix}, \quad (118)$$

$$\mathcal{F} = \begin{bmatrix} M \\ F \end{bmatrix}, \quad (119)$$

where M and F are the magnitudes of $\mathbf{M}$ and $\mathbf{F}$, positives in the directions indicated by the arrows in Fig. 1. The two components of the generalized coordinates error vector $e_q(q,t)$ given by (5) are

$$e_1(q_1,t) = q_1 - q_{r_1}(t) = q_1 - \pi \sin\left(\frac{\pi}{6}t\right) \quad (120)$$

and

$$e_2(q_2,t) = q_2 - q_{r_2}(t) \quad (121)$$

$$= q_2 - 2l\left(1 - 0.5\cos\left(\pi \sin\left(\frac{\pi}{6}t\right)\right)\right). \quad (122)$$

Hence, the kinematic deviation norm measure function ϕ given by (6) is

$$\phi = \| e_q(q,t) \|^2 = e_1^2(q_1,t) + e_2^2(q_2,t). \quad (123)$$

The matrix $C_m(q,u_r,t)$ is given by

$$C_m(q,u_r,t) = m_2 q_2 \begin{bmatrix} u_{r_2} & u_{r_1} \\ -u_{r_1} & 0 \end{bmatrix}. \quad (124)$$

The maximum singular value of $C_m(q,u_r,t)$ is found to be

$$\sigma_{max}(C_m(q,u_r,t)) = m_2|q_2|\sqrt{2u_{r_1}^2 + u_{r_2}^2 + \sqrt{u_{r_2}^4 + 4u_{r_1}^2 u_{r_2}^2}}. \quad (125)$$

The manipulator geometric and inertia constants are taken to be $l_1 = 1$ m, $m_1 = 10.5$ kg, $m_2 = 7.0$ kg, $I_{zz1} = 30$ kg.m^2 and $I_{zz2} = 15$ kg.m^2. Upper bounds on the variables u_{r_1}, u_{r_2} are obtained by time differentiating the expressions of q_{r_1} and q_{r_2} given by (114) and (115) as $\pi^2/6$ rad/sec and $\pi^2/6$ m/sec, respectively. A sufficiently conservative upper bound on q_2 is obtained from (113) as 3.5 m. Therefore, a value of γ that satisfies the condition given by (83) is taken to be 10^2, and a matrix Q that satisfies (68) and (71) is taken to be

$$Q = 60 I_{2\times 2}. \quad (126)$$

The servo-constraint dynamics constants in (10) are chosen to be $a_1 = 7$, $a_2 = 4$. With initial conditions $q_0 = [-\pi/2 \quad 2.8]^T$ and $u_0 = [0.4 \quad -0.2]^T$, the values of $\|e_u(t_0)\|$ and $\|e_{u_\gamma}\|$ are 1.26 and 1.3, respectively. Fig. 2 shows time history of generalized coordinates θ and d, where p, β, and δ are taken 4, 0.6, and 0.1, respectively. Excellent asymptotically stable trajectory tracking performance is noticed. Figs. 3 and 4 show time histories of the corresponding angular velocity $\dot{\theta}$ and linear velocity $\dot{d}$, and the control variables M and F, respectively.

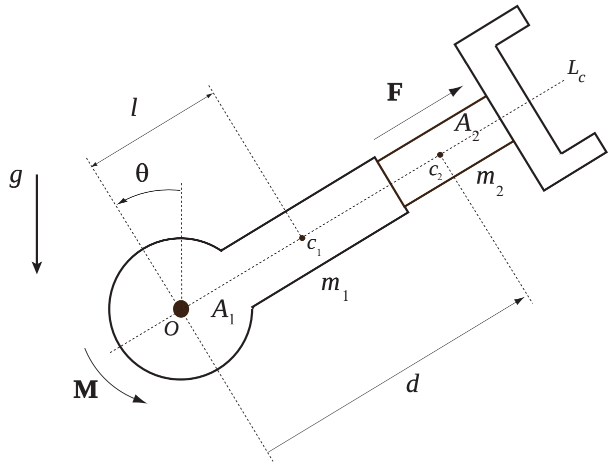

Figure 1: Schematic for RP robot manipulator.

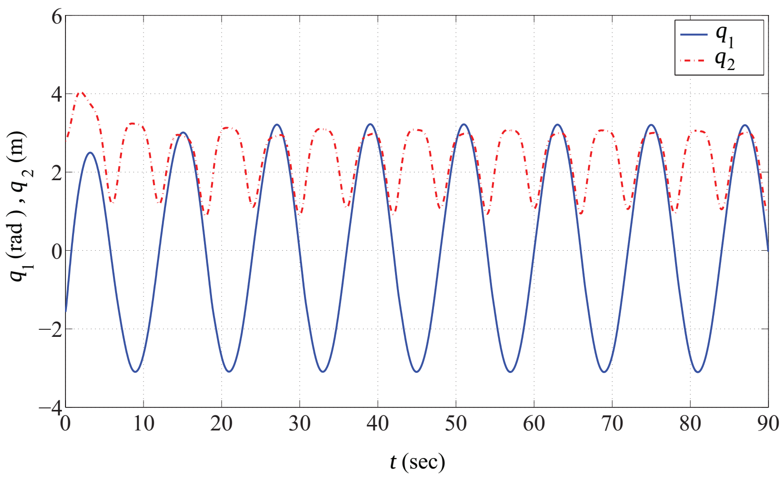

Figure 2: Generalized coordinates

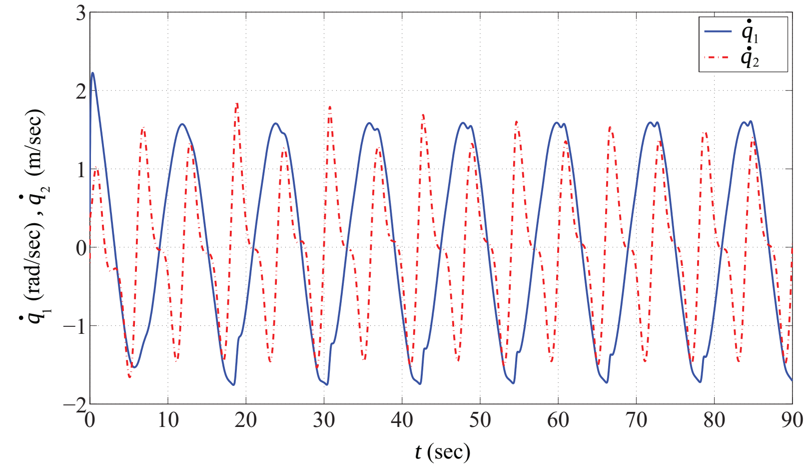

Figure 3: Generalized velocities.

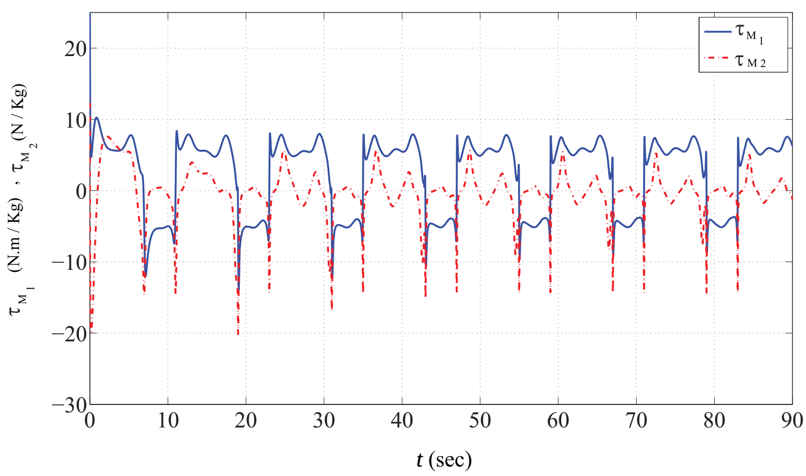

Figure 4: Scaled control forces.

13 Conclusions

The paper presents an approach that unifies the treatments of inverse kinematics and inverse dynamics, which have ever been made distinctive in the robot control literature. The vectorial representation of kinematical errors and their time derivatives in classical inverse dynamics is unfavorable, because the kinematical error is a scalar variable. More importantly, modeling the kinematical error as a vector that has the same number of elements as the number of manipulator's degrees of freedom restricts the inner loop design problem to have a unique solution, and hence it causes the methodology to lose a useful design freedom and makes it susceptible to dynamic inversion singularity. By observing that a control law that realizes any dynamic process on a controllable dynamical system is not unique, this paper removes the restriction on inverse dynamics by redefining the kinematical error as a deviation norm measure scalar. The paper applies the GID control paradigm to robot arm tracking of desired smooth trajectories. The outer loop design is made by generalized inversion of a stable servo-constraint dynamics differential equation in the kinematic deviation norm. The dynamically scaled generalized inverse in the particular part of the control law is capable of overcoming controls coefficient generalized inversion singularity, and it converges to the standard Moore-Penrose generalized inverse as closed loop steady state response approaches. The inner loop design is made by constructing the null-control vector in the auxiliary part of the control law. The null-control vector is designed to be linear in the internal states by means of a quadratic positive semidefinite control Lyapunov function and a controls coefficient nullprojected Lyapunov equation. Future works include utilizing the nullspace parametrization feature associated with generalized inversion and provided by the null-control vector in performing secondary objectives on top of generalized inverse dynamics.

References

[1] Bajodah, A.H., Hodges, D.H., and Chen, Ye-Hwa Inverse dynamics of servo-constraints based on the generalized inverse. *Nonlinear Dynamics* **39** (1-2) (2005) 179–196.

[2] Bajodah, A.H. Generalized Dynamic Inversion Spacecraft Control Design Methodologies. *IET Control Theory & Applications* **3** (2) (2009) 239–251.

[3] Greville, T.N.E. The pseudoinverse of a rectangular or singular matrix and its applications to the solutions of systems of linear equations. *SIAM Review* **1** (1) (1959) 38–43.

[4] Ben-Israel, A. and Greville, T.N.E. *Generalized Inverses, Theory and Applications.* Springer-Verlag New York, Inc., 2003, Second Edition.

[5] Bajodah, A.H. Servo-constraint Generalized Inverse Dynamics for Robot Manipulator Control Design. *International Journal of Robotics and Automation* **25** (1) (2010) 38–47.

[6] Moore, E.H. On the reciprocal of the general algebraic matrix. *Bulletin of the American Mathematical Society* **26** (1920) 394–395.

[7] Penrose, R. A generalized inverse for matrices. *Proceedings of the Cambridge Philosophical Society* **51** (1955) 406–413.

[8] Bajodah, A.H. Singularly Perturbed Feedback Linearization with Linear Attitude Deviation Dynamics Realization. *Nonlinear Dynamics* **53** (4) (2008) 321–343.

[9] Siciliano, B. and Khatib, O. *Springer Handbook of Robotics.* Springer, 2008, 245–268.

[10] Siciliano, B., Sciavicco, L., Villani, L., and Oriolo, G. *Robotics: Modeling, Planning, and Control.* Springer-Verlag London Limited, 2009.

[11] Bajodah, A.H. Stabilization of underactuated spacecraft dynamics via singularly perturbed feedback linearization. *Journal of King Abdulaziz University: Engineering Sciences* **16** (2) (2006) 35–53.

[12] Bajodah, A.H. Asymptotic Perturbed Feedback Linearization of Underactuated Euler's Dynamics. *International Journal of Control* **82** (10) (2009) 1856–1869.

[13] Iqqidr, A., Kalitine, B., and Outbib, R. Semidefinite Lyapunov functions stability and stabilization. *Mathematics of Control, Signals and Systems* **9** (2) (1996) 95–106.

[14] Bernstein, D.S. *Matrix mathematics: theory, facts, and formulas with application to linear system theory*. Princeton university press, 2009, Second Edition.

[15] Slotine, J.E. and Li, W. *Applied Nonlinear Control*. Prentice-Hall, Englewood Cliffs, NJ, 1991.

[16] Khalil, H.K. *Nonlinear Systems*. Prentice-Hall, Inc., 2002, Third Edition.

Nonlinear Dynamics and Systems Theory, **13** (1) (2013) 47–53

A Poiseuille Flow of an Incompressible Fluid with Nonconstant Viscosity

Y. Hataya [1*], M. Ito [2] and M. Shiba [2]

[1] *Department of Mathematics, Yamaguchi University, Yamaguchi, 753-8512, Japan*
[2] *Department of Applied Mathematics, Hiroshima University, Hiroshima 739-8527, Japan*

Received: March 19, 2012; Revised: January 23, 2013

Abstract: The viscosity coefficient in steady Navier-Stokes equations is determined for a particular velocity vector which arises from the study of conformal embedding of a Riemann surface.

Keywords: *Poiseuille flow; conformal embedding; nonconstant viscosity.*

Mathematics Subject Classification (2010): 76D06, 76M40, 35F10.

1 Introduction

Consider the steady Navier-Stokes equations

$$\begin{aligned} (\boldsymbol{u}\cdot\nabla)\boldsymbol{u} + \frac{1}{\rho}\nabla p &= \nu\Delta\boldsymbol{u} && \text{in } \Omega,\\ \nabla\cdot\boldsymbol{u} &= 0 && \text{in } \Omega,\\ \boldsymbol{u} &= \boldsymbol{0} && \text{on } \partial\Omega, \end{aligned}$$

in a long uniform tube $\Omega = \Omega_0 \times \mathbb{R}$ with the circular section

$$\Omega_0 := \{(x_1, x_2) \in \mathbb{R}^2;\ (x_1 - a)^2 + (x_2 - b)^2 < R^2\}.$$

Here, $\boldsymbol{u} = (u_1, u_2, u_3), p, \nu$ and ρ stand for the velocity field, the pressure, the viscosity and the density, respectively. We assume that ν and ρ are constant.

The solution of this problem with the additional assumption $u_1 = u_2 = 0$ is known as the Poiseuille flow. If this is the case, the pressure has a constant gradient $(0, 0, dp/dx_3)$ and u_3 is given by

$$u_3 = \frac{R^2 - (x_1 - a)^2 - (x_2 - b)^2}{4\nu\rho}\frac{dp}{dx_3}$$

* Corresponding author: mailto:hataya@yamaguchi-u.ac.jp

(see, e.g. [1]).

In the present paper we shall consider another kind of Poiseuille flow; the viscosity ν is not a priori supposed to be constant. The corresponding Navier-Stokes equations are then

$$(\boldsymbol{U}\cdot\nabla)\boldsymbol{U}+\frac{1}{\rho}\nabla p=\nabla\cdot(\nu\mathbb{T}(\boldsymbol{U})) \qquad \text{in } \Omega, \tag{1}$$

$$\nabla\cdot\boldsymbol{U}=0 \qquad \text{in } \Omega, \tag{2}$$

$$\boldsymbol{U}=\boldsymbol{0} \qquad \text{on } \partial\Omega, \tag{3}$$

where $\mathbb{T}(\boldsymbol{U})=(U_{i,x_j}+U_{j,x_i})_{ij}$ stands for the deformation tensor. We assume furthermore that $b>R$, i.e., the section Ω_0 lies entirely in the upper half plane $\{(x_1,x_2)\in\mathbb{R}\,;\,x_2>0\}$ and that the velocity field $\boldsymbol{U}=(U_1,U_2,U_3)$ in (2) satisfy

$$U_1=U_2=0,\ U_3=\frac{R^2-(x_1-a)^2-(x_2-b)^2}{2Rx_2}. \tag{4}$$

This assumption means that the section is a non-euclidean disk and the velocity component U_3 describes a paraboloid in the non-euclidean sense.

We now explain shortly the reason why we are interested in U_3. For this purpose we first note that the function u_3 is closely connected with the theory of conformal mapping of a multiply connected plane domain. To be more precise, let D be an arbitrary but fixed domain in the (finite) complex z plane and $\zeta\in D$ be a fixed point. We consider all the (one-to-one) conformal mapping f of D into the Riemann sphere $\hat{\mathbb{C}}=\mathbb{C}\cup\{\infty\}$ such that

$$f(z)=\frac{1}{z-\zeta}+\kappa_f(z-\zeta)+\lambda_f(z-\zeta)^2+\cdots, \qquad \kappa_f,\lambda_f,\cdots\in\mathbb{C},$$

about ζ. It is a classical result that κ_f describes a (euclidean) closed disk in the complex plane. If we realize the disk as Ω_0, then $u_3(x_1,x_2)$ represents the maximum area of $\hat{\mathbb{C}}\setminus f(D)$ for the function f with $\kappa_f=x_1+ix_2$. We thus see that the velocity of the classical Poiseuille flow coincides with the (maximum) area function in the theory of conformal mapping of a planar Riemann surface.

We have shown in [3] that an analogous theorem holds for the conformal embeddings of a noncompact Riemann surface S of genus one into (marked compact) tori T. The moduli of T accept the rôle which the coefficients κ_f played in the planar case, and the maximum area $|f(S)|$ of $f(S)$ for various conformal embeddings f of S into a fixed torus T is described by a constant multiple of the function u_3. That is, the function u_3 works for the Riemann surface R of genus one as well as for the plane domain D. In [3] we have proved more: the function U_3 describes the maximum ratio $|f(S)|/|T|$ for the fixed torus T.

Note that the unknown function in (2) is not the velocity $\boldsymbol{U}$ but the viscosity coefficient ν. We shall find a smooth function ν so that the vector $\boldsymbol{U}=(0,0,U_3)$ is the velocity of a steady flow in the tube of an incompressible fluid with the viscosity ν.

Since the viscosity ν is affected by, say, the temperature, it may change point to point in the tube, when the ambient space of the tube is of nonconstant temperature. Hence, the nonconstant character of ν would be expected to be realistically important.

2 Main Theorem

In the following, we assume the density $\rho > 0$ to be constant. The problem with which we are concerned in the present paper is:

Problem. *Find the pressure* $p = p(x_3)$ *and the smooth viscosity* $\nu = \nu(x_1, x_2)$, *for which* $(\boldsymbol{U}, p)$ *satisfies* (1)–(3).

Our goal is the following:

Theorem 2.1 *The system* (1)–(3) *has a unique smooth solution* $(\nu(x_1, x_2), p(x_3))$. *The pressure is given by* $p = \gamma\rho x_3 + \gamma'$, *where* γ, γ' *are constants with* $\gamma < 0$, *and* ν *is given by*

$$\nu(x_1, x_2) = \begin{cases} -\dfrac{\gamma R x_2^2}{(x_1 - a)^2}\left[-x_2 + c + \dfrac{(x_1 - a)^2 + x_2^2 - c^2}{2(x_1 - a)}\right. \\ \qquad\qquad \left. \times \mathrm{Sin}^{-1}\dfrac{2(x_1 - a)(x_2 + c)}{(x_1 - a)^2 + (x_2 + c)^2}\right], & \textit{if } x_1 \neq a, \\ -\dfrac{2}{3}\gamma R \dfrac{x_2^2(x_2 + 2c)}{(x_2 + c)^2}, & \textit{if } x_1 = a, \end{cases} \tag{5}$$

where $c = \sqrt{b^2 - R^2}$.

3 Proof of Theorem

In this proof, we shall denote U_3 by U for simplicity. The deformation tensor of the velocity (4) is then written as

$$\mathbb{T}(\boldsymbol{U}) = \begin{pmatrix} 0 & 0 & U_{x_1} \\ 0 & 0 & U_{x_2} \\ U_{x_1} & U_{x_2} & 0 \end{pmatrix}.$$

We thus rewrite equation (1) as

$$\frac{1}{\rho}\nabla p = (0, 0, (\nu U_{x_1})_{x_1} + (\nu U_{x_2})_{x_2}).$$

From this equation we see first of all that $dp/dx_3 = \gamma\rho$ holds with a constant γ. We have then a PDE for ν of the first order:

$$\nu_{x_1} U_{x_1} + \nu_{x_2} U_{x_2} + \nu \Delta U = \gamma. \tag{6}$$

For later use we first note the following basic expressions.

$$U_{x_1}(x_1, x_2) = -\frac{x_1 - a}{R x_2}, \tag{7}$$

$$U_{x_2}(x_1, x_2) = \frac{(x_1 - a)^2 - x_2^2 + c^2}{2R x_2^2}, \tag{8}$$

$$\Delta U(x_1, x_2) = -\frac{(x_1 - a)^2 + x_2^2 + c^2}{R x_2^3}. \tag{9}$$

Associated with (6) we now consider another equation

$$dx_1/U_{x_1} = dx_2/U_{x_2}, \tag{10}$$

or

$$\left\{(x_1-a)^2 - x_2^2 + c^2\right\} dx_1 + 2(x_1-a)x_2\,dx_2 = 0. \tag{11}$$

A solution of (10) (or (11)) is called a characteristic curve of (6). For general discussion of characteristic curves, see e.g. [2].

We can solve (11) and obtain the family of curves

$$C_k : \begin{cases} x_2^2 = c^2 - (x_1-a)(x_1-k), & \text{if } k \neq a, \\ x_1 = a,\ x_2 > 0, & \text{if } k = a. \end{cases} \tag{12}$$

It is easy to see that C_a is a characteristic curve. On the other hand for $k \neq a$, the function

$$\Phi(x_1,x_2) := \frac{x_1(x_1-a) + x_2^2 - c^2}{x_1-a} \quad \left[= x_1 + \frac{x_2^2-c^2}{x_1-a}\right] \tag{13}$$

satisfies

$$\frac{\partial \Phi}{\partial x_1} = \frac{(x_1-a)^2 - x_2^2 + c^2}{(x_1-a)^2}, \tag{14}$$

$$\frac{\partial \Phi}{\partial x_2} = \frac{2x_2}{x_1-a}. \tag{15}$$

Then, along the curve

$$\Phi(x_1,x_2) = k \tag{16}$$

for a constant k, the identity

$$0 = d\Phi = \frac{\partial \Phi}{\partial x_1}dx_1 + \frac{\partial \Phi}{\partial x_2}dx_2 = \frac{(x_1-a)^2 - x_2^2 + c^2}{(x_1-a)^2}dx_1 + \frac{2x_2}{x_1-a}dx_2$$

holds, which shows that (16) is a characteristic curve of (6) for any constant k. That is, (12) are the characteristic curves of (6). We observe that each characteristic curve C_k $(k \neq a)$ represents a half-circle

$$\left(x_1 - \frac{a+k}{2}\right)^2 + x_2^2 = d_k^2, \qquad x_2 > 0, \tag{17}$$

of the radius d_k:

$$d_k := \sqrt{c^2 + \left(\frac{a-k}{2}\right)^2}. \tag{18}$$

We remark that each curve C_k $(k \in \mathbb{R})$ passes through the point (a,c). Furthermore for each (x_1,x_2) other than (a,c), there exists a unique $k \in \mathbb{R}$ such that C_k passes through (x_1,x_2).

We now fix a $k \in \mathbb{R} \setminus \{a\}$ and consider the characteristic curve C_k. On this curve we can express x_2 as a single-valued function of x_1, since $x_2 > 0$ for the present problem. We next consider the function $\tilde{\nu}(x_1) := \nu(x_1, x_2(x_1))$ on (17). Since

$$\frac{d\tilde{\nu}}{dx_1} = \frac{\partial \nu}{\partial x_1} + \frac{\partial \nu}{\partial x_2}\frac{dx_2}{dx_1} = (\nu_{x_1}U_{x_1} + \nu_{x_2}U_{x_2})\,\frac{1}{U_{x_1}},$$

our equation (6) becomes now of the form

$$\frac{d\tilde{\nu}}{dx_1} + \tilde{\nu}\frac{\Delta U}{U_{x_1}} = \frac{\gamma}{U_{x_1}}, \tag{19}$$

or, equivalently

$$\frac{d}{dx_1}\left(\tilde{\nu}(x_1)\exp\int\frac{\Delta U}{U_{x_1}}\,dx_1\right) = \frac{\gamma}{U_{x_1}}\exp\int\frac{\Delta U}{U_{x_1}}\,dx_1. \tag{20}$$

To solve this equation explicitly we first observe that

$$\frac{\Delta U(x_1,x_2)}{U_{x_1}(x_1,x_2)} = \frac{(x_1-a)^2+x_2^2+c^2}{(x_1-a)x_2^2}, \tag{21}$$

which follows immediately from (7) and (9). This, together with equation (12), yields

$$\frac{\Delta U(x_1,x_2)}{U_{x_1}(x_1,x_2)} = \frac{(x_1-a)(x_1-k)-(x_1-a)^2-2c^2}{(x_1-a)\{(x_1-a)(x_1-k)-c^2\}}. \tag{22}$$

If we denote by α and β the roots of the quadratic equation $(x_1-a)(x_1-k)-c^2=0$, we have

$$\frac{\Delta U(x_1,x_2)}{U_{x_1}(x_1,x_2)} = \frac{2}{x_1-a} - \frac{1}{x_1-\alpha} - \frac{1}{x_1-\beta}. \tag{23}$$

As usual, we can ignore an integration constant and obtain

$$\int\frac{\Delta U}{U_{x_1}}dx_1 = \log\frac{(x_1-a)^2}{c^2-(x_1-a)(x_1-k)}. \tag{24}$$

Hence we have

$$\frac{\gamma}{U_{x_1}}\exp\int\frac{\Delta U}{U_{x_1}}\,dx_1 = -\gamma R\cdot\frac{x_1-a}{x_2} \tag{25}$$

along the characteristic curve C_k $(k \neq a)$.

In order to integrate (20), it is convenient to parametrize the curve (17). Namely, for each k, we consider the parametrization

$$\begin{cases} x_1 = -d_k\sin\theta + \dfrac{a+k}{2}, \\ x_2 = d_k\cos\theta, \end{cases} \quad (-\pi/2 < \theta < \pi/2) \tag{26}$$

of the curve (12). Then, according to (17), (18) and (26), the function $\tilde{\nu}(x_1) = \nu(x_1, x_2(x_1))$ can be expressed as $\tilde{\nu}(k,\theta) = \nu(x_1(k,\theta), x_2(k,\theta))$. Let θ_k $(-\pi/2 < \theta_k < \pi/2)$ be the value of θ for which

$$\begin{cases} a = -d_k\sin\theta_k + \dfrac{a+k}{2}, \\ c = d_k\cos\theta_k, \end{cases} \tag{27}$$

holds.

Because of the relation $dx_1 = -d_k \cos\theta d\theta = -x_2 d\theta$ on C_k we have

$$\begin{aligned}\int_a^{x_1} \left(\frac{\gamma}{U_{x_1}} \exp \int \frac{\Delta U}{U_{x_1}} \, dx_1 \right) dx_1 &= -\gamma R \int_a^{x_1} \frac{x_1 - a}{x_2} \, dx_1 \\ &= \gamma R \left\{ d_k(\cos\theta - \cos\theta_k) + \frac{k-a}{2}(\theta - \theta_k) \right\}.\end{aligned}$$

Noting that $\dfrac{k-a}{2} = d_k \sin\theta_k$, we have

$$\int_a^{x_1} \left(\frac{\gamma}{U_{x_1}} \exp \int \frac{\Delta U}{U_{x_1}} \, dx_1 \right) dx_1 = d_k \gamma R \{ (\cos\theta - \cos\theta_k) + (\theta - \theta_k) \sin\theta_k \}. \tag{28}$$

Now, in virtue of equation (25) we obtain

$$\tilde{\nu}(k, \theta) = d_k \gamma R \cos^2\theta \cdot \frac{(\cos\theta - \cos\theta_k) + (\theta - \theta_k)\sin\theta_k}{(\sin\theta - \sin\theta_k)^2}. \tag{29}$$

This is the solution of (19) on C_k $(k \neq a)$.

We shall next solve (6) on the characteristic curve C_a. On the half line $\{(a, x_2)\,;\, x_2 > 0\}$, equations (1)–(3) reduce to

$$\nu'(a, x_2) \frac{c^2 - x_2^2}{2Rx_2^2} - \nu \frac{x_2^2 + c^2}{Rx_2^3} = k.$$

It has a unique continuous solution

$$\nu(a, x_2) = -\frac{2}{3} \gamma R \, \frac{x_2^2(x_2 + 2c)}{(x_2 + c)^2}. \tag{30}$$

The function

$$\nu(x_1, x_2) := \begin{cases} \tilde{\nu}(k(x_1, x_2), \theta(x_1, x_2)), & \text{for } (x_1, x_2) \in C_k, \ k \neq a, \\ \nu(a, x_2), & \text{for } (x_1, x_2) \in C_a \end{cases}$$

is now well-defined on $\Omega_0 \setminus (a, c)$, since for each $(x_1, x_2) \neq (a, c)$ we can find a unique $k \in \mathbb{R}$ with $(x_1, x_2) \in C_k$. If (x_1, x_2) approaches to (a, c) along a characteristic curve C_k, the function $\nu(x_1, x_2)$ has a finite limit which is independent of k. To show this, we first discuss the case $k \neq a$. We can then apply the de l'Hôpital theorem to obtain

$$\lim_{\theta \to \theta_k} \frac{(\cos\theta - \cos\theta_k) + (\theta - \theta_k)\sin\theta_k}{(\sin\theta - \sin\theta_k)^2} = \lim_{\theta \to \theta_k} \frac{-\sin\theta + \sin\theta_k}{2(\sin\theta - \sin\theta_k)\cos\theta} = -\frac{1}{2\cos\theta_k}.$$

Consequently along each C_k, we have

$$\lim_{(x_1, x_2) \to (a, c)} \nu(x_1, x_2) = -\frac{c\gamma R}{2}.$$

If $k = a$, it is easy to see $\nu(a, x_2) \to -c\gamma R/2$ as $x_2 \to c$ along C_a. Hence, $\nu(x_1, x_2)$ is a continuous function on Ω_0.

We next rewrite the function ν explicitly in terms of the euclidean coordinates (x_1, x_2). In virtue of (26), we have

$$\sin(\theta - \theta_k) = -\frac{1}{2d_k^2}\frac{(x_2+c)\{(x_1-a)^2+(x_2-c)^2\}}{x_1-a}.$$

Since

$$d_k^2 = \frac{\{(x_1-a)^2+(x_2+c)^2\}\{(x_1-a)^2+(x_2-c)^2\}}{4(x_1-a)^2},$$

by (16) and (18), we obtain

$$\sin(\theta - \theta_k) = \frac{-2(x_1-a)(x_2+c)}{(x_1-a)^2+(x_2+c)^2}. \tag{31}$$

If we substitute (26), (27) and (31) into (29), we conclude

$$\nu(x_1,x_2) = -\frac{\gamma R x_2^2}{(x_1-a)^2}\left[-x_2+c+\frac{(x_1-a)^2+x_2^2-c^2}{2(x_1-a)} \times \mathrm{Sin}^{-1}\frac{2(x_1-a)(x_2+c)}{(x_1-a)^2+(x_2+c)^2}\right]$$

for $x_1 \neq a$.

Finally we shall show ν is $C^1(\Omega_0)$. In fact, putting $y = \dfrac{2(x_1-a)(x_2+c)}{(x_1-a)^2+(x_2+c)^2}$ in the Maclaurin series

$$\mathrm{Sin}^{-1}y = \sum_{j=0}^{\infty}\frac{(2j)!}{2^{2j}\,(j!)^2}\,\frac{y^{2j+1}}{2j+1},$$

we have the expansion

$$-\frac{\nu(x_1,x_2)}{\gamma R x_2^2} = \frac{2}{3}\frac{x_2+2c}{(x_2+c)^2} + O(|x_1-a|^2).$$

Thus $\dfrac{\partial\nu}{\partial x_1}(a,x_2)$ exists and equals to 0. Since the regularity of $\nu(x_1,x_2)$ is obvious except the half line $\{(a,x_2)\,;\,x_2>0\}$, we conclude that ν is continuously differentiable in Ω_0.

Remark. From (5), we can see $\gamma < 0$ if the viscous constant ν is positive.

References

[1] Batchelor, G. K. An Introduction to Fluid Dynamics. Cambridge University Press, Cambridge, 1970.

[2] Garabedian, P. Partial Differential Equations. Wiley, New York, 1964.

[3] Shiba, M. The euclidean, hyperbolic, and spherical spans of an open Riemann surface of low genus and the related area theorems. *Kodai Math. J.* **16** (1993) 118–137.

Nonlinear Dynamics and Systems Theory, **13** (1) (2013) 55–68

Double Hyperchaotic Encryption for Security in Biometric Systems

E. Inzunza-González [1] and C. Cruz-Hernández [2*]

[1] *Faculty of Engineering, Architecture and Design, Baja California Autonomous University (UABC), Km. 103 Carret. Tijuana-Ensenada, Ensenada, B.C., 22860, México.*
[2] *Electronics and Telecommunications Department, Scientific Research and Advanced Studies of Ensenada (CICESE), Carretera Ensenada-Tijuana No. 3918, Zona Playitas, 22860 Ensenada, B.C. México.*

Received: November 12, 2012; Revised: January 21, 2013

Abstract: In this paper, a novel method for double image encryption is proposed by using different hyperchaotic maps. The proposed algorithm is implemented in a biometric system. In particular, for face pattern recognition, the eigenfaces approach is used, and to encrypt biometric information the Rössler and Chen hyperchaotic maps are exploited. The simulation and experimental results show that the security analysis performed to the double encryption algorithm implemented, is strong against known different attacks, such as: brute force, statistical, differential, and information entropy. Therefore, the proposed double encryption algorithm is suitable for use in biometric systems based on face recognition which operate remotely.

Keywords: *chaotic encryption; hyperchaotic maps; biometric systems; eigenface; face recognition; information security.*

Mathematics Subject Classification (2010): 68P25, 94A60, 11T71, 14G50, 68T10.

* Corresponding author: mailto:ccruz@cicese.mx

1 Introduction

A facial recognition system is an application run by computer to automatically identify a person from a digital image, by comparing selected facial features from a digital image or a frame from a video source. One way to do this is by comparing selected facial features with a facial image database, see Figure 1. The face recognition systems have less uniqueness than recognition systems based on fingerprint and iris, however, provides a more direct form of identification, friendly and is more acceptable compared with other biometric personal identification systems [32]. Therefore, research on face recognition has become one of the most important issues in biometric systems.

The first semi-automated system for face recognition required the administrator to located features (such as eyes, ears, nose, and mouth) on the photographs before it calculated distances and ratios to a common reference point, which were compared with reference data. Goldstein *et al.* [14] used 21 specific subjective markers such as hair and lip thickness to automate the recognition. The problem was that the measurements and locations were manually computed.

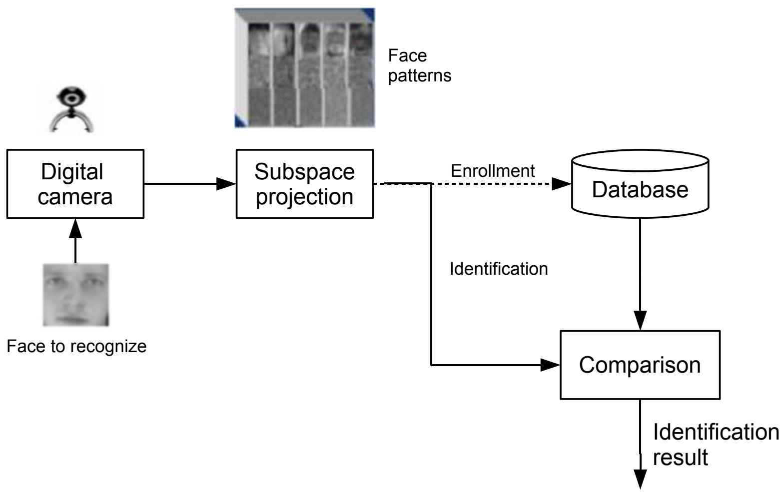

Figure 1: Scheme of a general biometric system based on face image.

On the other hand, the idea of using eigenfaces was motivated by a technique developed by Sirovich and Kirby in [28] and by Kirby and Sirovich in [19] for efficiently representing pictures of faces by using *Principal Components Analysis (PCA).* They argued that a collection of face images can be approximately reconstructed by storing a small collection of weights for each face and a small set of standard pictures. PCA method reported in [28] and [19] is also called *eigenfaces* by Turk and Pentland in [29, 30], this appearance-based technique is used widely for the dimensionality reduction and recorded a great performance in face recognition. PCA is a standard linear algebra technique, to the face recognition problem [28]. This was considered somewhat of a milestone as it showed that less than one hundred values were required to accurately code a suitably aligned and normalized face image [28]. Turk and Pentland discovered that while using the eigenfaces technique, the residual error could be used to detect faces in images [29,30].

This was a discovery that enabled reliable real-time automated face recognition systems. Although the approach was somewhat constrained by environmental factors, it nonetheless created significant interest in furthering development of automated face recognition technologies. Among the most important methods for face recognition are: eigenface [32], fisherface [7], dual eigen space [32], and neural networks [20].

Current literature reports many techniques for human face recognition, see e.g. [7, 14, 16, 19, 20, 25, 28–30, 32], on the other hand, there are many works about image encryption algorithms based on chaos for secure communications, see e.g. [1–3,6,9,10,21,24]. Recently, encryption in biometric systems has been applied, see e.g. [4, 5, 8, 15, 18, 22] with the purpose of protecting biometric information. Nevertheless, to our knowledge, any approach of a secure biometric system, particularly about face patterns recognition that works remotely with double hyperchaotic encryption has not been reported. Hyperchaotic maps are theoretically proofed with good randomness, infinite period, and unpredictability on long term [11]. These complex maps are usually defined as a system characterized at least by two positive Lyapunov exponents which provide more complex waveforms than simply chaotic maps. Consequently, these hyperchaotic maps have the characteristics of high capacity, high security, and high efficiency [11].

The aim of this paper, is to improve the security encryption in a biometric system based on human face recognition. In particular, we use a double hyperchaotic encryption in a face recognition system which works remotely, the eigenface method to get the face patterns is used, see e.g. [7, 29, 30, 32], next, Rössler and Chen hyperchaotic maps to encrypt face patterns are used. In this work, the proposed secure biometric system, is similar to the reported in [22], but there are fundamental differences with respect to that work: (1) they encrypt iris templates by using the generalized Hénon map and 1D logistic map. In this paper, the Rössler and Chen hyperchaotic maps for face pattern double encryption are used; (2) they used in the quantizer a threshold equal to 0.5, however, we optimize the threshold to improve security; (3) they extracted iris features, in this work we extract face patterns; (4) for features extraction they used a test of statistical independence reported in [12], we use eigenface method reported in [29, 30]; (5) they only reported brief analysis on sensitivity of initial conditions. Nevertheless, we provide a complete security analysis.

The organization of this paper is as follows: In Section 2, a brief review on eigenfaces approach is given. In Section 3, the proposed algorithm to encrypt and decrypt is described. In Section 4, the main results of this work are presented. The paper is concluded with some remarks in Section 5.

2 Review on Eigenfaces Approach

PCA approaches include two phases: enrollment and identification (see Figure 1). In the enrollment phase, an eigenspace is established from the training samples by using PCA and the training face images are mapped to the eigenspace for identification. In the identification phase, an input face is projected to the same eigenspace and identified by an appropriate classifier. For details of this method, see e.g. [29, 30, 32]. The approach for face recognition involves the following initial operations:

1. Acquire an initial set of face images (the training set).

2. Calculate the eigenfaces from the training set, keeping only M images that correspond to the highest eigenvalues. These M images define the face space. As new

faces are experienced, the eigenfaces can be updated or recalculated.

3. If it is a face, classify the weight pattern as either a known person or as unknown.

4. Update the eigenfaces and/or weight patterns (optional).

5. If the same unknown is seen several times, calculate its characteristic weight pattern and incorporate into the known faces (optional).

2.1 Calculating eigenfaces

A human face image can be considered as a stochastic sample, and each face image is considered as a higher dimensional vector and each pixel corresponds to a component. If all the face images lie in the same subspace of the higher dimensional space, this subspace is a good representation of face images because it shows the common features of faces. So, detection of faces is to find the subspace.

Suppose $A = [a_{ij}]_{r\times c}$ as a human face image, where r and c are the number of rows and columns of the images, respectively; a_{ij} is the gray value of the pixel in *i-th* row and *j-th* column. Re-arrange a_{ij} and make it a column vector

$$x^i = [a_{11}\ a_{21}\ ...\ a_{r1}\ a_{12}\ a_{22}\ ...\ a_{r2}\ ...\ a_{1c}\ a_{2c}\ ...\ a_{rc}]^T, \tag{1}$$

where x^i is a *D-dimensional* vector, $D = r\times\ c$.

Next, the images are *mean centered* by subtracting the mean image from each image vector,

$$\overline{x}^{\,i} = x^i - m, \tag{2}$$

where m is the average vector of the training specimens set, and is given by

$$m = \frac{1}{M}\sum_{i=0}^{M-1} x^i. \tag{3}$$

Vectors from Eq. (2) are combined side by side to create a data matrix of size $D\times M$, where M is the number of images in the training specimens set,

$$\overline{X} = \left\{\ \overline{x}^1 \mid \overline{x}^2 \mid ... \mid \overline{x}^P\ \right\}, \tag{4}$$

the covariance matrix can be calculated as

$$\Omega = \overline{X}\cdot\overline{X}^T. \tag{5}$$

This covariance matrix has up to d eigenvectors associated with non-zero eigenvalues, assuming $d < D$.

Let $\lambda_1,\ \lambda_2,\ ...\ ,\ \lambda_d$ ($\lambda_1 \geqslant \lambda_2 \geqslant\ ...\ \geqslant \lambda_d > 0$) and $u_1,\ u_2,\ ...\ ,\ u_d$ be eigenvalues and corresponding eigenvectors of the covariance matrix Ω, respectively. So, every human face image, x^i, can be represented by the linear combination of the eigenvectors. According to the algebra theory, we know that $u_1,\ u_2\ ,\ ...\ ,\ u_d$ will be orthogonal one another and unit vector. Usually, $M < D$, can be satisfied because D is larger than the number of the specimens. Then $d < D$ is derived. In other words, the given human face image can be represented by fewer base vectors (d vectors) [32].

Some values λ_i, in d eigenvalues are very small, whose corresponding eigenvectors give little contribution to represent the face image specimens, hence they can be ignored. Thus, we sort the eigenvectors according to the decreasing eigenvalues, and select the top k eigenvectors to represent the specimens [32].

If we choose k as a very big number, for example $k = d$. But we know some eigenvectors have little contribution to face space. On the contrary, if we select k as a very small number, for example $k = 1$, then the subspace is not sufficient to represent the face image specimens. Usually, we can select the smallest k which satisfies the following expression [32]

$$\frac{\sum\limits_{i=0}^{k} \lambda_i}{\sum\limits_{i=0}^{M-1} \lambda_i} \geqslant \alpha, \tag{6}$$

where α is a real number, which is close to 100%, such as 99%. It states that the top k axes have 99% energy of all axes.

2.1.1 Ordering eigenvectors

Order the eigenvectors $u_i \in U$ according to their corresponding eigenvalues λ_i from high to low. Keep only the eigenvectors associated with non-zero eigenvalues. This matrix of eigenvectors is the eigenspace U, where each column of U is an eigenvector,

$$U = [\, u_1 \mid u_2 \mid \cdots \mid u_d \,]. \tag{7}$$

2.1.2 Projecting training images

To project the training images, each of the centered training images from Eq. (2) must be projected into the eigenspace. To project an image into the eigenspace, we need to calculate the dot product of the image with each of the ordered eigenvectors from Eq. (7) as follows,

$$\widetilde{x}^{\,i} = U^{T} \overline{x}^{i}. \tag{8}$$

Therefore, the dot product of the image and the first eigenvector will be the first value in the new vector. The new vector calculated from Eq. (8) of the projected image must contain the same values as eigenvectors.

2.1.3 Identifying test images

Each test image is first mean centered by subtracting the mean image, and is then projected into the same eigenspace defined by U as follows,

$$\overline{y}^{\,i} = y^i - m, \tag{9}$$

where m is calculated from Eq. (3), and $\overline{y}^{\,i}$ is the centered test image.

Then project this centered test image according to

$$\widetilde{y}^{\,i} = U^{T}\, \overline{y}^{\,i}. \tag{10}$$

The projected test image ($\widetilde{y}^{\,i}$) is compared to every projected training image and the training image that is found to be nearest to the test image is used to identify the input image (test images).

These images can be compared by using any number of similarity measures, the most common is the L_2 norm or Euclidian distance as follows,

$$\varepsilon^2 = \left\| \widetilde{y}^{\,i} - \widetilde{x}^{\,k} \right\|_2, \tag{11}$$

where $\widetilde{x}^{\,k}$ is a vector describing the k^{th} face class. A face is classified as belonging to class k when the minimum ε is below some chosen threshold θ_ε. Otherwise the face is classified as "unknown".

3 Encryption and Decryption Algorithm

3.1 Double encryption algorithm

The Rössler hyperchaotic map is described by the following equations [2]:

$$\begin{aligned} x_1(k+1) &= \alpha x_1(k)(1 - x_1(k)) - \beta(x_3 + \gamma)(1 - 2x_2(k), \\ x_2(k+1) &= \delta x_2(k)(1 - x_2(k) + \zeta x_3(k), \\ x_3(k+1) &= \eta((x_3(k) + \gamma)(1 - 2x_2(k)) - 1)(1 - \theta x_1(k)), \end{aligned} \tag{12}$$

with parameters $\alpha = 3.8$, $\beta = 0.05$, $\gamma = 0.35$, $\delta = 3.78$, $\zeta = 0.20$, $\eta = 0.10$, $\theta = 1.9$, and initial conditions: $x_1(0) = 0.10$, $x_2(0) = 0.15$, and $x_3(0) = 0.01$; the map (12) exhibits hyperchaotic dynamics [2]. Figure 2 shows the hyperchaotic attractor generated by the Rössler map projected on the (x_1, x_2, x_3)-plane.

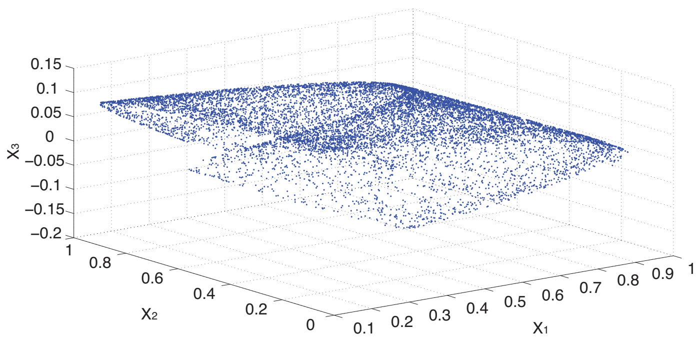

Figure 2: Hyperchaotic attractor generated by Rössler map (12).

On the other hand, the Chen hyperchaotic map is described by the following equations [1]:

$$\begin{aligned} x_1(k+1) &= 1 - a(x_1^2(k) + x_2^2(k)), \\ x_2(k+1) &= -2abx_1(k)x_2(k), \end{aligned} \tag{13}$$

with parameters $a = 1.95$ y $b = 1$, and initial conditions: $x_1(0) = 0.025$ and $x_2(0) = 0.025$; the map (12) exhibits hyperchaotic dynamics [1]. Figure 3 shows the

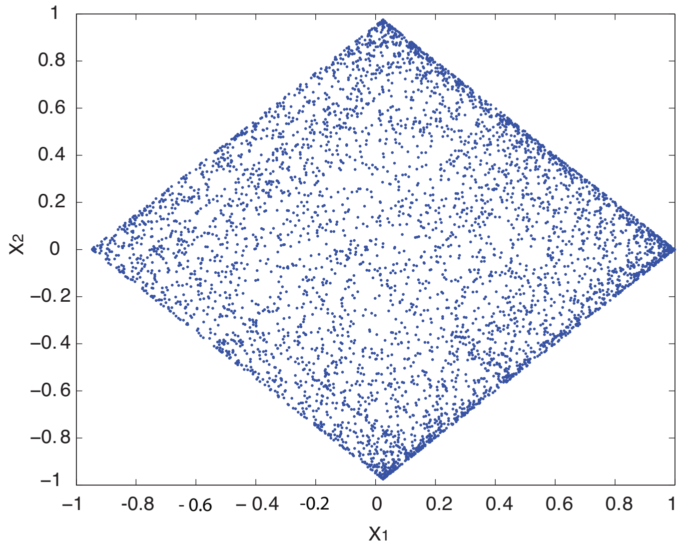

Figure 3: Hyperchaotic attractor generated by Chen map (13).

hyperchaotic attractor generated by the Chen map projected on the (x_1, x_2)-plane.

The proposed double encryption scheme in this work to encrypt face patterns is shown in Figure 4. Where the inputs to the scheme are the face patterns and initial conditions as encryption key for the hyperchaotic maps Eq. (12) and (13). Later, the face pattern is converted to binary secuence, and then the two X-OR operation is performed with the generated hyperchaotic signal by Rössler map, prior to operating X-OR, the hyperchaotic signal, also has to be digitized, this is done by using a quantizer. In the quantizer a threshold can be established between 0 and 1, for example in [22] 0.5 was used for the Hénon map. When the amplitude of the hyperchaotic signal is greater than or equal to 0.5, the output of the quantizer is at a higher level, whereas when the amplitude of the hyperchaotic signal is less than 0.5, the quantizer output is at a low-level. In this work, the threshold was optimized to obtain the best entropy and therefore better security levels, so the best threshold for Rössler and Chen hyperchaotic map are 0.59 and 0.14 respectively. Then, the result of the X-OR operation between the digitized face pattern and the hyperchaotic signals in binary format, also is a binary signal called encrypted face pattern, which is sent through a public network.

3.2 Double decryption algorithm

Figure 5 shows the double decryption scheme, to recover the original face pattern at the receiver end, the reverse process of encryption must be followed, i.e., it receives the encrypted face pattern and introduces the same key used for the encryption (the same initial conditions of the two hyperchaotic maps). Similarly, the generated hyperchaotic signal, is applied to a quantizer to be converted to a binary format, the threshold of the quantizer has to be the same as the two used to encrypt the face pattern. Then apply the two X-OR operation between the encrypted face pattern and hyperchaotic binary signals. The result of this operation is also a string of bits, then these bits are grouped

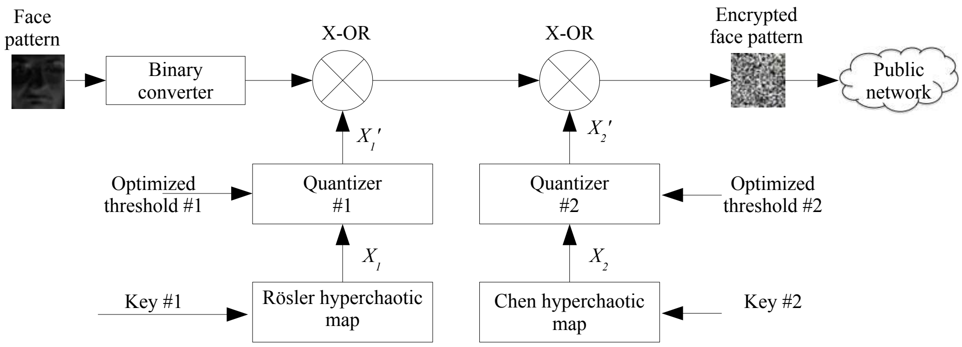

Figure 4: Double encryption scheme for face patterns.

into 8 bits to form the corresponding level of gray of each pixel, lastly it rebuilds the image of the recovered face pattern.

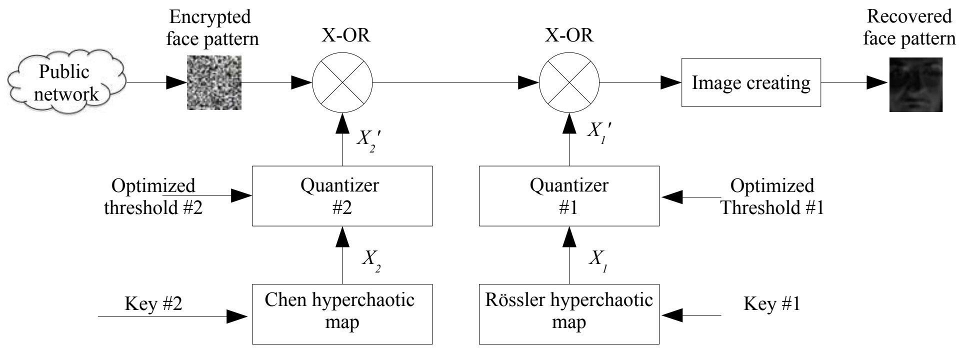

Figure 5: Double decryption scheme for recovered face patterns.

4 Results

4.1 Security analysis

4.1.1 Key space analysis

The key of the proposed cryptosystem consists of two parts: a) the initial conditions of the two hyperchaotic maps (Rössler and Chen), (b) the control parameters of these maps. Thus, there are five initial conditions and nine parameters in our algorithm. According to the IEEE standard for floating point arithmetic [17], the computational precision of 64 bits numbers is 1×10^{-16}, so the secret key's space is $10^{16} \times 10^{16} \times 10^{16} \times 10^{16} \times 10^{16} \times 10^{16} \times 10^{16} \times 10^{16} \times 10^{16} \times 10^{16} \times 10^{16} \times 10^{16} \times 10^{16} \times 10^{16} = 10^{224}$, therefore in a binary system it is equal to 2^{744}, so the secret key's space is large enough to resist exhaustive attack.

4.1.2 Statistical analysis

Figure 6(a) shows the face pattern #1 and the Figure 6(d) shows its corresponding histogram, this pattern was encrypted by using the Rössler and Chen hyperchaotic maps and approach explained in Section 3. Figure 6(b) shows the encrypted face pattern with different maps using the initial conditions as an encryption key: $x_1(0) = 0.10$, $x_2(0) = 0.15$, $x_3(0) = 0.01$ and $x_1(0) = 0.025$ and $x_2(0) = 0.025$ of Rössler and Chen maps, respectively. The optimized threshold for quantizing the state x_1 of the Rössler map is 0.59, while the optimized threshold for quantizing the state x_2 of the Chen map is 0.14. Figure 6(e) shows its corresponding histogram, we can see, in the histogram from the original image 6(d), that most of the information is concentrated among the pixels that are in the range of gray level between 0 and 100. While in the histogram in Figure 6(e) the information is distributed over the entire range from 0 to 255 of the grayscale level, therefore, we can say that the system is robust against statistical attacks. Figure 6(c) shows the recovered face pattern at the receiver end, and Figure 6(f) shows its corresponding histogram, we can see that both, the recovered face pattern and the histogram are equal to the original pattern, therefore recovering 100% of the original information.

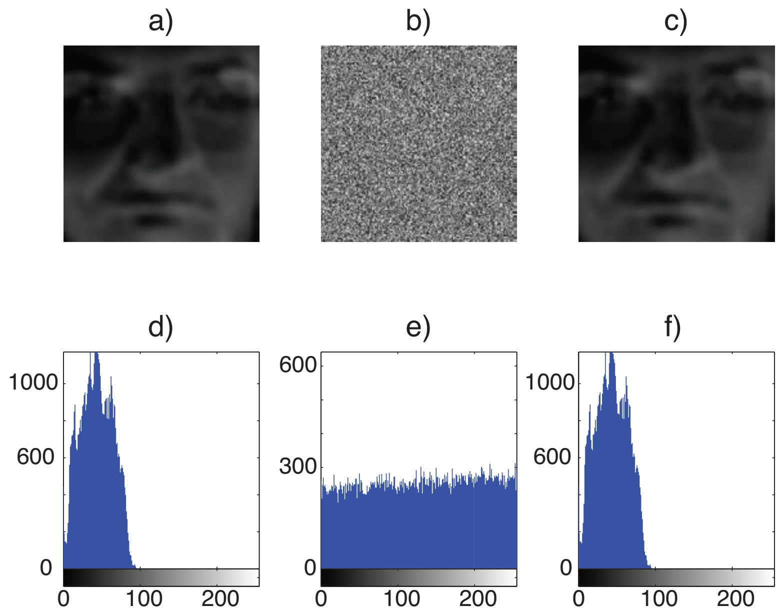

Figure 6: Top: (a) Original face pattern, (b) Encrypted face pattern, (c) Recovered face pattern. Bottom: (d) Histogram of the original face pattern, (e) Histogram of the face pattern, (f) Histogram of the recovered face pattern.

4.1.3 Correlation analysis of adjacent pixels

Shannon proposed two techniques based on the design of encrypters [26,27], the *diffusion* and *confusion*, these two properties above can be demonstrated by a test correlation of adjacent pixels in the encrypted image [9]. The correlation between two adjacent pixels was examined horizontally, vertically and diagonally. To do this, we randomly selected 2025 pairs of pixels (x_i, y_i) of the image pattern under analysis (original or encrypted), generated by scattering graphics with these pairs of adjacent pixels, i.e., the pixel is plotted x_i vs y_i. Then their corresponding correlation coefficients (r_{xy}) are calculated [9] by using the next expression,

$$r_{xy} = \frac{cov(x, y)}{\sqrt{D(x)}\sqrt{D(y)}}, \tag{14}$$

with

$$cov(x, y) = \frac{1}{N}\sum_{i=1}^{N}(x_i - E(x))(y_i - E(y)), \tag{15}$$

where $cov(x,\ y)$ is the covariance, $D(x)$ is the variance, x and y denote the scale values of gray level in the image pattern under analysis. For this numerical case, the following discrete forms were used:

$$E(x) = \frac{1}{N}\sum_{i=1}^{N} x_i, \tag{16}$$

$$D(x) = \frac{1}{N}\sum_{i=1}^{N}(x_i - E(x))), \tag{17}$$

where $E(x)$ is the average gray levels of pixels.

Figure 7(a) shows the correlation distribution of two adjacent pixels in horizontal direction of the original face pattern. Using Eq. (14), we obtain the correlation coefficient of 0.9976. Figure 7(b) shows the correlation distribution of two adjacent horizontal pixels from the encrypted face pattern, in the same way, using (14) to compute the correlation coefficient, which is -0.0082. Table 1 shows the horizontal, vertical and diagonal correlation coefficients of adjacent pixels in the original face pattern and in the encrypted face pattern. From the results of Table 1, we find that the correlation coefficients of the encrypted face pattern are close to zero, it can clearly be seen that our algorithm can destroy the relativity effectively; the proposed image encryption algorithm has a strong ability to resist statical attack.

Table 1: Correlation of adjacent pixels in the original face pattern and in the encrypted face pattern.

Pixels	**Original face pattern**	**Encrypted face pattern**
Horizontal	0.9976	-0.0082
Vertical	0.9986	0.0073
Diagonal	0.9961	0.0089

4.1.4 Differential attacks

To perform an analysis against differential attacks [9] and understand the differences between encrypted images, two measures in common are used, NPCR (Number of Pixels

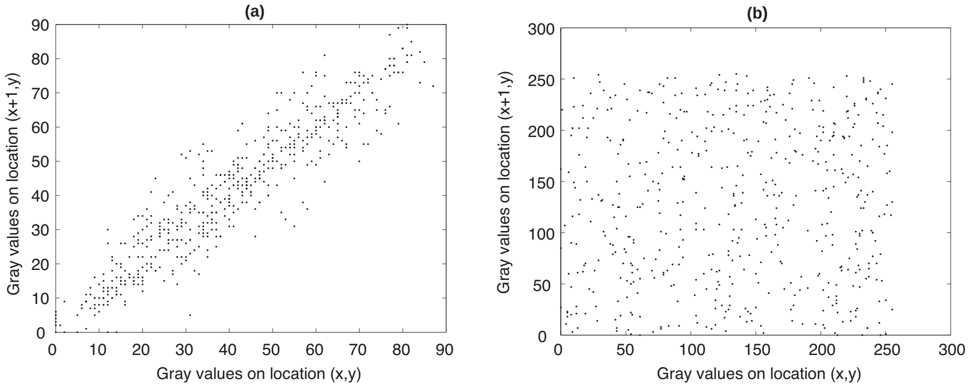

Figure 7: Correlations of two horizontally adjacent pixels in the original image and in the ciphered image: (a) Original face pattern, (b) Encrypted face pattern.

Change Rate) and UACI (Unified Average Changing Intensity). These measures are used to test the influence of change of a pixel in the whole encrypted pattern.

Number of pixels change rate (NPCR) Measures the percentage of the number of different pixels between two encrypted image patterns and can be calculated by using the following expression [9, 24],

$$NPCR = \frac{\sum_{i,j} D(i,j)}{W \times H} \times 100\%, \tag{18}$$

where $D(i,j)$ is a binary arrangement, so that:

$D(i,j) = 0$, if $C_1(i,j) = C_2(i,j)$,
$D(i,j) = 1$, where $C_1(i,j \neq C_2(i,j)$,

C_1 and C_2 are encrypted image patterns obtained with keys (initial conditions) that are very similar. W and H define the size of the image under analysis.

Unified average changing intensity (UACI) Measures the average intensity differences between two encrypted images (C_1 and C_2) by the expression [9, 24],

$$UACI = \frac{1}{W \times H} \sum_{i,j} \frac{|C_1(i,j) - C_2(i,j)|}{255} \times 100\%, \tag{19}$$

where C_1, C_2, W, and H were computed previously.

To realize the analysis against differential attacks, very similar keys are used to encrypt the original face pattern. In this case, the first encryption keys used for Rössler map are $x_1(0) = 0.10$, $x_2(0) = 0.15$, and $x_3(0) = 0.01$, for Chen map are $x_1(0) = 0.025$ and $x_2(0) = 0.025$, also we used the same parameters described in Section 3 for Rössler and Chen maps, so with these keys we obtain the encrypted face pattern C_1, the following keys used for Rössler map are $x_1(0) = 0.10 + 1e^{-10}$, $x_2(0) = 0.15$, and $x_3(0) = 0.01$, for Chen map are $x_1(0) = 0.025$ and $x_2(0) = 0.025$, also we used the same parameters described in Section 3, so we obtain the encrypted face pattern C_2. Using expressions

(18) and (19), we obtain $NPCR = 99.71\%$ and $UACI = 34.26\%$. These results show that the encryption algorithm is strong against differential attacks, because the $NPCR$ is approximate the ideal value of 100% and $UACI$ is slightly higher than 33%.

4.1.5 Information entropy

Shannon [26, 27] introduced the mathematic fundamentals of the information theory applied to communications and data storage. The information entropy is a criterion that shows the randomness of the data. In addition, it can be used to evaluate the security of encryption [31]. To calculate the entropy $H(s)$ [6] from a source (s), we have

$$H(s) = \sum_{i=0}^{2^N-1} P(s_i) \cdot Log_2(\frac{1}{P(s_i)})\ bits, \tag{20}$$

where $P(s_i)$ represents the probability of the symbol s_i.

For a purely random source, which is emitting 2^N symbols with same probability, after evaluating Eq. (20), we have an entropy $H(s) = N$, in this case, encrypted images with completely random pixels in 8 bit grayscale, have entropy $H(s) = 8$ bits. When images of patterns are encrypted, ideally its entropy must be 8. When a cryptographic system emits symbols with entropy less than 8, the encrypter has some degree of predictability, so its security is set at risk [6].

To evaluate the information entropy, from the algorithm of hyperchaotic encryption used in this paper, Eq. (20) was used. First, we calculate the probability of occurrence of each symbol (pixel), with the help of the corresponding histogram of the encrypted face pattern. In the case, of the encrypted face pattern obtained with the encryption keys $x_1(0) = 0.10$, $x_2(0) = 0.15$, and $x_3(0) = 0.01$, the entropy calculated is $H(s_i) = 7.9956$. This is a good result, because it is near (similar) to its ideal value of 8.

5 Conclusion

In this paper, we have applied double hyperchaotic encryption to face patterns in a biometric system, particularly in face recognition system which operates remotely and uses eigenface approach, this was for illustrative purposes, but other methods can be implemented easily. The double encryption algorithm presents an extremely large key space and very good statistical properties, so it effectively resists statistic attacks. Also, it has a high sensitivity to withstand differential attacks. Therefore, because the algorithm used in this work has a high security level, it can be suggested to encrypt confidential biometric information (face, iris, fingerprint, palmprint, retina, hand geometry, and facial thermogram, etc.), that will be transmitted securely through a public network, such as the internet. As future work, we propose to use 3D Discrete Generalized Hénon Map [13] and quantum dynamics [23] to encrypt biometric information.

Acknowledgment

This work was supported by CONACYT, Mexico under Research Grants No. 166654.

References

[1] Aguilar Bustos, A.Y. and Cruz-Hernández, C. Synchronization of discrete time hyperchaotic systems: An application in communications. *Chaos, Solitons and Fractals* **41**(3) (2009) 1301–1310.

[2] Aguilar Bustos A.Y., Cruz-Hernández C., López-Gutiérrez R. M. and Posadas Castillo C. Synchronization of Different Hyperchaotic Maps for Encryption. *Nonlinear Dynamics and Systems Theory* **8**(3) (2008) 221–236.

[3] Aguilar Bustos A.Y., Cruz-Hernández C., López-Gutiérrez R. M., Tlelo Cuatle E. and Posadas Castillo. C. Hyperchaotic Encryption for Secure E-mail Communication. In: *Emergent Web Intelligence, Advanced Information Retrieval*. Springer, London, 2010, 471–486.

[4] Anil K. J., Karthik N. and Abhishek N. Biometric Template Security. *EURASIP Journal on Advances in Signal Processing* **2008**(1) 1–17.

[5] Anil, K. J. and Umut Uludag. Hiding Fingerprint Minutiae in Images. In: *Third Workshop on Automatic Identification Advanced Technologies (AutoID)*. IEEE, Tarrytown, New York, 2002, 97–102.

[6] Behnia S., Akhshani A., Mahmodi H. and Akhavan A. A novel algorithm for image encryption based on mixture of chaotic maps. *Chaos, Solitons and Fractals* **35**(2) (2008) 408–419.

[7] Belhumeur P. N., Hespanha J. P. and Kriegman D. J. Eigenfaces vs. Fisherfaces: Recognition using class specific linear projection. *IEEE Trans. on Pattern Analysis and Machine Intelligence* **19**(7) (1997) 711–720.

[8] Bremananth, R. and Chitra, A. An efficient biometric cryptosystem using autocorrelators. *International Journal of Signal Processing* **2**(3) (2005) 158–164.

[9] Chen G., Mao, Y. and Chui, C. K. Asymmetric image encryption based on 3D chaotic maps. *Chaos, Solitons and Fractals* **21**(3) (2004) 749–761.

[10] Cruz-Hernández, C. Synchronization of time-delay Chua's oscillator with application to secure communication. *Nonlinear Dynamics and Systems Theory* **4**(1) (2004) 1–13.

[11] Cruz-Hernández, C. and Martynyuk, A. A. Advances in chaotic dynamics and applications, In: Stability, Ocillations, and Optimization of Systems, Cambridge Scientific Publishers, Kiev, 2010.

[12] Daugman, J. High confidence visual recognition of persons by a test of statistical independence. *IEEE Trans. on Pattern Analysis and Machine Intelligence* **15**(11) (1993) 1148–1161.

[13] Filali R. L., Hammami S., Benrejeb M. and Borne P. On Synchronization, Antisynchronization and Hybrid Synchronization of 3D Discrete Generalized Hénon Map. *Nonlinear Dynamics and Systems Theory* **12**(1) (2012) 81–95.

[14] Goldstein A.J., Harmon L.D. and Lesk, A.B. Identification of human faces. In: *Proceedings of the IEEE* **59**(5) (1971) 748–760.

[15] Haiping L., Karl M., Bui F., Plataniotis K. N. and Hatzinakos D. Face recognition with biometric encryption for privacy-enhancing self-exclusion. In: *16th international conference on Digital signal processing*, Aegean island of Santorini, 2009, 1–8.

[16] Hsu, C. W. and Lin, C. J. A comparison of methods for multi-class support vector machines. *IEEE Trans. Neural Networks* **13** (2) (2002) 415–425.

[17] IEEE Computer Society. IEEE Standard for Floating-Point arithmetic. In: IEEE std 754 – 2008, New York, 2008, 1–58.

[18] Inzunza-González E., Cruz-Hernández C. and Serrano-Guerrero H., Hyperchaotic encryption: An application in biometric systems based on face recognition, submitted in *AEÜ - International Journal of Electronics and Communications.*

[19] Kirby, M. and Sirovich, L. Application of the Karhunen-Loeve procedure for the characterization of human faces. *IEEE Transactions on Pattern Analysis and Machine Intelligence* **12**(1) (1990) 103–108.

[20] Kresimir Delac, M. G. and Stewart, B. M. Recent advances in face recognition. In-Teh, Vienna, 2008.

[21] López-Mancilla, D. and Cruz-Hernndez, C. Output synchronization of chaotic systems: model-matching approach with application to secure communication. *Nonlinear Dynamics and Systems Theory* **5** (2) (2005) 141–15.

[22] Muhammad K. K., Zhang J. and Tian L. Chaotic secure content-based hidden transmission of biometric templates. *Chaos, Solitons and Fractals* **32**(5) (2007) 1749–1759.

[23] Mukhopadhyay S., Demircioglu B. and Chatterjee A. Quantum Dynamics of a Nonlinear Kicked Oscillator. *Nonlinear Dynamics and Systems Theory* **11**(2) (2011) 173–182.

[24] Peng J., Zhang D. and Xiaofeng L. A digital image encryption based on hyper-chaotic cellular neural network. *Fundamenta Informaticae* **90**(3) (2009) 269–282.

[25] Sani M. M., Ishak K. A., Samad S. A. Classification using adaptive multiscale retinex and support vector machine for face recognition system. *Journal of Applied Sciences* **10**(6) (2010) 506–511.

[26] Shannon C. E. Communication theory of security systems. *The Bell System Technical Journal* **27**(3) (1948) 379-423, 623–656.

[27] Shannon C. E. Communication theory of secrecy system. *The Bell System Technical Journal* **28**(4) (1949) 656–715.

[28] Sirovich, L. and Kirby, M. A low-dimensional procedure for the characterization of human faces. *J. Optical Soc. Am. A* **4**(3) (1987) 519–524.

[29] Turk, M. and Pentland, A. Eigen face for recognition. *Journal of Cognitive Neuroscience* **3**(1) (1991) 71–86.

[30] Turk, M. and Pentland, A. Face recognition using eigenfaces. In: Proceedings of IEEE Conf. on Computer Vision and Pattern Recognition. IEEE, La Haina Maui, 1991, 586–591.

[31] Yongyi, M. and Zichao, D. A New Image Encryption Algorithm of Input-Output Feedback Based on Multi-chaotic System. Applied Mechanics and Materials **40-41** (1) (2011) 924–929.

[32] Zhang, D. D. Automated biometrics technologies and systems. Kluwer Academic Publishers, Beijing, 2000.

Nonlinear Dynamics and Systems Theory, **13** (1) (2013) 69–78

On the Approximate Controllability of Fractional Order Control Systems with Delay

S. Kumar* and N. Sukavanam

Department of Mathematics, Indian Institute of Technology, Roorkee (IITR), Roorkee-247667, India.

Received: December 14, 2011; Revised: January 30, 2013

Abstract: In this paper, sufficient conditions of the approximate controllability for a class of fractional order semilinear control systems with bounded delay are established. To illustrate the theory an example is given.

Keywords: *fractional order system; semilinear delay systems; mild solution; reachable set; approximate controllability.*

Mathematics Subject Classification (2010): 34H05, 34K30, 34K37, 47D60, 93B05.

1 Introduction

Let V and $\hat{V}$ be real Hilbert spaces. Also, let $Z = L_2([0,\tau];V)$ and $Y = L_2([0,\tau];\hat{V})$ be the corresponding function spaces defined on $[0,\tau]$. Let $C([-h,0],V)$ be the Banach space of all continuous functions from $[-h,0]$ to V with the supremum norm.

Consider the following fractional order semilinear control system with bounded delay

$$\left.\begin{array}{ll} {}^CD_t^\alpha x(t) = Ax(t) + Bu(t) + f(t,x_t), & t \in]0,\tau]; \\ x(t) = \varphi(t), & t \in [-h,0]. \end{array}\right\} \tag{1}$$

Here ${}^CD_t^\alpha$ is the Caputo fractional derivative of order α, where $1/2 < \alpha < 1$; the state $x(\cdot)$ takes its values in the space V; $A : D(A) \subseteq V \to V$ is a closed linear operator with dense domain $D(A)$ generating a C_0-semigroup $T(t)$; the control function $u(\cdot)$ takes its values in $\hat{V}$. The operator B is a bounded linear operator from $\hat{V}$ to V; $f : [0,\tau] \times C([-h,0],V) \to V$ is a continuous function and φ is the element of $C([-h,0];V)$.

* Corresponding author: mailto:mathdma@gmail.com

The investigation of the theory of fractional calculus have been started about three decades before. Fractional order differential equations are generalizations of ordinary differential equations to an arbitrary (noninteger) order. Fractional order nonlinear equations are abstract formulations for many problems arising in engineering, physics and many other fields. In particular, the fractional calculus is used in diffusion process, electrical science, electrochemistry, viscoelasticity, control science, electro magnetic theory and several more. For more details one can see [1–6] and the references cited therein. In [7] phase synchronizations in coupled chaotic systems presented by fractional differential equations has been considered. The existence and uniqueness of solutions of a nonlinear multi-variables fractional differential equations have been investigated in [8] by using Schauder's fixed points theorems and Global contraction mapping theory.

The problems of optimal control [9, 10] and various type of controllability like exact controllability [11–13], boundary controllability [14] and the approximate controllability [15, 16] of fractional order systems have been studied in the area of control theory in infinite dimension spaces.

To prove exact controllability and the boundary controllability, the main tool used by the authors is to convert the controllability problem into a fixed point problem together with the assumption that the controllability operator has an induced inverse on a quotient space. In [12–14], to prove the controllability results for fractional order semilinear systems authors made an assumption that the semigroup associated with the linear part is compact. However, if the operator B is compact or C_0-semigroup $T(t)$ is compact then the controllability operator is also compact and hence inverse of it does not exist if the state space V is infinite dimensional [17]. Thus, the concept of exact controllability is too strong in infinite dimensional space and the approximate controllability is more appropriate for these control systems.

The approximate controllability of the systems of integer order ($\alpha = 1, 2$) has been proved in [18–23] and the references therein. To show the results on the approximate controllability a relation between the reachable set of a semilinear system and that of the corresponding linear system is proved. In [15] Sakthivel et al. proved the approximate controllability by assuming that the C_0-semigroup $T(t)$ is compact and the nonlinear function is continuous and uniformly bounded. Sukavanam et al. [16] proved the approximate controllability for a class of semilinear delayed control system of fractional order by assuming that the corresponding linear system is approximately controllable and nonlinear function satisfies the Lipschitz condition. Recently, Kumar et al. [24] established sufficient conditions for the approximate controllability of a class of semilinear delay control systems of fractional order by using Schauder's fixed point theorem and the compactness of the C_0-semigroup together with the Lipschitz continuity of nonlinear term.

In this paper, sufficient conditions for the approximate controllability of fractional order semilinear control system (1) are established.

The paper is organized as follows: in Section 2, we present some necessary preliminaries. The approximate controllability of semilinear system (1) is proved in Section 3. In Section 4, an example is given to illustrate the theory.

2 Preliminaries

This section is devoted to the basic definitions and lemma, which are useful for further development.

Definition 2.1 A real function $f(t)$ is said to be in the space C_α, $\alpha \in \mathbb{R}$ if there exists a real number $p > \alpha$, such that $f(t) = t^p g(t)$, where $g \in C[0, \infty[$ and it is said to be in the space C_α^m iff $f^{(m)} \in C_\alpha$, $m \in N$.

Definition 2.2 The Riemann-Liouville fractional integral operator of order $\beta > 0$ of function $f \in C_\alpha$, $\alpha \geq -1$ is defined as

$$I^\beta f(t) = \frac{1}{\Gamma(\beta)} \int_0^t (t-s)^{\beta-1} f(s) ds,$$

where Γ is the Euler gamma function.

Definition 2.3 If the function $f \in C_{-1}^m$ and m is a positive integer then we can define the fractional derivative of $f(t)$ in the Caputo sense as

$${}^C D_t^\alpha f(t) = \frac{1}{\Gamma(m-\alpha)} \int_0^t (t-s)^{m-\alpha-1} f^m(s) ds, \quad m-1 \leq \alpha < m.$$

Definition 2.4 [25] A function $x(\cdot) \in C([-h, \tau]; V)$ is said to be the mild solution of (1) if it satisfies

$$x(t) = \begin{cases} S_\alpha(t)\varphi(0) + \int_0^t (t-s)^{\alpha-1} T_\alpha(t-s)[Bu(s) + f(s, x_s)] ds, & t \in [0, \tau], \\ \varphi(t), & t \in [-h, 0], \end{cases}$$

where $S_\alpha(t)x = \int_0^\infty \phi_\alpha(\theta) T(t^\alpha \theta) x d\theta$ and $T_\alpha(t)x = \alpha \int_0^\infty \theta \phi_\alpha(\theta) T(t^\alpha \theta) x d\theta$. Here $\phi_\alpha(\theta) = \frac{1}{\alpha}\theta^{-1-1/\alpha}\psi_\alpha(\theta^{-1/\alpha})$ is the probability density function defined on $(0, \infty)$, that is $\phi_\alpha(\theta) \geq 0$, and $\int_0^\infty \phi_\alpha(\theta) d\theta = 1$. Also the term $\psi_\alpha(\theta)$ is defined as $\psi_\alpha(\theta) = \frac{1}{\pi}\Sigma_{n=1}^\infty (-1)^{n-1} \theta^{-n\alpha-1} \frac{\Gamma(n\alpha+1)}{n!} \sin(n\pi\alpha)$, $\theta \in (0, \infty)$.

Define the solution mapping Φ from Z to $C([0, \tau]; V)$ as

$$(\Phi u)(t) = x(t).$$

Definition 2.5 The set $K_\tau(f) = \{x(\tau) \in V : \ x(t) \text{ is a mild solution of (1)}\}$ is called the reachable set of the system (1).

Definition 2.6 Let $x(\tau)$ be the state value of system (1) at time τ corresponding to the control u. The system (1) is said to be approximately controllable in time interval $[0, \tau]$, if for every desired final state ξ and $\epsilon > 0$ there exists a control function $u(\cdot) \in Y$ such that the mild solution $x(t)$ of (1) satisfies

$$\|x(\tau) - \xi\| < \epsilon.$$

The system (1) is said to be approximately controllable on $[0, \tau]$ iff $\overline{K_\tau(f)} = V$, where $\overline{K_\tau(f)}$ denotes the closure of $K_\tau(f)$.

Lemma 2.1 *[25] For any fixed $t \geq 0$, $S_\alpha(t)$ and $T_\alpha(t)$ are bounded linear operators, that is, for any $x \in V$, $\|S_\alpha(t)x\| \leq M\|x\|$ and $\|T_\alpha(t)x\| \leq \frac{M\alpha}{\Gamma(1+\alpha)}\|x\|$, where M is a constant such that $\|T(t)\| \leq M$, for all $t \in [0, \tau]$.*

Define a continuous linear operator $\mathcal{L}$ from Z to $C([0,\tau];V)$ by

$$\mathcal{L}p = \int_0^\tau (\tau - s)^{\alpha-1} T_\alpha(\tau - s)p(s)ds, \text{ for } p(\cdot) \in Z.$$

Assumption: We need the following hypotheses to prove our results:
(H1) The nonlinear operator $f(t,x)$ satisfies the Lipschitz condition i.e. there exists a positive constant l such that

$$\|f(t,x) - f(t,y)\|_V \leq l\|x - y\|_V, \text{ for all } x, y \in V \text{ and } t \in [0,\tau],$$

and $\|f(t,0)\|_V \leq l_f$.
(H2) For any given $\epsilon > 0$, and $p(\cdot) \in Z$, there exists some $u(\cdot) \in Y$ such that

$$\|\mathcal{L}p - \mathcal{L}Bu\|_V < \epsilon.$$

(H3) $\|Bu(\cdot)\|_Z \leq \lambda\|p(\cdot)\|_Z$, where λ is a positive constant independent of $p(\cdot)$.
(H4) The constant λ satisfies $\frac{M\alpha\tau^\alpha\lambda l}{\Gamma(1+\alpha)\sqrt{2\alpha-1}} \exp\left(\frac{Ml\tau^\alpha}{\Gamma(1+\alpha)}\right) < 1$.

3 Controllability Results

In this section, we prove the approximate controllability for a class of fractional order semilinear control system (1) with bounded delay.

Lemma 3.1 *Under hypotheses (H1) the solution mapping* $(\Phi u)(\cdot)$ *satisfies*

$$\|(\Phi u)(t)\|_V \leq K \exp\left(\frac{Ml\tau^\alpha}{\Gamma(1+\alpha)}\right),$$

where $K = M\left[\|\varphi(0)\| + \frac{\alpha}{\Gamma(1+\alpha)}\sqrt{\frac{\tau^{2\alpha-1}}{2\alpha-1}}\|Bu\|_Z + \frac{l_f\tau^\alpha}{\Gamma(1+\alpha)}\right]$.

Let $u_1(\cdot)$ *and* $u_2(\cdot)$ *be in* Y. *Then*

$$\|x_1 - x_2\|_Z \leq \frac{M\alpha\tau^\alpha}{\Gamma(1+\alpha)\sqrt{2\alpha-1}} \exp\left(\frac{Ml\tau^\alpha}{\Gamma(1+\alpha)}\right)\|Bu_1(\cdot) - Bu_2(\cdot)\|_Z,$$

where $x_n(t) = (\Phi u_n)(t),\ n = 1, 2, \cdots$.

Proof. The solution mapping $(\Phi u)(t) = x(t)$ is given by

$$x(t) = x_t(0) = S_\alpha(t)\varphi(0) + \int_0^t (t-s)^{\alpha-1} T_\alpha(t-s)[Bu(s) + f(s, x_s)]ds.$$

Taking the norm on both sides, we have

$$\begin{aligned}
\|x_t\|_V &= \|S_\alpha(t)\|\|\varphi(0)\| + \int_0^t (t-s)^{\alpha-1}\|T_\alpha(t-s)\|\|Bu(s)+f(s,x_s)\|ds \\
&\leq M\|\varphi(0)\| + \frac{M\alpha}{\Gamma(1+\alpha)}\int_0^t (t-s)^{\alpha-1}\|Bu(s)\|ds \\
&\quad + \frac{M\alpha}{\Gamma(1+\alpha)}\int_0^t (t-s)^{\alpha-1}\|f(s,x_s)\|ds, \\
&\leq M\|\varphi(0)\| + \frac{M\alpha}{\Gamma(1+\alpha)}\sqrt{\frac{\tau^{2\alpha-1}}{2\alpha-1}}\|Bu\|_Z \\
&\quad + \frac{M\alpha l}{\Gamma(1+\alpha)}\int_0^t (t-s)^{\alpha-1}\|x_s\|_C ds + \frac{Ml_f\tau^\alpha}{\Gamma(1+\alpha)}. \\
&\leq K + \frac{M\alpha l}{\Gamma(1+\alpha)}\int_0^t (t-s)^{\alpha-1}\|x_s\|_C ds.
\end{aligned}$$

This implies that

$$\|x_t\|_C = \sup\|x_t\|_V \leq K + \frac{M\alpha l}{\Gamma(1+\alpha)}\int_0^t (t-s)^{\alpha-1}\|x_s\|_C ds.$$

Now, using the Gronwall's inequality, we get

$$\|x(t)\| \quad \leq \quad K\exp\Big(\frac{Ml\tau^\alpha}{\Gamma(1+\alpha)}\Big).$$

Thus, we have

$$\|(\Phi u)(t)\|_V \leq K\exp\Big(\frac{Ml\tau^\alpha}{\Gamma(1+\alpha)}\Big).$$

Let us define $y(\cdot,\varphi):[-h,\tau]\to V$ as

$$y(t,\varphi) = \begin{cases} \varphi(t), & t\in[-h,0], \\ S_\alpha(t)\varphi(0), & t\in[0,\tau]. \end{cases}$$

Let $x(t) = y(t) + z(t)$, $t\in[-h,\tau]$. It is easy to see that $x(\cdot)$ satisfies (1) if and only if $z_0 = 0$ and for $t\in[0,\tau]$, we have

$$z(t) = \int_0^t (t-s)^{\alpha-1}T_\alpha(t-s)[Bu(s)+f(s,y_s+z_s)]ds.$$

Now, let us take $x_1(\cdot),\ x_2(\cdot)\in V$ and $u_1,\ u_2\in Y$, then

$$\begin{aligned}
&\|(z_1)_t-(z_2)_t\|_V \\
&\quad\leq \frac{M\alpha}{\Gamma(1+\alpha)}\int_0^t (t-s)^{\alpha-1}\|Bu_1(s)-Bu_2(s)\|ds \\
&\qquad + \frac{M\alpha}{\Gamma(1+\alpha)}\int_0^t (t-s)^{\alpha-1}\|f(s,y(s)+(z_1)_s)-f(s,y(s)+(z_2)_s)\|ds \\
&\quad\leq \frac{M\alpha}{\Gamma(1+\alpha)}\sqrt{\frac{\tau^{2\alpha-1}}{2\alpha-1}}\|Bu_1-Bu_2\|_Z \\
&\qquad + \frac{M\alpha l}{\Gamma(1+\alpha)}\int_0^t (t-s)^{\alpha-1}\|(z_1)_s-(z_2)_s\|_C ds.
\end{aligned}$$

Using the Gronwall's inequality, we get

$$\begin{aligned}\sup\|(z_1)_t-(z_2)_t\|_V &= \|(z_1)_t-(z_2)_t\|_C\\ &\le \frac{M\alpha}{\Gamma(1+\alpha)}\sqrt{\frac{\tau^{2\alpha-1}}{2\alpha-1}}\exp\Big(\frac{Ml\tau^\alpha}{\Gamma(1+\alpha)}\Big)\|Bu_1-Bu_2\|_Z.\end{aligned}$$

Hence, we have

$$\begin{aligned}\|x_1-x_2\|_Z &= \Big(\int_0^\tau \|x_1(s)-x_2(s)\|_V^2 ds\Big)^{1/2}\\ &= \Big(\int_0^\tau \|z_1(s)-z_2(s)\|_V^2 ds\Big)^{1/2}\\ &\le \frac{M\alpha\tau^\alpha}{\Gamma(1+\alpha)\sqrt{2\alpha-1}}\exp\Big(\frac{Ml\tau^\alpha}{\Gamma(1+\alpha)}\Big)\|Bu_1(\cdot)-Bu_2(\cdot)\|_Z.\end{aligned}$$

This completes the proof of lemma.

Theorem 3.1 *Under hypotheses (H1)–(H4) the fractional order semilinear control system (1) is approximately controllable.*

Proof. Since the domain $D(A)$ of the operator A is dense in Z, it is sufficient to prove that $D(A)\subset\overline{K_\tau(f)}$. For this, let us take $\xi\in D(A)$, then for any given $\epsilon>0$, there exists a control function $u_\epsilon(\cdot)\in Y$ such that

$$\|\xi-S_\alpha(\tau)\varphi(0)-\mathcal{L}f(s,x_\epsilon(s))-\mathcal{L}Bu_\epsilon\|<\epsilon,$$

where $x_\epsilon(t)=(\Phi u_\epsilon)(t)$ satisfies

$$x_\epsilon(t)=S_\alpha(t)\varphi(0)+\int_0^t(t-s)^{\alpha-1}T_\alpha(t-s)[Bu_\epsilon(s)+f(s,(x_\epsilon)_s)]ds.$$

Now, we construct a sequence recursively as follows.

Assume that $u_1(\cdot)\in Y$ is arbitrarily given. By hypothesis (H2), there exists some $u_2(\cdot)\in Y$ such that

$$\|\xi-S_\alpha(\tau)\varphi(0)-\mathcal{L}f(s,(x_1)_s)-\mathcal{L}Bu_2\|<\frac{\epsilon}{2^2}, \tag{2}$$

where $x_1(t)=(\Phi u_1)(t)$, for all $t\in[0,\tau]$.

For $u_2(\cdot)\in Y$ thus obtained, we determine $w_2(\cdot)\in Y$ by hypotheses (H2) and (H3) such that

$$\|\mathcal{L}[f(s,(x_2)_s)-f(s,(x_1)_s)]-\mathcal{L}Bw_2\|<\frac{\epsilon}{2^3}, \tag{3}$$

and by Lemma 3.1, we have

$$\begin{aligned}\|Bw_2(\cdot)\|_{L_2([0,\tau];V)} &\le \lambda\|f(s,(x_2)_s)-f(s,(x_1)_s)\|_Z\\ &\le \lambda\Big(\int_0^\tau\|f(s,(x_2)_s)-f(s,(x_1)_s)\|_V^2ds\Big)^{1/2}\\ &\le \lambda l\Big(\int_0^\tau\|(x_2)_s-(x_1)_s\|_V^2ds\Big)^{1/2}\\ &\le \lambda l\|x_2-x_1\|_Z\\ &\le \frac{M\alpha\tau^\alpha\lambda l}{\Gamma(1+\alpha)\sqrt{2\alpha-1}}\exp\Big(\frac{Ml\tau^\alpha}{\Gamma(1+\alpha)}\Big)\|Bu_1(\cdot)-Bu_2(\cdot)\|_Z,\end{aligned}$$

where $x_n(t) = (\Phi u_n)(t)$, $n = 1, 2$, for all $t \in [0, \tau]$.

Thus, we may define $u_3 = u_2 - w_2$ in Y which has the following property

$$\begin{aligned}\|\xi - S_\alpha(\tau)\varphi(0) \quad &- \quad \mathcal{L}f(s,(x_2)_s) - \mathcal{L}Bu_3\| \\ &\leq \quad \|\xi - S_\alpha(\tau)\varphi(0) - \mathcal{L}f(s,(x_1)_s) - \mathcal{L}Bu_2 \\ &\qquad +\mathcal{L}Bw_2 - \mathcal{L}[f(s,(x_2)_s) - f(s,(x_1)_s)]\| \\ &\leq \quad \|\xi - S_\alpha(\tau)\varphi(0) - \mathcal{L}f(s,(x_1)_s) - \mathcal{L}Bu_2\| \\ &\qquad +\|\mathcal{L}Bw_2 - \mathcal{L}[f(s,(x_2)_s) - f(s,(x_1)_s)]\|.\end{aligned}$$

Using Eq. (2) and (3), we get

$$\|\xi - S_\alpha(\tau)\varphi(0) - \mathcal{L}f(s,(x_2)_s) - \mathcal{L}Bu_3\| \leq \left(\frac{1}{2^2} + \frac{1}{2^3}\right)\epsilon.$$

Mathematical induction implies that there exists a sequence $u_n(\cdot) \in Y$ such that

$$\|\xi - S_\alpha(\tau)\varphi(0) - \mathcal{L}f(s,(x_n)_s) - \mathcal{L}Bu_{n+1}\| \leq \left(\frac{1}{2^2} + \cdots + \frac{1}{2^{n+1}}\right)\epsilon, \tag{4}$$

where $x_n(t) = (\Phi u_n)(t)$, $n = 1, 2, \cdots$, for all $t \in [0, \tau]$ and

$$\begin{aligned}\|Bu_{n+1}(\cdot) \quad &- \quad Bu_n(\cdot)\|_Z \\ &\leq \quad \frac{M\alpha\tau^\alpha\lambda l}{\Gamma(1+\alpha)\sqrt{2\alpha-1}} \exp\left(\frac{Ml\tau^\alpha}{\Gamma(1+\alpha)}\right)\|Bu_n(\cdot) - Bu_{n-1}(\cdot)\|_Z.\end{aligned}$$

Clearly, by hypothesis (H4), the sequence $\{Bu_n;\ n = 1, 2, \cdots\}$ is a Cauchy sequence in the Banach space Z and there exists some $v(\cdot) \in Z$ such that

$$\lim_{n\to\infty} Bu_n(t) = v(t), \text{ in } Z.$$

Therefore for any given $\epsilon > 0$, there exists some integer N_ϵ such that

$$\|\mathcal{L}Bu_{N_\epsilon+1} - \mathcal{L}Bu_{N_\epsilon}\| < \frac{\epsilon}{2}. \tag{5}$$

Hence, we obtain

$$\begin{aligned}\|\xi - S_\alpha(\tau)\varphi(0) \quad &- \quad \mathcal{L}f(s,(x_{N_\epsilon})_s) - \mathcal{L}Bu_{N_\epsilon}\| \\ &\leq \quad \|\xi - S_\alpha(\tau)\varphi(0) - \mathcal{L}f(s,(x_{N_\epsilon})_s) - \mathcal{L}Bu_{N_\epsilon+1}\| \\ &\qquad +\|\mathcal{L}Bu_{N_\epsilon+1} - \mathcal{L}Bu_{N_\epsilon}\|,\end{aligned}$$

where $x_{N_\epsilon}(t) = (\Phi u_{N_\epsilon})(t)$, for all $t \in [0, \tau]$. Using Eq. (4) and (5), we get

$$\begin{aligned}\|\xi - S_\alpha(\tau)\varphi(0) - \mathcal{L}f(s,(x_{N_\epsilon})_s) - \mathcal{L}Bu_{N_\epsilon}\| \quad &\leq \quad \left(\frac{1}{2^2} + \cdots + \frac{1}{2^{N_\epsilon+1}}\right)\epsilon + \frac{\epsilon}{2} \\ &\leq \quad \epsilon.\end{aligned}$$

This means that $\xi \in \overline{K_\tau(f)}$. Hence the fractional order semilinear system (1) is approximately controllable on $[0, \tau]$. This completes the proof.

Theorem 3.2 *Suppose that the range of the operator B i.e. $R(B)$ is dense in Z. Then under hypothesis (H1) the semilinear system (1) is approximately controllable.*

Proof. Since the range of the operator B is dense in Z, for any given point $p(\cdot) \in Z$ and every $\delta > 0$, there exists some point $Bu(\cdot) \in R(B)$, where $u(\cdot) \in Y$ such that

$$\|Bu(\cdot) - p(\cdot)\|_Z < \delta \|p(\cdot)\|_Z. \tag{6}$$

Now, we have

$$\begin{aligned}
\|\mathcal{L}p - \mathcal{L}Bu\| &\leq \frac{M\alpha}{\Gamma(1+\alpha)} \int_0^\tau (\tau - s)^{\alpha-1} \|p(s) - Bu(s)\| ds \\
&\leq \frac{M\alpha}{\Gamma(1+\alpha)} \sqrt{\frac{\tau^{2\alpha-1}}{2\alpha-1}} \|p(\cdot) - Bu(\cdot)\|_Z \\
&\leq \frac{M\alpha}{\Gamma(1+\alpha)} \sqrt{\frac{\tau^{2\alpha-1}}{2\alpha-1}} \delta \|p(\cdot)\|_Z \\
&< \epsilon.
\end{aligned}$$

Thus from (6), we have

$$\begin{aligned}
\|Bu(\cdot)\|_Z &= \|Bu(\cdot) - p(\cdot) + p(\cdot)\|_Z \\
&\leq \|Bu(\cdot) - p(\cdot)\|_Z + \|p(\cdot)\|_Z \\
&\leq \delta \|p(\cdot)\|_Z + \|p(\cdot)\|_Z \\
&\leq (\delta + 1)\|p(\cdot)\|_Z.
\end{aligned}$$

This implies that the conditions (H2) and (H3) are satisfies, if we choose $\delta > 0$ in such a manner that (H4) is verified. Then the approximate controllability of (1) follows from Theorem 3.1.

4 Example

Let $V = L_2(0, \pi)$ and $A = \frac{\partial^2}{\partial x^2}$ with $D(A)$ consisting of all $y \in V$ with $\frac{\partial^2 y}{\partial x^2}$ and $y(0) = 0 = y(\pi)$. Put $e_n(x) = \sqrt{2/\pi}\sin(nx);\ 0 \leq x \leq \pi,\ n = 1, 2, \cdots$, then $\{e_n,\ n = 1, 2, \cdots\}$ is an orthonormal basis for V and e_n is the eigenfunction corresponding to the eigenvalue $\lambda_n = -n^2$ of the operator A. Then the C_0-semigroup $T(t)$ generated by A has $\exp(\lambda_n t)$ as the eigenvalues and e_n as their corresponding eigenfunctions [26]. Define an infinite-dimensional space $\hat{V}$ by

$$\hat{V} = \left\{ u \mid u = \sum_{n=2}^{\infty} u_n e_n,\ \text{with} \sum_{n=2}^{\infty} u_n^2 < \infty \right\}.$$

The norm in $\hat{V}$ is defined by

$$\|u\|_{\hat{V}} = \left(\sum_{n=2}^{\infty} u_n^2 \right)^{1/2}.$$

Define a continuous linear map B from $\hat{V}$ to V as

$$Bu = 2u_2 e_1 + \sum_{n=2}^{\infty} u_n e_n,\ \text{for } u = \sum_{n=2}^{\infty} u_n e_n \in \hat{V}. \tag{7}$$

Let us consider the following fractional order semilinear control system of the form

$$\begin{aligned}
&{}^{C}D_t^{\alpha} y(t,x) = \frac{\partial^2}{\partial x^2} y(t,x) + Bu(t,x) + f(t, y(t-h,x)); \ t \in [0,\tau], \ 0 < x < \pi, \\
&y(t,0) = y(t,\pi) = 0; \ t \in [0,\tau], \\
&y(t,x) = \varphi(t,x); \ t \in [-h,0],
\end{aligned} \tag{8}$$

where $\varphi(t,x)$ is continuous. The system (8) can be written in the abstract form given by (1). The operator B is defined in (7) and the control function $u(t,x) \in L_2([0,\tau]; \hat{V}) = L_2([0,\tau] \times (0,\pi))$. Here the nonlinear term f is considered as an operator satisfying Hypothesis (H1). If the conditions (H2)-(H4) are satisfied, then the approximate controllability of system (8) follows from Theorem 3.1. For example, if we consider the function f as $f(t,z) = l\|z\|\phi_3(z)$, where $l > 0$ is a constant. The function f satisfies (H1) with Lipschitz constant l.

Conclusion

The approximate controllability for a class of semilinear delay control system of fractional order has been proved provided that it holds for the corresponding linear system. These results hold only for the fractional order such that $1/2 < \alpha < 1$.

Acknowledgment

The first author is thankful to Council of Scientific & Industrial Research (CSIR) for the financial support with grant number 09/143(0621)/2008-EMR-I.

References

[1] Fitt, A.D., Goodwin, A.R.H. and Wakeham, W.A. A fractional differential equation for a MEMS viscometer used in the oil industry. *J. Comput. Appl. Math.* **229** (2009) 373–381.

[2] Diethelm, K. and Freed, A.D. On the solution of nonlinear fractional order differential equations used in the modeling of viscoplasticity. In: *Scientifice Computing in Chemical Engineering II-Computational Fluid Dynamics, Reaction Engineering and Molecular Properties* (F. Keil, W. Mackens, H. Voss, J. Werther, Eds.), Springer-Verlag, Heidelberg, (1999) 217–224.

[3] Hilfer, R. *Applications of Fractional Calculus in Physics*, World Scientific, Singapore, 2000.

[4] Kilbas, A.A., Srivastava, H.M. and Trujillo, J.J. *Theory and Applications of Fractional Differential Equations*, Elsevier, Amsterdam, 2006.

[5] Oldham, K.B. and Spanier, J. *The Fractional Calculus,Theory and Applications of Differentiation and Integration to Arbitrary Order*, Academic Press, New York, London, 1974.

[6] Podlubny I. *Fractional Differential Equations*, Academic Press, New York, 1999.

[7] Erjaee, G.H. and Taghvafard, H. Stability analysis of phase synchronization in coupled chaotic systems presented by fractional differential equations. *Nonlinear Dynamics and Systems Theory.* **11**(2) (2011) 147–154.

[8] Yu, J.M., Luo, Y.W., Zhou, S.B. and Lin, X.R. Existence and uniqueness for nonlinear multi-variables fractional differential equations. *Nonlinear Dynamics and Systems Theory.* **11**(2) (2011) 213–221.

[9] Wang, J. and Zhou, Y. A class of fractional evolution equations and optimal controls. *Nonlinear Analysis: Real World Applications.* **12** (2011) 262-272.

[10] Wang, J. Zhou, Y. and Wei, W. A class of fractional delay nonlinear integrodifferential controlled systems in Banach spaces. *Commun Nonlinear Sci Numer Simulat.* doi:10.1016/j.cnsns.2011.02.003, (2011).

[11] Debbouche, A. and Baleanu, D. Controllability of fractional evolution nonlocal impulsive quasilinear delay integro-differential systems. *Computers and Mathematics with Applications.* **62** (2011) 1442–1450.

[12] Tai, Z. and Wang, X. Controllability of fractional-order impulsive neutral functional infinite delay integrodifferential systems in Banach spaces. *Applied Mathematics Letters.* **22** (2009) 1760–1765.

[13] Yan, Z. Controllability of fractional-order partial neutral functional integrodifferential inclusions with infinite delay. *Journal of the Franklin Institute.* **348** (2011) 2156–2173.

[14] Ahmed, H.M. Boundary controllability of nonlinear fractional integrodifferential systems. *Advances in Difference Equations.* **2010** (2010) Article ID 279493.

[15] Sakthivel, R., Ren, Y. and Mahmudov, N.I. On the approximate controllability of semilinear fractional differential systems. *Computers and Mathematics with Applications.* **62** (2011) 1451–1459.

[16] Sukavanam, N. and Kumar, S. Approximate controllability of fractional order semilinear delay systems. *J Optim Theory Appl.* **151** (2011) 373–384.

[17] Triggiani, R. A note on the lack of exact controllability for mild solutions in Banach spaces. *SIAM J. Control Optim.* **15** (1977) 407–411.

[18] Balasubramaniam, P., Park, J.Y. and Muthukumar, P. Approximate controllability of neutral stochastic functional differential systems with infinite delay. *Stochastic Analysis and Applications.* **28** (2010) 389–400.

[19] Henríquez, H.R. and Hernández, E.M. Approximate controllability of second-order distributed implicit functional systems. *Nonlinear Analysis.* **70** (2009) 1023–1039.

[20] Kwun, Y.C., Park, J.Y. and Ryu, J.W. Approximate controllability and controllability for delay volterra system. *Bull. Korean Math. Soc.* **28**(2) (1991) 131–145.

[21] Sukavanam, N. and Tafesse, S. Approximate controllability of a delayed semilinear control system with growing nonlinear term. *Nonlinear analysis.* **74** (2011) 6868–6875.

[22] Tomar, N.K. and Sukavanam, N. Approximate controllability of non-densely defined semilinear delayed control systems. *Nonlinear Studies.* **18**(2) (2011) 229–234.

[23] Zhou, H.X. Approximate controllability for a class of semilinear abstract equations. *SIAM J. Control and Optimization.* **21**(4) (1983) 551–565.

[24] Kumar, S. and Sukavanam, N. Approximate controllability of fractional order semilinear systems with bounded delay, J. Differential Equations (2012): doi:10.1016/j.jde.2012.02.014.

[25] Zhou, Y. and Jiao, F. Existence of mild solutions for fractional neutral evolution equations. *Computers and Mathematics with Applications.* **59** (2010) 1063–1077.

[26] Naito, K. Controllability of semilinear control systems dominated by the linear part. *SIAM J. Control and Optimization.* **25**(3) (1987) 715–722.

Nonlinear Dynamics and Systems Theory, **13** (1) (2013) 79–92

Asymptotic Stability for a Model of Cell Dynamics after Allogeneic Bone Marrow Transplantation

R. Precup *, M-A. Şerban and D. Trif

Department of Mathematics, Babeş–Bolyai University, 400084 Cluj-Napoca, Romania

Received: March 13, 2012;   Revised: January 18, 2013

Abstract: The paper presents stability analysis of steady-states of a dynamic system modeling cell evolution after stem cell transplantation. The border of the basins of attraction of the stable equilibria is found providing the theoretical basis for post-transplant correction therapies.

Keywords: *stability; dynamical system; numerical simulation; mathematical modeling.*

Mathematics Subject Classification (2010): 37C75, 37N25, 34D23.

1 Introduction

In [1] a mathematical model essentially owed to Dingli and Michor [2] was used in order to characterize normal and leukemic states and to explain basic pathways through which the robustness of the hematopoietic system can fail leading to leukemia.

Assume that at each time t, the cell population divides into two: the normal population $x(t)$ and the leukemic population $y(t)$. By x_0, y_0 we denote the normal and leukemic populations at a fixed moment of time $t = 0$. Denote by a, b, c and A, B, C (model parameters) the intrinsic (i.e., in the absence of any constraints) growth, microenvironment sensitivity and death rates of normal and leukemic cells, respectively. The conservation laws for normal and leukemic cells can be expressed as a system of two differential equations:

$$\begin{cases} x' = \frac{a}{1+b(x+y)}x - cx, \\ \\ y' = \frac{A}{1+B(x+y)}y - Cy. \end{cases} \tag{1}$$

* Corresponding author: mailto:r.precup@math.ubbcluj.ro

Here the term $\frac{a}{1+b(x(t)+y(t))}x\left(t\right)$ represents the new normal cell population at time t, and $cx\left(t\right)$ are the removed normal cells at time t. Similar interpretations hold for y. The terms $\frac{1}{1+b(x+y)}$ and $\frac{1}{1+B(x+y)}$ simulate the crowding effect in the bone marrow microenvironment and introduce competition between normal and leukemic cells. The cell proliferation is faster while the total cell population $x+y$ is small, and slower for large $x+y$. Thus these terms simulate the feedback of the proliferation system. We assume that for both cell populations, the intrinsic growth rate is greater than the death rate, i.e., $a>c$ and $A>C$. Denote

$$d:=\frac{1}{b}\left(\frac{a}{c}-1\right)\quad\text{and}\quad D:=\frac{1}{B}\left(\frac{A}{C}-1\right).$$

Then the *steady-states* or *equilibria* of system (1) are:

$$(0,0)\,;\ \ (d,0)\,;\ \ (0,D)$$

if $d\neq D$, and

$$(0,0)\,;\ \ (\alpha,d-\alpha)\ \ \text{for}\ \ 0\leq\alpha\leq d$$

when $d=D$.

The stability analysis in [1] shows that the zero solution $(0,0)$ is always unstable and if $d>D$, then $(d,0)$ is the unique asymptotically stable equilibrium and the normal cell population $x\left(t\right)$ approaches the equilibrium abundance d (normal homeostatic level) while the leukemic cell population $y\left(t\right)$ tends to zero; if $d<D$, then $(0,D)$ is the unique asymptotically stable equilibrium and the leukemic cell population becomes dominant approaching to its equilibrium abundance D (leukemic homeostatic level) and leads in the limit to the elimination of the normal cells, that is $x\left(t\right)$ tends to zero. These happen no matter the initial concentrations $x_0>0$, $y_0>0$ are. Thus we may say that the normal hematopoietic state is characterized by the inequality $d>D$, the leukemic hematopoietic state corresponds to the inequality $d<D$ and that equality $d=D$ characterizes the transitory state between normal and leukemic states.

The basic idea of the stem cell transplantation (see [5, 7]) consists in adding, say at time $t=0$, in competition with x_0, y_0 (host cells) a new population (donor cells) z_0. If the aggressiveness of z against x,y (graft-versus-host and graft-versus-leukemia) compensates that of the x and y against z (anti-graft effect), and if the initial concentrations x_0,y_0 are smaller enough as compared with z_0, then, in time, host cells are eliminated and completely replaced by donor cells guaranteeing the elimination of cancer.

Mathematically, this means that a new equation in z is added to the previous system in x and y which is itself modified in order to incorporate the new competition (mutual "aggressiveness") between z, on one side, and x and y, on the other. Assuming that intrinsic growth, sensitivity and death rates of the donor cell population are those of the normal host cell population (human invariant kinetic parameters), namely a,b,c, in [5] it was proposed the following model for the cellular dynamics after bone marrow transplantation:

$$\begin{cases} x'=\frac{a}{1+b(x+y+z)}\frac{x+y+\varepsilon}{x+y+\varepsilon+gz}x-cx,\\ \\ y'=\frac{A}{1+B(x+y+z)}\frac{x+y+\varepsilon}{x+y+\varepsilon+Gz}y-Cy,\\ \\ z'=\frac{a}{1+b(x+y+z)}\frac{z+\varepsilon}{z+\varepsilon+h(x+y)}z-cz.\end{cases}\tag{2}$$

Here the growth inhibitory factors

$$\frac{1}{1+g\frac{z}{x+y+\varepsilon}}, \quad \frac{1}{1+G\frac{z}{x+y+\varepsilon}}, \quad \frac{1}{1+h\frac{x+y}{z+\varepsilon}}$$

take into account the cell-cell interactions, quantitatively by ratios $\frac{z}{x+y+\varepsilon}$ and $\frac{x+y}{z+\varepsilon}$, and qualitatively by parameters h, g, G standing for the intensity of anti-graft, anti-host and anti-leukemia effects, respectively. Constant $\varepsilon > 0$ is taken in order to avoid singularity.

Numerical simulations performed in [5] for the leukemic case $d < D$ have proved that the evolution can ultimately lead either to the normal homeostatic equilibrium $(0, 0, d)$ achieved by the expansion of the donor cells and the elimination of the host cells, or to the leukemic homeostatic equilibrium $(0, D, 0)$ characterized by the proliferation of the cancer line and the suppression of the other cell lines. One state or the other is reached depending on cell-cell interactions (anti-host, anti-leukemia and anti-graft effects) and initial cell concentrations at transplantation.

The aim of this paper is to provide a rigorous mathematical base for the conclusions obtained in [5] by simulations. Thus in the present paper we find the equilibria of the system (2), we study their stability and we find the boundary of the attraction basins of the stable equilibria. This boundary allows us to calculate an initial cell concentration (x_0, y_0, z_0) in the attraction basin of the normal homeostatic equilibrium $(0, 0, d)$. Section 2 contains an analysis of the proposed system concerning its dynamics, Section 3 shows some numerical simulations with physiological parameters and in Section 4 a brief summary is given.

2 Equilibria of the Augmented System

Let us consider the system (2) with $\varepsilon \to 0$,

$$\begin{cases} x' = \left(\dfrac{a}{1+b(x+y+z)}\dfrac{x+y}{x+y+gz} - c\right) x \equiv U(x,y,z), \\[2ex] y' = \left(\dfrac{A}{1+B(x+y+z)}\dfrac{x+y}{x+y+Gz} - C\right) y \equiv V(x,y,z), \\[2ex] z' = \left(\dfrac{a}{1+b(x+y+z)}\dfrac{z}{z+h\,(x+y)} - c\right) z \equiv W(x,y,z), \end{cases} \tag{1}$$

where $a, b, c, A, B, C, g, G, h$ are positive parameters and $x \geq 0$, $y \geq 0$, $z \geq 0$ are such that $x + y + z > 0$. The main assumptions on the parameters are

$$a > c, \quad A > C, \quad d < D.$$

a) At the origin $O(0, 0, 0)$ we have

$$\lim_{(x,y,z)\to(0,0,0)} U(x,y,z) = \lim_{(x,y,z)\to(0,0,0)} V(x,y,z) = \lim_{(x,y,z)\to(0,0,0)} W(x,y,z) = 0$$

so that we will define $U(0, 0, 0) = V(0, 0, 0) = W(0, 0, 0) = 0$.

b) On the Ox axis, we have the equilibrium $P_1(d, 0, 0)$. The eigenvalues of the Jacobian calculated by MAPLE at this point are

$$-c, \quad -\frac{c(a-c)}{a}, \quad -\frac{CBa - CBc - Abc + Ccb}{bc + aB - cB}.$$

We have $-c < 0$, $-c(a-c)/a < 0$ and

$$-\frac{CBa - CBc - Abc + Ccb}{bc + aB - cB} = \frac{BC(D-d)}{1+Bd} > 0$$

so that P_1 is an unstable equilibrium for all considered values of the parameters. On the Ox axis, the first equation of (1) becomes

$$x' = bcx\frac{d-x}{1+bx}$$

and the origin $x = 0$ has a behavior of an unstable equilibrium.

c) On the Oy axis we have the equilibrium $P_2(0, D, 0)$. The eigenvalues of the Jacobian at this point are

$$-c, \quad -\frac{C(A-C)}{A}, \quad \frac{CBa - CBc - Acb + Ccb}{CB + Ab - Cb}.$$

Again $-c < 0$, $-C(A-C)/A < 0$ but

$$\frac{CBa - CBc - Acb + Ccb}{CB + Ab - Cb} = \frac{bc(d-D)}{1+bD} < 0$$

so that P_2 is a stable node for all considered values of the parameters – this is the "bad" equilibrium. On the Oy axis, the second equation of (1) becomes

$$y' = BCy\frac{D-y}{1+By}$$

so that the origin $y = 0$ has a behavior of an unstable equilibrium.

d) On the Oz axis the equilibrium is $P_3(0, 0, d)$. The eigenvalues of the Jacobian at this point are $-c < 0$, $-C < 0$, $-c(a-c)/a < 0$, so that P_3 is a stable node for all considered values of the parameters – this is the "good" equilibrium. On the Oz axis, the third equation of (1) becomes

$$z' = bcz\frac{d-z}{1+bz}$$

so that the origin $z = 0$ has again a behavior of an unstable equilibrium.

e) In the Oxy plane the equilibrium conditions lead us to the system

$$\left(\frac{a}{1+b(x+y)} - c\right)x = 0, \qquad \left(\frac{A}{1+B(x+y)} - C\right)y = 0,$$

from where, for $(x, y) \neq (0, 0)$ we obtain $x + y = d = D$. Consequently, this system is inconsistent for $d < D$. In a neighborhood of the origin, the above system becomes

$$x' = bcx\frac{d-(x+y)}{1+b(x+y)}, \qquad y' = BCy\frac{D-(x+y)}{1+B(x+y)},$$

so that $x' > 0$, $y' > 0$ have again a behavior of an unstable equilibrium.

f) In the Oxz plane the equilibrium condition leads us to the system

$$\begin{cases} \dfrac{a}{1+b(x+z)}\dfrac{x}{x+gz} - c = 0, \\ \dfrac{a}{1+b(x+z)}\dfrac{z}{z+hx} - c = 0, \end{cases} \tag{2}$$

from where, for $(x,z) \neq (0,0)$ we obtain $\dfrac{x}{x+gz} = \dfrac{z}{z+hx}$ or $hx^2 = gz^2$. Consequently, we have a solution $P_4(x^+,0,z^+)$, where

$$x^+ = \frac{\dfrac{a}{c\left(1+\sqrt{hg}\right)} - 1}{b\left(1+\sqrt{\dfrac{h}{g}}\right)}, \quad z^+ = \sqrt{h/g}x^+. \tag{3}$$

There exists an admissible solution $(x^+ > 0, z^+ > 0)$ if and only if

$$\sqrt{hg} < \frac{a}{c} - 1 = bd.$$

We remark here that $z = \sqrt{h/g}x$ is an invariant manifold in Oxz.

In order to study the stability of this solution we calculate the Jacobian J of the system (1) at this point,

$$J = \begin{pmatrix} -\frac{bcx^+}{1+b(x^++z^+)} + \frac{cgz^+}{x^++gz^+} & \square & -\frac{bcx^+}{1+b(x^++z^+)} - \frac{cgx^+}{x^++gz^+} \\ 0 & Q & 0 \\ -\frac{bcz^+}{1+b(x^++z^+)} - \frac{hcz^+}{z^++hx^+} & \square & -\frac{bcz^+}{1+b(x^++z^+)} + \frac{hcx^+}{z^++hx^+} \end{pmatrix},$$

where $\square$ means that the values of J_{12} and J_{32} are useless for the calculation of the eigenvalues. An eigenvalue is

$$Q = \frac{Ax^+}{\left(1+B\left(x^++z^+\right)\right)\left(x^++Gz^+\right)} - C$$

and from the expressions of x^+ and z^+ we obtain

$$Q = \frac{C}{1+\frac{B}{b}\left(\dfrac{a}{c\left(1+\sqrt{hg}\right)} - 1\right)} \frac{\frac{A}{C}\sqrt{gh}}{\sqrt{gh}+Gh} - C.$$

The other two eigenvalues have the product

$$\begin{vmatrix} J_{11} & J_{13} \\ J_{31} & J_{33} \end{vmatrix} < 0$$

so that they have opposite signs. Consequently, the equilibrium $(x^+,0,z^+)$ is hyperbolic unstable. If $Q < 0$, system (1) has a two-dimensional local stable invariant manifold and a one-dimensional local unstable invariant manifold. If $Q > 0$ the system has a two-dimensional local unstable invariant manifold and a one-dimensional local stable invariant manifold (see [3], Theorem 1.3.2–Stable Manifold Theorem for a Fixed Point).

g) In the Oyz plane the equilibrium condition leads us to the system

$$\begin{cases} \dfrac{A}{1+B(y+z)} \dfrac{y}{y+Gz} = C, \\ \dfrac{a}{1+b(y+z)} \dfrac{z}{z+hy} = c, \end{cases} \tag{4}$$

which becomes

$$F_1(y,z) \equiv CBy^2 + CB(G+1)yz + CBGz^2 + (C-A)y + CGz = 0,$$
$$F_2(y,z) \equiv cbhy^2 + cb(h+1)yz + cbz^2 + chy + (c-a)z = 0.$$

This means that the equilibrium point is the intersection of these two conics and it is admissible if its coordinates are both positive.

Obviously, the two conics pass through the origin. We also have

$$F_1(y,0) = CBy^2 + (C-A)y = 0 \Longrightarrow y = 0,\ y = D,$$
$$F_1(0,z) = CBGz^2 + CGz = 0 \Longrightarrow z = 0,\ z = -\frac{1}{B},$$

and

$$F_2(y,0) = cbhy^2 + chy = 0 \Longrightarrow y = 0,\ y = -\frac{1}{b},$$
$$F_2(0,z) = cbz^2 + (c-a)z = 0 \Longrightarrow z = 0,\ z = d.$$

But

$$\delta_1 = \begin{vmatrix} CB & \frac{CB(G+1)}{2} \\ \frac{CB(G+1)}{2} & CBG \end{vmatrix} = C^2B^2G - \frac{C^2B^2(G+1)^2}{4} = -\frac{C^2B^2(G-1)^2}{4} < 0$$

for F_1 and

$$\delta_2 = \begin{vmatrix} cbh & \frac{cb(h+1)}{2} \\ \frac{cb(h+1)}{2} & cb \end{vmatrix} = c^2b^2h - \frac{c^2b^2(h+1)^2}{4} = -\frac{c^2b^2(h-1)^2}{4} < 0$$

for F_2 so that the conics are hyperbolas if $G \neq 1$, $h \neq 1$, see Figure 1.

The center of $F_1(y,z) = 0$ has the coordinates

$$y_0 = \frac{G(C-A) - AG - CG^2}{CB(G-1)^2} < 0, \quad z_0 = \frac{G(C+A) + A - C}{CB(G-1)^2} > 0$$

and the asymptotes are

$$z - z_0 = -\frac{1}{G}\left(y - y_0\right), \quad z - z_0 = -\left(y - y_0\right).$$

If $G > 1$, the first asymptote intersects Oy at $y_0 + Gz_0 > D$ and intersects Oz at $\frac{y_0+Gz_0}{G} > 0$, while the second asymptote intersects both Oy and Oz at $y_0 + z_0 < -\frac{1}{B}$.

If $G < 1$, the first asymptote intersects Oy at $y_0 + Gz_0 < 0$ and intersects Oz at $\frac{y_0+Gz_0}{G} < -\frac{1}{B}$, while the second asymptote intersects both Oy and Oz at $y_0 + z_0 > D$. Consequently, the hyperbola $F_1(y,z) = 0$ has a unique branch into the first quadrant of Oyz.

Analogously, the center of $F_2(y,z) = 0$ has the coordinates

$$y_0 = \frac{h(c+a) + a - c}{bc(h-1)^2} > 0, \quad z_0 = \frac{h(c-a) - ah - ch^2}{bc(h-1)^2} < 0$$

and the asymptotes are

$$z - z_0 = -h\left(y - y_0\right), \quad z - z_0 = -\left(y - y_0\right).$$

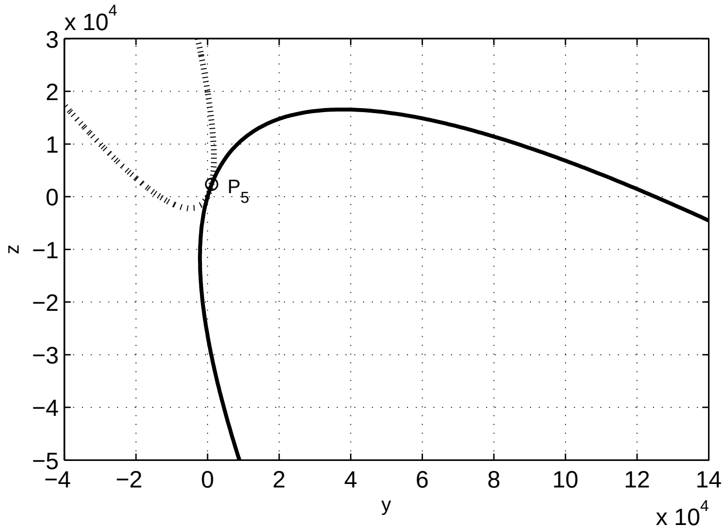

Figure 1: The equilibrium point $P_5 \in Oyz$.

If $h > 1$ the first asymptote intersects Oy at $\frac{hy_0+z_0}{h}$ and intersects Oz at $z_0 + hy_0 > d$ while the second asymptote intersects both Oy and Oz at $y_0 + z_0 < -\frac{1}{b}$.

If $h < 1$ the first asymptote intersects Oy at $\frac{hy_0+z_0}{h} < -\frac{1}{b}$ and intersects Oz at $z_0 + hy_0$ while the second asymptote intersects both Oy and Oz at $y_0 + z_0 > d$.

Consequently, the hyperbola $F_2(y, z) = 0$ has a unique branch into the first quadrant of Oyz.

The intersection of these branches depends on their slopes at the origin

$$z_y = -\frac{F_{1y}(0,0)}{F_{1z}(0,0)} = \frac{A-C}{CG} > 0$$

for F_1 and

$$z_y = -\frac{F_{2y}(0,0)}{F_{2z}(0,0)} = \frac{ch}{a-c} > 0$$

for F_2. We have an intersection point $P_5(0, y^*, z^*)$ solution of the system (4) with positive coordinates if and only if

$$\frac{A-C}{CG} > \frac{ch}{a-c},$$

i.e.

$$hG < BbDd = \left(\frac{A}{C} - 1\right)\left(\frac{a}{c} - 1\right).$$

The stability of this point is given by the eigenvalues of the Jacobian

$$J = \begin{pmatrix} P & 0 & 0 \\ \Box & -\frac{BCy^*}{1+B(y^*+z^*)} + \frac{GCz^*}{y^*+Gz^*} & -\frac{BCy^*}{1+B(y^*+z^*)} - \frac{GCy^*}{y^*+Gz^*} \\ \Box & -\frac{bcz^*}{1+b(y^*+z^*)} - \frac{chz^*}{z^*+hy^*} & -\frac{bcz^*}{1+b(y^*+z^*)} + \frac{chy^*}{z^*+hy^*} \end{pmatrix}.$$

One eigenvalue is

$$P = \frac{ay^*}{(1 + b(y^* + z^*))\,(y^* + gz^*)} - c.$$

The product of the other two eigenvalues is

$$\begin{vmatrix} J_{22} & J_{23} \\ J_{32} & J_{33} \end{vmatrix} < 0$$

so that they have opposite signs. Consequently, the equilibrium $(0, y^*, z^*)$ is hyperbolic unstable. If $P < 0$ the system (1) has a two-dimensional local stable invariant manifold and a one-dimensional local unstable invariant manifold. If $P > 0$ the system has a two-dimensional local unstable invariant manifold and a one-dimensional local stable invariant manifold.

From the system (4) verified by (y^*, z^*), we have

$$P = \frac{a\left(hy^{*2} - gz^{*2}\right)}{(1 + b(y^* + z^*))\,(y^* + gz^*)\,(z^* + hy^*)}$$

whose sign is given by $hy^{*2} - gz^{*2}$. More precisely,

$$\frac{y^*}{z^*} < \sqrt{\frac{g}{h}} \Longrightarrow P < 0,$$
$$\frac{y^*}{z^*} > \sqrt{\frac{g}{h}} \Longrightarrow P > 0.$$

In order to evaluate the sign of P, we eliminate $y^* + z^*$ from the system (4). We obtain

$$\frac{B}{A}\frac{a}{b} = \frac{\frac{1}{C}\frac{y^*}{y^*+Gz^*} - \frac{1}{A}}{\frac{1}{c}\frac{z^*}{z^*+hy^*} - \frac{1}{a}}.$$

and by denoting $\frac{y^*}{z^*} = t^*$ we have

$$\frac{A}{B}\left(\frac{1}{C}\frac{t^*}{t^* + G} - \frac{1}{A}\right) = \frac{a}{b}\left(\frac{1}{c}\frac{1}{1 + ht^*} - \frac{1}{a}\right).$$

Consequently, t^* is a positive root of the equation

$$f(t) \equiv \frac{A}{BC}\frac{t}{t + G} - \frac{a}{bc}\frac{1}{1 + ht} - \frac{1}{B} + \frac{1}{b} = 0.$$

But

$$f'(t) = \frac{A}{BC}\frac{G}{(t + G)^2} + \frac{a}{bc}\frac{h}{(1 + ht)^2} > 0,$$

and

$$f(0) = -\frac{a}{bc} - \frac{1}{B} + \frac{1}{b} = \frac{c - a}{bc} - \frac{1}{B} < 0,$$
$$\lim_{t\to\infty} f(t) = \frac{A}{BC} - \frac{1}{B} + \frac{1}{b} = \frac{A - C}{BC} + \frac{1}{b} > 0$$

so that

$$f\left(\sqrt{\frac{g}{h}}\right) > 0 = f(t^*) \Longleftrightarrow t^* < \sqrt{\frac{g}{h}} \Longleftrightarrow P < 0,$$
$$f\left(\sqrt{\frac{g}{h}}\right) < 0 = f(t^*) \Longleftrightarrow t^* > \sqrt{\frac{g}{h}} \Longleftrightarrow P > 0.$$

Consequently, the sign of P is opposite to the sign of

$$f\left(\sqrt{\frac{g}{h}}\right) = \frac{A}{BC}\frac{\sqrt{gh}}{\sqrt{gh}+Gh} - \frac{a}{bc}\frac{1}{1+\sqrt{gh}} - \frac{1}{B} + \frac{1}{b}.$$

If the equilibrium P_5 exists but P_4 does not exist, i.e.

$$Gh < \left(\frac{A}{C}-1\right)\left(\frac{a}{c}-1\right), \qquad \sqrt{gh} > \frac{a}{c}-1,$$

then

$$0 < Gh < \left(\frac{A}{C}-1\right)\sqrt{gh}$$

and

$$f\left(\sqrt{\frac{g}{h}}\right) > \frac{A}{BC}\frac{1}{1+\frac{\left(\frac{A}{C}-1\right)\left(\frac{a}{c}-1\right)}{\sqrt{gh}}} - \frac{a}{bc}\frac{1}{1+\sqrt{hg}} - \frac{1}{B} + \frac{1}{b} >$$
$$> \frac{A}{BC}\frac{1}{1+\frac{A}{C}-1} - \frac{a}{bc}\frac{1}{1+\frac{a}{c}-1} - \frac{1}{B} + \frac{1}{b} = 0.$$

In this case, $P < 0$ and the equilibrium $P_5(0, y^*, z^*)$ has a two-dimensional local stable manifold and a one-dimensional local unstable manifold.

If the equilibrium P_5 does not exist, but P_4 exists, i.e.

$$Gh > \left(\frac{A}{C}-1\right)\left(\frac{a}{c}-1\right), \qquad \sqrt{gh} < \frac{a}{c}-1,$$

then

$$Gh > \left(\frac{A}{C}-1\right)\sqrt{gh}$$

and

$$Q = \frac{C}{1+\frac{B}{b}\left(\frac{a}{c\left(1+\sqrt{hg}\right)}-1\right)}\frac{\frac{A}{C}\sqrt{gh}}{\sqrt{gh}+Gh} - C < C\left(\frac{\frac{A}{C}\sqrt{gh}}{\sqrt{gh}+Gh}-1\right) < 0.$$

In this case, $Q < 0$ and the equilibrium $P_4(x^+, 0, z^+)$ has a two-dimensional local stable manifold and a one-dimensional local unstable manifold.

If both equilibria P_4 and P_5 exist, i.e.

$$Gh < \left(\frac{A}{C}-1\right)\left(\frac{a}{c}-1\right), \qquad \sqrt{gh} < \frac{a}{c}-1,$$

we have

$$Q = \frac{C}{1 + \frac{B}{b}\left(\frac{a}{c\left(1+\sqrt{hg}\right)} - 1\right)} \frac{\frac{A}{C}\sqrt{gh}}{\sqrt{gh}+Gh} - C,$$

$$f\left(\sqrt{\frac{g}{h}}\right) = \frac{A}{BC}\frac{\sqrt{hg}}{\sqrt{hg}+Gh} - \frac{a}{bc}\frac{1}{1+\sqrt{hg}} - \frac{1}{B} + \frac{1}{b}.$$

By eliminating $\frac{\frac{A}{C}\sqrt{gh}}{\sqrt{gh}+Gh}$ we obtain

$$\frac{\frac{A}{C}\sqrt{gh}}{\sqrt{gh}+Gh} = Bf\left(\sqrt{\frac{g}{h}}\right) + \frac{B}{b}\left(\frac{a}{c}\frac{1}{1+\sqrt{hg}} - 1\right) + 1,$$

$$Q = \frac{C\left(Bf\left(\sqrt{\frac{g}{h}}\right) + \frac{B}{b}\left(\frac{a}{c}\frac{1}{1+\sqrt{hg}} - 1\right) + 1\right)}{1 + \frac{B}{b}\left(\frac{a}{c\left(1+\sqrt{hg}\right)} - 1\right)} - C = \frac{BCf\left(\sqrt{\frac{g}{h}}\right)}{1 + \frac{B}{b}\left(\frac{a}{c\left(1+\sqrt{hg}\right)} - 1\right)}.$$

Consequently, Q has the same sign as $f\left(\sqrt{\frac{g}{h}}\right)$, so that Q and P have opposite signs. This means that either $P_5(0, y^*, z^*)$ or $P_4(x^+, 0, z^+)$ has a two-dimensional local stable manifold.

h) Finally, if we search equilibrium points (x, y, z) with $x > 0$, $y > 0$, $z > 0$, we are led to the system

$$\begin{cases} \frac{a}{1+b(x+y+z)}\frac{x+y}{x+y+gz} - c = 0, \\ \frac{A}{1+B(x+y+z)}\frac{x+y}{x+y+Gz} - C = 0, \\ \frac{a}{1+b(x+y+z)}\frac{z}{z+h\left(x+y\right)} - c = 0. \end{cases}$$

By denoting $u = x + y$, this system becomes

$$\begin{aligned} au &= c\left(1 + b(u+z)\right)\left(u + gz\right), \\ Au &= C\left(1 + B(u+z)\right)\left(u + Gz\right), \\ az &= c\left(1 + b(u+z)\right)\left(z + hu\right). \end{aligned}$$

But

$$\frac{u}{z} = \frac{u+gz}{z+hu} = \frac{\frac{u}{z}+g}{1+h\frac{u}{z}},$$

hence we obtain $\frac{u}{z} = \sqrt{\frac{g}{h}}$. Now, from the first equation we get

$$u + z = \frac{1}{b}\left(\frac{\frac{a}{c}}{1+\sqrt{gh}} - 1\right).$$

Obviously, $u + z > 0$, if $\sqrt{gh} < \frac{a}{c} - 1$.

We obtain now from the second equation the consistency condition

$$\frac{\frac{A}{C}\sqrt{gh}}{\sqrt{gh}+Gh} = 1 + \frac{B}{b}\left(\frac{\frac{a}{c}}{1+\sqrt{gh}} - 1\right), \tag{5}$$

from where

$$Gh < \left(\frac{A}{C} - 1\right)\sqrt{gh} < \left(\frac{A}{C} - 1\right)\left(\frac{a}{c} - 1\right).$$

For the existence of such an equilibrium it is necessary that equilibria P_4 and P_5 exist and, moreover, $P = Q = 0$. In this very particular case, the equilibrium is not unique. The solutions (x, y, z) verify $x + y = u_0$, $z = z_0$, where

$$u_0 = \frac{1}{b}\left(\frac{\frac{a}{c}}{1+\sqrt{gh}} - 1\right)\frac{\sqrt{gh}}{\sqrt{gh}+h}, \quad z_0 = \frac{\frac{1}{b}\left(\frac{\frac{a}{c}}{1+\sqrt{gh}} - 1\right)}{1+\sqrt{\frac{g}{h}}}. \tag{6}$$

Now if we put together the above results, we can state the following

Theorem 2.1 *Let* $a, b, c, A, B, C, g, G, h$ *be positive parameters such that* $a > c$, $A > C$, $d < D$, *where* $d = \frac{1}{b}\left(\frac{a}{c} - 1\right)$ *and* $D = \frac{1}{B}\left(\frac{A}{C} - 1\right)$. *Then system* (1), *considered for* $x \geq 0$, $y \geq 0$, $z \geq 0$, *has the following steady-states:*

a) $O(0,0,0)$ *and* $P_1(d,0,0)$ *as unstable equilibria,*

b) $P_2(0,D,0)$ *and* $P_3(0,0,d)$ *as asymptotically stable equilibria,*

c) $P_4(x^+,0,z^+)$ *given by* (3) *if* $hg < \left(\frac{a}{c} - 1\right)^2$ *and*

d) $P_5(0,y^*,z^*)$ *given by* (4) *if* $hG < \left(\frac{a}{c} - 1\right)\left(\frac{A}{C} - 1\right)$, *as hyperbolic unstable equilibria. Only one of* P_4 *or* P_5 *has a two-dimensional local stable invariant manifold. Finally, the system* (1) *has*

e) *a line of equilibria* $P(x,y,z)$ *in the case* (5), *where* $x + y = u_0$, $z = z_0$ *are given by* (6).

We remark that the local stable invariant manifolds W^s_{loc} of hyperbolic equilibria have global analogues W^s obtained by letting points in W^s_{loc} flow backwards in time.

These manifolds act as boundaries between different regions of the phase space. For a system with multiple attractors, a boundary of a basin of attraction can often be recovered as a codimension-one stable manifold of a saddle point, such as P_4 or P_5.

In general, such manifolds can not be expressed in closed-form and therefore must be approximated numerically for particular values of the parameters. In our paper we have used an efficient algorithm of Moore [4], based on Laguerre functions and modified in order to apply our MATLAB package *LaguerreEig* [8].

3 Numerical Simulations

In order to verify and to illustrate the above theoretical results, we will perform some numerical tests, with the physiological values of the parameters chosen from [2]:

$$\begin{array}{lll} a = 0.005, & A = 0.0115, & g = 2, \\ b = 0.000075, & B = 0.000038, & G = 2, \\ c = 0.002, & C = 0.002, & h = 2, \end{array}$$

such that

$$a > c, \quad A > C, \quad d = 20000 < D = 125000.$$

The condition

$$Gh = 4 < \left(\frac{A}{C} - 1\right)\left(\frac{a}{c} - 1\right) = 4.75 \times 1.5$$

is fulfilled, but

$$hg = 4 > \left(\frac{a}{c} - 1\right)^2 = (1.5)^2$$

so that we have no equilibrium P_4 in the Oxz plane – in this case $x^+ < 0$. The consistency condition (5) is not satisfied:

$$\frac{\frac{0.0115}{0.002}\sqrt{4}}{\sqrt{4}+4} \neq 1 + \frac{0.000038}{0.000075}\left(\frac{\frac{0.005}{0.002}}{1+\sqrt{4}} - 1\right)$$

or $1.9167 \neq 0.91556$. We have $P_5(0, 1149.089506, 2342.140461)$ and the corresponding eigenvalues of the Jacobian are $-.0003471757542, .002588209809, -.001219452669$. This point P_5 is an unstable equilibrium with a two-dimensional stable manifold. The numerical tests show that this manifold indeed separates the attraction basins of the asymptotically stable equilibria $P_2(0, 125000, 0)$ and $P_3(0, 0, 20000)$ in the computational domain of physiological significance, see Figure 2.

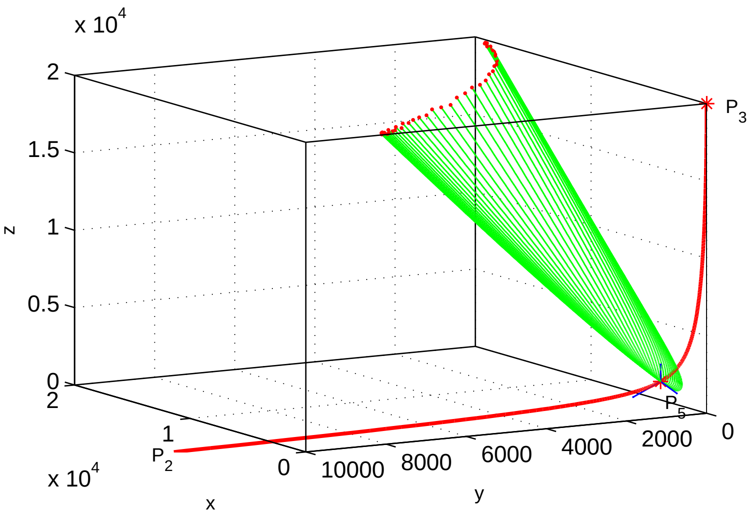

Figure 2: Case $C = 0.002$. The numerically calculated two-dimensional stable manifold of P_5. The continuous line that connects P_5P_2 and P_5P_3 in the plane Oyz is the numerically calculated one-dimensional unstable manifold of P_5.

If therapeutic agents are used in order to increase the death rate of the leukemic cells, i.e. to increase C from $C = 0.002$ to $C = 0.006$ for example, the equilibria P_4 and P_5 do not exist in the considered domain. Again $A > C$ and $d < D$, as above, but the numerical tests show that the border between the attraction basins of P_2 and P_3 is now a numerically calculated two-dimensional invariant manifold which behaves as a two-dimensional stable manifold of the origin O. In this case the attraction basin of $P_3(0, 0, 20000)$ increases, see Figure 3.

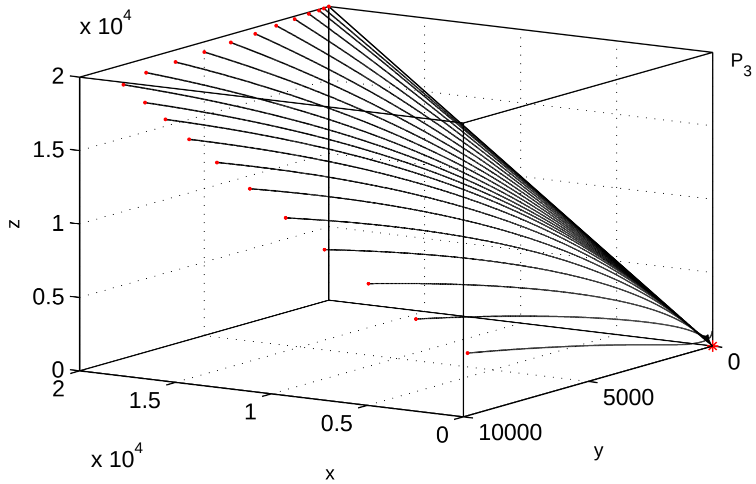

Figure 3: case $C = 0.006$. The border between the attraction basins of P_2 and P_3.

4 Conclusion

A mathematical model of Dingli and Michor [2] was augmented in [5] in order to simulate the cell dynamics after bone marrow transplantation. The new model (1) introduces the parameters h, g, G standing for the intensity of anti-graft, anti-host and anti-leukemia effects.

This model has only two asymptotically stable equilibria, $P_2(0, D, 0)$ and $P_3(0, 0, d)$. Other important unstable hyperbolic equilibria are $P_4(x^+, 0, z^+)$, which exists if and only if $hg < \left(\frac{a}{c} - 1\right)^2$, and $P_5(0, y^*, z^*)$, which exists if and only if $hG < \left(\frac{A}{C} - 1\right)\left(\frac{a}{c} - 1\right)$.

If, after an appropriate therapy, h is sufficiently small, i.e. the anti-graft effect becomes small enough, then one or both equilibria P_4 or P_5 exist and, by the stable manifold theorem for a hyperbolic fixed point, one of them always has a stable two-dimensional invariant manifold.

This stable manifold provides important information about the system's global dynamics, for example it indicates the boundary of the attraction basins of the asymptotically stable equilibria P_2 and P_3. Given the initial host cell concentrations x_0, y_0, we may calculate an initial concentration (dose of infused cells at transplantation) z_0 in the attraction basin of P_3 so that, in time, host cells will be eliminated and completely replaced by donor cells, guaranteeing the elimination of cancer. Based on the stability analysis in this paper, a theoretical basis for the control of post-transplant evolution can be provided and therapy planning algorithms for guiding the correction treatment after transplant can be established. This is the goal of the subsequent paper [6].

Acknowledgment

This work was supported by a grant of the Romanian National Authority for Scientific Research, CNCS UEFISCDI, project number PN-II-ID-PCE-2011-3-0094.

References

[1] Cucuianu, A. and Precup, R. A hypothetical-mathematical model of acute myeloid leukaemia pathogenesis. *Comput. Math. Methods Med.* **11** (2010) 49–65.

[2] Dingli, D. and Michor, F. Successful therapy must eradicate cancer stem cells. *Stem Cells* **24** (2006) 2603–2610.

[3] Guckenheimer, J. and Holmes, P. *Nonlinear Oscillations, Dynamical Systems, and Bifurcation of Vector Fields.* Springer-Verlag, New York, 1983.

[4] Moore, G. Laguerre approximation of stable manifolds with application to connecting orbits. *Math. Comp.* **73** (2004) 211–242.

[5] Precup, R., Arghirescu, S., Cucuianu, A. and Serban, M. Mathematical modeling of cell dynamics after allogeneic bone marrow transplantation in acute myeloid leukemia. *Int. J. Biomath.* **5**(2012), 1250026 [18 pages] DOI: 10.1142/S1793524511001684.

[6] Precup, R., Serban, M-A., Trif, D. and Cucuianu, A. A planning algorithm for correction therapies after allogeneic stem cell transplantation. *J. Math. Model. Algor.* **11** (2012) 309–323.

[7] Precup, R., Trif, D., Serban, M-A. and Cucuianu A. A mathematical approach to cell dynamics before and after allogeneic bone marrow transplantation. *Ann. Tiberiu Popoviciu Semin. Funct. Equ. Approx. Convexity* **8** (2010) 167–175.

[8] Trif, D. *LaguerreEig* (2009), Available from:
http://www.mathworks.com/ matlabcentral/fileexchange/24266-laguerreeig.

Nonlinear Dynamics and Systems Theory, **13** (1) (2013) 93–106

Adaptive Synchronization for Oscillators in ϕ^6 Potentials

U. E. Vincent [1,2*] and R. Guo [3]

[1] *Department of Physics, Lancaster University, Lancaster LA1 4YB, United Kingdom*
[2] *Department of Physical Sciences, Redeemer's University, Km 46, Lagos – Ibadan Expressway, P.M.B 3005, Redemption City, Nigeria*
[3] *Department of Mathematical and Physical Sciences, Shandong Institute of Light Industry, Jinan 250353, PR China*

Received: February 29, 2012 Revised: January 19, 2013

Abstract: In this paper, we investigate adaptive synchronization for multi-parameter oscillators with ϕ^6 potentials. We consider the synchronization for known and unknown system parameters for the ϕ^6 Van-der Pol and Duffing oscillator based on a simple adaptive control technique; and show that a single-state adaptive feedback is sufficient to steer two identical oscillators to stable synchronization. We obtain some estimates of the unknown parameters for both systems and present numerical simulations to show the effectiveness of our approach.

Keywords: *synchronization; adaptive control; ϕ^6 oscillators.*

Mathematics Subject Classification (2010): 34C28, 34D06, 93C40, 93D21.

1 Introduction

The synchronization of chaotic oscillator is an intriguing phenomenon that has received considerable research attention during the last two decades. The increasing and enormous research activities on chaos synchronization is partly motivated by several promising real life applications; spanning areas such as secure communications, chaos generators design, chemical reactions, lasers, biological systems, information science, neural networks, etc [1–7]. For this reason, the study of chaos synchronization has grown rapidly since its discovery in 1990 by Pecora and Carroll [1]; and a wide variety of linear and nonlinear approaches have been proposed and well developed for achieving specific synchronization

* Corresponding author: `mailto:u.vincent@lancaster.ac.uk`

`http://e-ndst.kiev.ua`

goals [1, 8–22]. These methods have been applied to many real physical model systems, such as the Nonlinear Bloch equations [31–33], lasers [34,35], Josephson junctions [36–38], various forms of the Van-der Pol and Duffing oscillators, including the ϕ^6 oscillators [23–29], to mention but a few.

The dynamics of nonlinear systems with ϕ^6 potentials [39–45], have become more fascinating because, ϕ^6 oscillators, in particular present more complex dynamics than their corresponding ϕ^4 oscillators. This property makes them better models for security of encrypted information during transmission. Thus, investigating chaos synchronization for ϕ^6 oscillators is very relevant for secure communications.

In [29], the author introduced a modified active control method for realizing the identical and non-identical synchronization of chaotic oscillators in ϕ^6 potentials. The proposed active control in [29] was specifically aimed at treating the problem of controller complexity arising in the application of the active control formalism. However, one of the two control inputs, that play the key role in driving the two oscillators to a synchronized state is still complex relative to the controlled systems, implying that the proposed approach remains questionable with regard to practical applications. Moreover, the parameters of the synchronizing systems in [29] were assumed to be known in advance, in all the cases considered. Since in practice the parameters of chaotic systems are not usually known in advance, it would be significant to investigate the synchronization for the case of unknown parameters as in [46]. In particular, for multi-parameter systems such as the ϕ^6 oscillators, estimating the unknown parameters of the systems is essential in the synchronization process.

In general, the problem of design flexibility and controller complexity has remained a crucial and long standing issue in control theory research [19, 47]. Recently, Guo [48], proposed a simple adaptive controller for the identical chaos synchronization. This technique was applied to achieve the adaptive and reduced-order synchronization for Josephson junctions and time-varying lower-order systems [38,49]; and further extended to realize the stabilization of chaotic systems [50, 51].

The goal of the present paper is to investigate the synchronization of ϕ^6 Van-der Pol and Duffing oscillators based on our proposed simple adaptive control [38, 48, 49]. We will show that for two identical ϕ^6 oscillators, a single-state adaptive feedback is sufficient to drive the oscillators to a stable synchronized state. Furthermore, we will consider the synchronization for unknown system parameters and obtain an estimate of all the unknown parameters of the systems. In the next section, we would give a brief theory of our proposed method. In Section 3, synchronization for identical ϕ^6 Van-der Pol and Duffing oscillators would be treated, both for known and unknown parameters; while in Section 4, we deal with the estimation of the unknown parameters. The paper is concluded in Section 5.

2 Theory of Adaptive-Feedback Control

2.1 Adaptive control for chaos synchronization

Let us introduce in this section, the adaptive control method [48] briefly. For a master chaotic system given as,

$$\dot{x} = f(x), \tag{1}$$

where $x = (x_1, x_2, \cdots, x_n)^T \in \mathrm{R}^n$, $f(x) = (f_1(x), f_2(x), \cdots, f_n(x))^T : \mathrm{R}^n \to \mathrm{R}^n$ is a nonlinear vector function. Without loss of generality, let $\Omega \subset \mathrm{R}^n$ be a chaotic bounded set of system (1) which is globally attractive. For the vector function $f(x)$, we give a general assumption.

Assumption 1 $\forall x = (x_1, x_2, \cdots, x_n)^T \in \Omega$ and $y = (y_1, y_2, \cdots, y_n)^T \in \Omega$ there exists a constant $l > 0$ satisfying

$$| f_i(x) - f_i(y) | \leq l \mid x - y \mid_\infty, i = 1, 2, \cdots, n, \tag{2}$$

where $\mid x - y \mid_\infty$ is the ∞-norm of $x - y$. i.e., $\mid x - y \mid_\infty = \max_j \mid x_j - y_j \mid, j = 1, 2, \cdots, n$.

Remark 1 This condition is very loose, and in fact, holds as long as $\partial f_i / \partial x_j (i, j = 1, 2, \cdots, n)$ are bounded. Thus, the class of systems in the form of (1) and (2) includes almost all well-known finite-dimensional chaotic and hyperchaotic systems. The corresponding slave system to system (1) is as follows,

$$\dot{y} = f(y) + k_1(y - x) = f(y) + u, \tag{3}$$

where the controller $u = k_1 e = (k_1 e_1, k_1 e_2, \cdots, k_1 e_n)^T, e_i = y_i - x_i$. Unlike the usual linear feedback control, the feedback gain k_1 is duly adapted according to the following update law,

$$\dot{k}_1 = -\gamma \sum_{i=1}^{n} e_i^2, \tag{4}$$

where γ is an arbitrary positive constant. The controller $u = k_1 e$ can realize the synchronization of the master and slave chaotic systems (1) and (2).

Remark 2 The feedback gain k_1 is automatically adapted to a suitable strength k_0 depending on the initial values, which is significantly different from the well known linear feedback.

Remark 3 The controller $u = k_1 e$ can employ only one feedback term e_i for some chaotic systems. The feedback term e_i is selected such that, if $e_i = 0$ then $e_j = 0, j = 1, 2, \cdots n, j \neq i$, so that the set $E = \{(e, k_1) \in \mathrm{R}^{n+1} | e = 0, k_1 = k_0\}$. Thus, leading to the above conclusion.

2.2 Adaptive control for chaos synchronization with unknown parameters

In our previous paper [49], we obtained a novel adaptive controller for chaos synchronization with unknown parameters. This is introduced in brief herein. Consider a nonlinear dynamical system

$$\dot{x} = f(x) + g(x)p, \tag{5}$$

where $x = (x_1, x_2, \cdots, x_n)^T \in \mathrm{R}^n$ denotes the state variables, $p = (p_1, p_2, \cdots, p_k)^T \in \mathrm{R}^k$ denotes the uncertain parameters, $f(x) = (f_1(x), f_2(x), \cdots, f_n(x))^T$ and $g(x) = [g(x)]_{n \times k}$ represent differential nonlinear vector function and matrix function respectively. The vector function $f(x)$ satisfies Assumption 1.

We consider system (5) as the master system and introduce a controlled slave system

$$\dot{y} = f(y) + g(y)p + u, \tag{6}$$

where $y = (y_1, y_2, \cdots, y_n)^T \in \mathrm{R}^n$ denotes the state variables, and $u = (u_1, u_2, \cdots, u_n)^T$ is a controller. The main goal is to design a suitable controller u to synchronize the two identical systems in spite of their uncertain parameters. We denote the synchronization error between the two systems as $e = y - x \in \mathrm{R}^n$ and subtract system (5) from system (6) and thus obtain the error dynamical system

$$\dot{e} = f(y) - f(x) + [g(y) - g(x)]p + u. \tag{7}$$

We can introduce the control function

$$u = -[g(y) - g(x)]\hat{p} + k_1 e, \tag{8}$$

where $\hat{p}$ is the estimate of p, and $k_1 e = (k_1 e_1, k_1 e_2, \cdots, k_1 e_n)^T \in \mathrm{R}^n$ is the linear feedback control with the updated gain $k_1 \in \mathrm{R}^1$. Thus, the synchronization error system is reduced to

$$\dot{e} = [f(y) - f(x)] + [g(y) - g(x)]\tilde{p} + k_1 e, \tag{9}$$

where $\tilde{p} = p - \hat{p}$ is the parameter estimation mismatch between the real value of the unknown parameter and its corresponding estimated value. Then the above discussion can be summarized in the following theorem.

Theorem 1 *If the estimations of the unknown parameters and the feedback gain contained in the adaptive controller (8) are updated by the following laws*

$$\begin{cases} \dot{\hat{p}} = [g(y) - g(x)]^T e, \\ \dot{k}_1 = -\gamma e^T e = -\gamma \sum_{i=1}^{n} e_i^2, \end{cases} \tag{10}$$

then, the synchronization between system (5) and (6) will be achieved.

Remark 4 The control term $k_1 e$ can include only one feedback term e_i for some chaotic systems. The feedback term e_i is selected such that if $e_i = 0$ then $e_j = 0, j = 1, 2, \cdots n, j \neq i$, therefore the set $E = \{(e, \tilde{p}, k_1) \in \mathrm{R}^{n+k+1} | e = 0, \tilde{p} = 0, k_1 = -k^*\}$, so that the conclusion in (10) is obtained.

3 Synchronization of Two Identical ϕ^6 Van-der Pol and Duffing Oscillators

3.1 Example 1. ϕ^6 Van-der Pol oscillators

The ϕ^6 Van-der Pol oscillators could be written as

$$\begin{aligned} \dot{x}_1 &= x_2, \\ \dot{x}_2 &= \mu(1 - x_1^2)x_2 - \alpha x_1 - \beta x_1^3 - \delta x_1^5 + f cos(\omega t), \end{aligned} \tag{11}$$

where $\mu, \alpha, \beta, \delta, f, \omega$ are parameters of the system (11). Let system (11) be the master system.

Case 1: The parameters $(\mu, \alpha, \beta, \delta, f, \omega)$ of the master system (11) are assumed to be known. According to Ref. [48], the slave system with adaptive controller is as follows,

$$\begin{aligned} \dot{y}_1 &= y_2 + k_1(y_1 - x_1), \\ \dot{y}_2 &= \mu(1 - y_1^2)y_2 - \alpha y_1 - \beta y_1^3 - \delta y_1^5 + f cos(\omega t), \end{aligned} \tag{12}$$

where the feedback gain k_1 is adapted according to the following update law $\dot{k}_1 = -\gamma e_1^2$. The strength of the arbitrary constant γ would influence the controller performance. For instance, large γ would lead to fast stabilization of the augment system; while the feedback gain k_1 would quickly approach a suitable negative constant. On the contrary, the speed of stabilization would be very slow for small γ; so that the feedback gain k_1 would slowly approach a suitable negative constant.

Next, we give numerical simulations to verify the above theoretical result. Firstly, let the initial conditions of the master system (11) be: $x_1(0) = 1, x_2(0) = 2$, the slave system (12): $y_1(0) = -3, y_2(0) = 4$ and $\mu = 0.4, \alpha = 1.0, \beta = -0.7, \delta = 0.1, f = 9, \omega = 3.14$. With the initial value of the controller $k_1(0) = -1$, Figure 1 shows the synchronization performance. The error system of two identical ϕ^6 Van-der Pol oscillators approaches zero asymptotically as $t \to \infty$, while the feedback gain k_1 tends to a negative constant. For other sets of initial conditions and system parameters, the synchronization is still achievable. For instance, let the initial conditions be $x_1(0) = 1, x_2(0) = 2$, and $y_1(0) = -3, y_2(0) = 1$; while the system parameters are: $\mu = 0.4, \alpha = 0.46, \beta = 1.0, \delta = 0.1, f = 4.5, \omega = 0.86$. Using the same initial value of the controller $k_1(0) = -1$, as before, Figure 2 shows that the two identical Φ^6 Van-der Pol oscillators achieves asymptotic synchronization as $t \to \infty$, while the feedback gain k_1 tends to a negative constant.

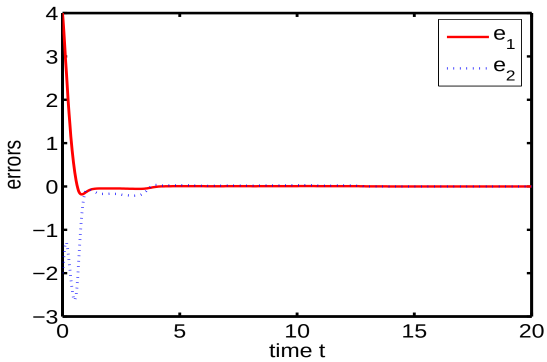

Figure 1: The error system of two identical Φ^6 Van-der Pol oscillators ($\mu = 0.4, \alpha = 1.0, \beta = -0.7, \delta = 0.1, f = 9, \omega = 3.14$) is asymptotically stable as $t \to \infty$.

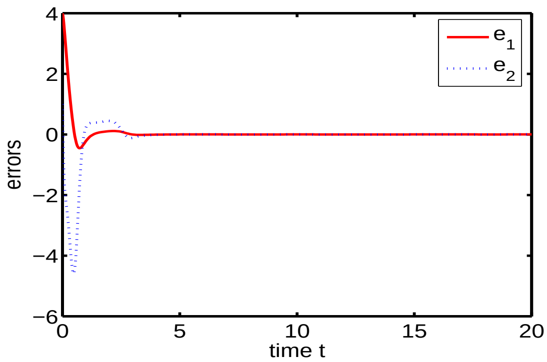

Figure 2: The error system of two identical Φ^6 Van-der Pol oscillators ($\mu = 0.4, \alpha = 0.46, \beta = 1.0, \delta = 0.1, f = 4.5, \omega = 0.86$) is asymptotically stable as $t \to \infty$.

Case 2: The parameters $(\mu, \alpha, \beta, \delta)$ of system (11) are unknown.

According to our method in Ref. [49], the slave system with adaptive controller is as follows,

$$\begin{aligned} \dot{y}_1 &= y_2 + u_1, \\ \dot{y}_2 &= \mu(1-y_1^2)y_2 - \alpha y_1 - \beta y_1^3 - \delta y_1^5 + f cos(\omega t) + u_2, \end{aligned} \tag{13}$$

where the controller $u = (u_1, u_2)^T$ is defined as,

$$\begin{aligned} u_1 &= k_1(y_1 - x_1), \\ u_2 &= -(1-y_1^2)y_2 - (1-x_1^2)x_2)\mu_e - (x_1 - y_1)\alpha_e - (x_1^3 - y_1^3)\beta_e - (x_1^5 - y_1^5)\delta_e. \end{aligned} \tag{14}$$

In eq. (14) μ_e, α_e, β_e, and δ_e are the estimated values of the parameters μ, α, β, and δ, respectively. Again, the feedback gain k_1 is dully adapted according to the update law $\dot{k}_1 = -\gamma e_1^2$.

To verify that the controller $u = (u_1, u_2)^T$ would drive the systems to synchrony, we give some numerical simulation results, firstly, by selecting the initial conditions of the master system (11): $x_1(0) = 1, x_2(0) = 2$, the slave system (12): $y_1(0) = -3, y_2(0) = 4$, $f = 9, \omega = 3.14$. The initial values of the estimated parameters are $\mu_e = 0.6, \alpha_e = 1.2, \beta_e = -0.4$, and $\delta_e = 0.3$. Using the same initial controller gain, $k_1(0) = -1$, we illustrate in Figure 3 the synchronization behaviour of the two identical ϕ^6 Van-der Pol oscillators with unknown parameters. Clearly, asymptotically synchronization is achieved as $t \to \infty$, while the feedback gain k_1 tends to a negative constant. We may also consider other sets of initial conditions and estimating parameters. For instance, let $x_1(0) = 1$, $x_2(0) = 2$, and $y_1(0) = -3$, $y_2(0) = 4$, $f = 9, \omega = 3.14$. Similarly, let the initial values of the estimated parameters be $\mu_e = 0.5$, $\alpha_e = 0.5$, $\beta_e = 1.1$, $\delta_e = 0.12$. This case is shown in Figure 4, confirming that the synchronization is fully guaranteed for the two identical ϕ^6 Van-der Pol oscillators.

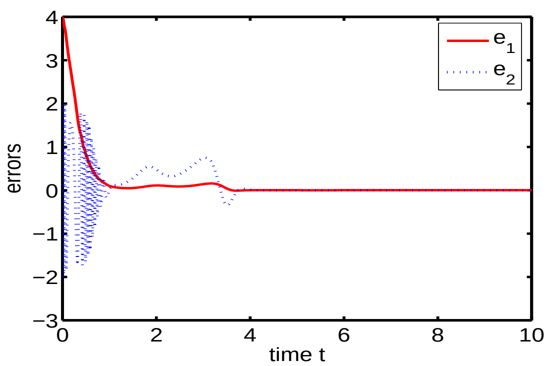

Figure 3: The error system of two identical Φ^6 Van-der Pol oscillators with unknown parameters is asymptotically stable as $t \to \infty$.

3.2 Example 2. ϕ^6 Duffing oscillators

$$\begin{aligned} \dot{x}_1 &= x_2, \\ \dot{x}_2 &= -\lambda x_2 - \alpha x_1 - \beta x_1^3 - \delta x_1^5 + f cos(\omega t), \end{aligned} \tag{15}$$

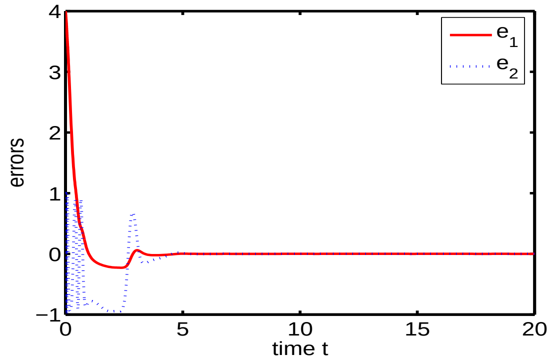

Figure 4: The error system of two identical Φ^6 Van der Pol oscillators with unknown parameters is asymptotically stable as $t \to \infty$.

where λ, α, β, δ, f, and ω are parameters of the system (15). Let system (15) be the master oscillator.

Case 1: All the parameters $(\lambda, \alpha, \beta, \delta, f, \omega)$ of system (15) are known in advance. According to our method in Ref. [48], the slave oscillator with adaptive controller is as follows,

$$\begin{aligned} \dot{y}_1 &= y_2 + k_1(y_1 - x_1), \\ \dot{y}_2 &= -\lambda y_2 - \alpha y_1 - \beta y_1^3 - \delta y_1^5 + f cos(\omega t), \end{aligned} \tag{16}$$

the feedback gain k_1 is adapted according to the following update law $\dot{k}_1 = -\gamma e_1^2$.

Again, we give numerical simulations to verify the above theoretical results. First, we select the initial states values of the master system (15) as follows: $x_1(0) = 1, x_2(0) = 2$, the slave system (16): $y_1(0) = -3, y_2(0) = 4$ and $\lambda = 0.4$, $\alpha = 1.0$, $\beta = -0.7$, $\delta = 0.1$, $f = 9$, $\omega = 3.14$. With the initial value of the adaptive controller $k_1(0) = -1$, Figure 5 shows that the two identical ϕ^6 Duffing oscillators achieve stable synchronization as $t \to \infty$, while the feedback gain k_1 tends to a negative constant. For other set of initial conditions, namely, for the master: $x_1(0) = 1, x_2(0) = 2$, the slave system: $y_1(0) = -3, y_2(0) = 1$ and $\lambda = 0.4$, $\alpha = 0.46$, $\beta = 1.0$, $\delta = 0.1$, $f = 4.5$, $\omega = 0.86$, Figure 6 shows that the synchronization is also attained with the initial adaptive controller $k_1(0) = -1$. The feedback gain k_1 also tends to a negative constant.

Case 2: The parameters $(\lambda, \alpha, \beta, \delta)$ of system (15) are unknown.

Using our method in Ref. [49], the slave system with adaptive controller is as follows,

$$\begin{aligned} \dot{y}_1 &= y_2 + u_1, \\ \dot{y}_2 &= -\lambda y_2 - \alpha y_1 - \beta y_1^3 - \delta y_1^5 + f cos(\omega t) + u_2, \end{aligned} \tag{17}$$

and the controller $u = (u_1, u_2)^T$ is as follows,

$$\begin{aligned} u_1 &= k_1(y_1 - x_1), \\ u_2 &= -(-y_2 + x_2)\lambda_e - (x_1 - y_1)\alpha_e - (x_1^3 - y_1^3)\beta_e - (x_1^5 - y_1^5)\delta_e, \end{aligned} \tag{18}$$

where $\lambda_e, \alpha_e, \beta_e, \delta_e$ are the estimating value of the parameters $\lambda, \alpha, \beta, \delta$ respectively, and the feedback gain k_1 is adapted according to the update law $\dot{k}_1 = -\gamma e_1^2$.

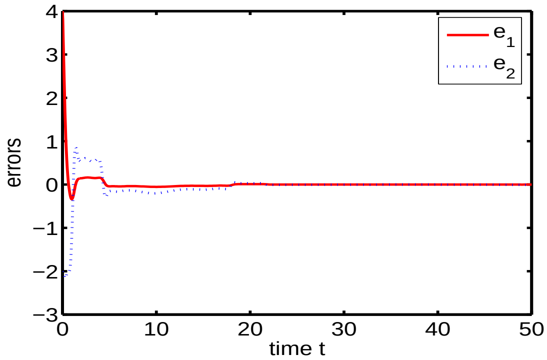

Figure 5: The error system of two identical Φ^6 Duffing oscillators ($\lambda = 0.4$, $\alpha = 1.0$, $\beta = -0.7$, $\delta = 0.1$, $f = 9$, $\omega = 3.14$) is asymptotically stable as $t \to \infty$.

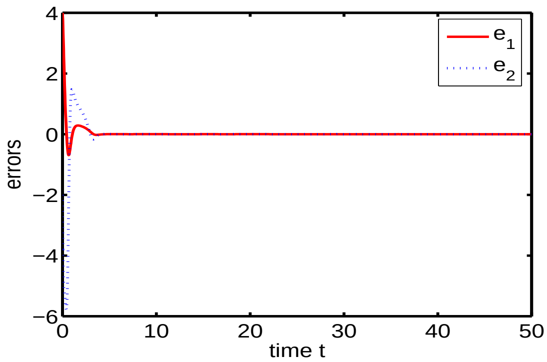

Figure 6: The error system of two identical Φ^6 Duffing oscillators ($\lambda = 0.4$, $\alpha = 0.46$, $\beta = 1.0$, $\delta = 0.1$, $f = 4.5$, $\omega = 0.86$) is asymptotically stable as $t \to \infty$.

Figure 7 shows the results of the numerical simulations. We first, selected the initial states values of the master system (17) as: $x_1(0) = 1, x_2(0) = 2$, and the slave system (18) as: $y_1(0) = -3, y_2(0) = 4$, $f = 9$, $\omega = 3.14$, the initial values of the estimating parameters are $\lambda_e = 0.6$, $\alpha_e = 1.2$, $\beta_e = -0.4$, $\delta_e = 0.3$. With the initial value of the controller being $k_1(0) = -1$, the error system of two identical ϕ^6 Duffing oscillators with unknown parameters is asymptotically stabilized as $t \to \infty$, while the feedback going k_1 tends to a negative constant; implying that synchronization is achieved. We consider also, other choice of initial conditions, namely, $x_1(0) = 1, x_2(0) = 2$ (master) and $y_1(0) = -3, y_2(0) = 4$ (slave) and the parameters values $f = 9, \omega = 3.14$, $\lambda_e = 0.5, \alpha_e = 0.5, \beta_e = 1.1$, and $\delta_e = 0.12$; and find that synchronization is still achieved as shown in Figure 8.

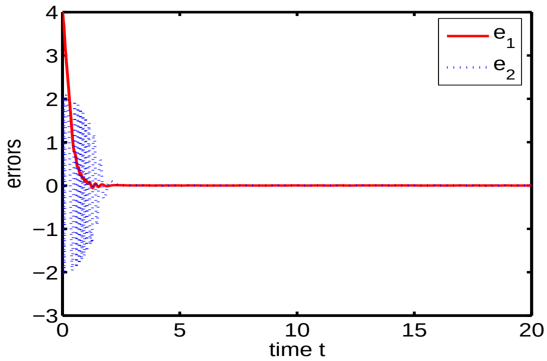

Figure 7: The error system of two identical Φ^6 Duffing oscillators with unknown parameters is asymptotically stable as $t \to \infty$.

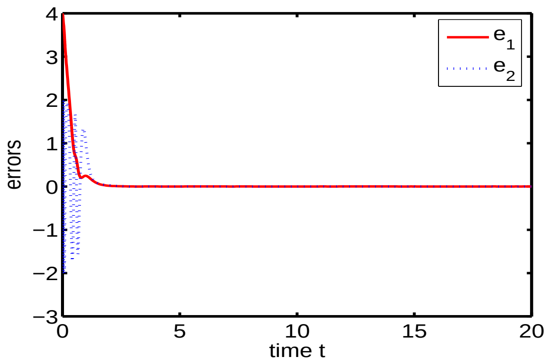

Figure 8: The error system of two identical Φ^6 Duffing oscillators with unknown parameters is asymptotically stable as $t \to \infty$.

4 Estimation of the Unknown Parameters of Van-der Pol and Duffing Oscillators

Example 1 ϕ^6 Van-der Pol oscillators:

$$\begin{aligned} \dot{x}_1 &= x_2, \\ \dot{x}_2 &= \mu(1-x_1^2)x_2 - \alpha x_1 - \beta x_1^3 - \delta x_1^5 + f cos(\omega t), \end{aligned} \tag{19}$$

where $\mu = 0.4$, $\alpha = 1$, $\beta - 0.7$, $\delta = 0.1$, $f = 9$, and $\omega = 3.14$ are parameters of the system (19), and we let system (19) be the master system; where the parameters μ, α, β are unknown. According to Ref. [46], the slave system with adaptive controller is as follows,

$$\begin{aligned} \dot{y}_1 &= y_2 + k_1(y_1 - x_1), \\ \dot{y}_2 &= \mu_e(1-y_1^2)y_2 - \alpha_e y_1 - \beta_e y_1^3 - \delta y_1^5 + f cos(\omega t) + k_1(y_2 - x_2), \end{aligned} \tag{20}$$

where μ_e, α_e, and β_e are the estimated parameters μ, α, and β, respectively, which are adapted according to the update law,

$$\begin{aligned}\dot{\mu}_e &= -(1-y_1^2)y_2(y_2-x_2),\\ \dot{\alpha}_e &= y_1(y_2-x_2),\\ \dot{\beta}_e &= y_1^3(y_2-x_2),\end{aligned} \tag{21}$$

and the feedback gain k_1 is adapted according to the update law $\dot{k}_1 = -(e_1^2+e_2^2)$.

In what follows, we give numerical simulations to verify the above theoretical results. Firstly, by selecting the initial state values of the master system (19): $x_1(0) = 1, x_2(0) = 2$, the slave system (8): $y_1(0) = -3, y_2(0) = 4$, $f = 9, \omega = 3.14$, the initial values of the estimating parameters are $\lambda_e = 0.6, \alpha_e = 1.2, \beta_e = -0.4$. With the initial value of the controller $k_1(0) = -1$, Figure 9 shows that the error system of two identical Φ^6 Van-der Pol oscillators with unknown parameters is asymptotically stable as $t \to \infty$, while the feedback gain k_1 tends to a negative constant. Figure 10 shows that the estimating parameters λ_e, α_e and β_e converge to its true value λ, α and β, respectively.

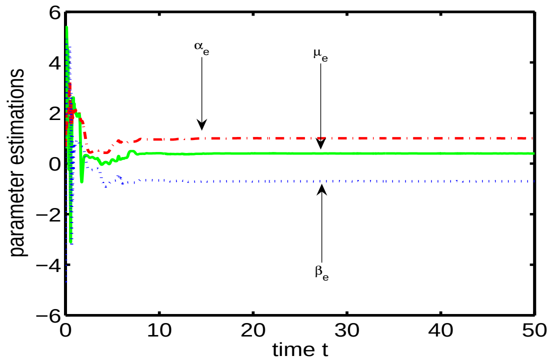

Figure 9: The estimated parameters μ_e, α_e, β_e, converge to its true value μ, α, β respectively.

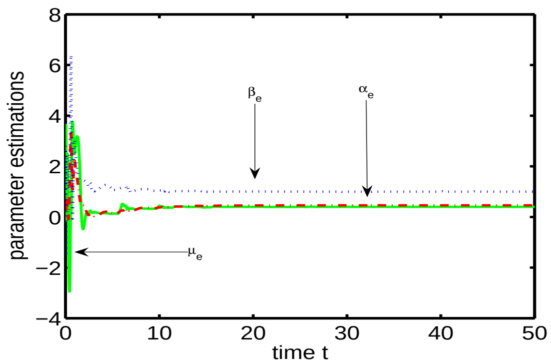

Figure 10: The estimated parameters μ_e, α_e, β_e, converge to its true value μ, α, β respectively.

Example 2 ϕ^6 Duffing oscillators:

$$\begin{aligned} \dot{x}_1 &= x_2, \\ \dot{x}_2 &= -\lambda x_2 - \alpha x_1 - \beta x_1^3 - \delta x_1^5 + f cos(\omega t), \end{aligned} \tag{22}$$

where $\lambda = 0.01$, $\alpha = 1.0$, $\beta - 0.495$, $\delta = 0.05$,f=0.78, and $\omega = 0.55$ are parameters of system (19). Let system (19) be the master system; where the parameters α, and β are unknown. Following Ref. [46], the slave system with adaptive controller is as follows,

$$\begin{aligned} \dot{y}_1 &= y_2 + k_1(y_1 - x_1), \\ \dot{y}_2 &= -\lambda y_2 - \alpha_e y_1 - \beta_e y_1^3 - \delta y_1^5 + f cos(\omega t) + k_1(y_2 - x_2), \end{aligned} \tag{23}$$

where α_e, β_e is the estimated parameters α, β respectively, which are adapted according to the update law,

$$\begin{aligned} \dot{\alpha}_e &= y_1(y_2 - x_2), \\ \dot{\beta}_e &= y_1^3(y_2 - x_2), \end{aligned} \tag{24}$$

and the feedback gain k_1 is adapted according to the update law $\dot{k}_1 = -(e_1^2 + e_2^2)$.

Numerical simulation results for the drive-response system (23) and (24), we carried out using the following initial conditions for the master system (23): $x_1(0) = 1, x_2(0) = 2$, and for the slave system (24): $y_1(0) = -3, y_2(0) = 4$. The other parameters are set as follows: $f = 9, \omega = 3.14$, while the initial values of the estimating parameters are $\alpha_e = 1.2$, and $\beta_e = -0.4$. With the initial value of the controller $k_1(0) = -1$, Figure 11 shows that the error system of two identical Φ^6 Duffing oscillators with unknown parameters is asymptotically stabilized as $t \to \infty$, while the feedback gain k_1 approaches a negative constant. Figure 12 shows also that the estimating parameters α_e, and β_e, converge to its true values α and β, respectively.

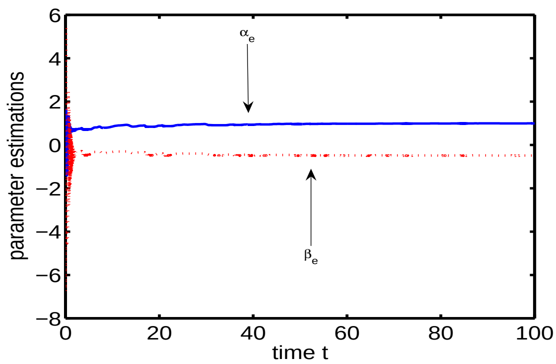

Figure 11: The estimated parameters α_e, β_e, converge to its true values α, β respectively.

5 Conclusion

In this paper, we have examined the synchronization of oscillating particles in ϕ^6 potentials based on adaptive control approach. The adaptive approach that we have employed is such that a single-state feedback is sufficient to steer the synchronization of two identical oscillators. We demonstrate this method for the ϕ^6 Van-der Pol and Duffing oscillators and realized the synchronization also for the case of unknown system parameters. For

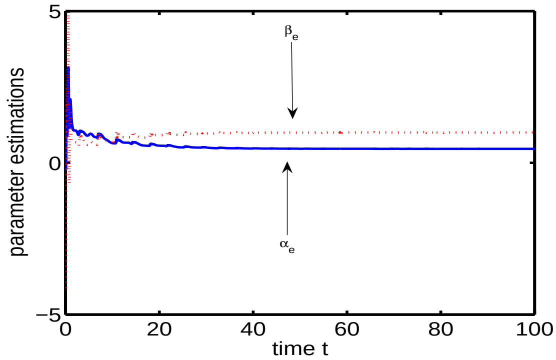

Figure 12: The estimated parameters α_e, β_e, converge to its true value α, β respectively.

the case of parameter unknown, we estimated the all the unknown parameters. We note that our proposed approach gives rise to simpler control control input, especially when the parameters are known in advance. Such adaptive control approach would have advantage in practical applications, since it could be easily realized compared to existing methods.

Acknowledgements

UEV is supported by the Royal Society of London, through the Newton Fellowships Alumni Funding.

References

[1] Pecora, L. M. and Carroll, T.L. Synchronization in chaotic systems. *Phys. Rev. Lett.* **64** (1990) 821–824.

[2] Ojalvo, J. and Roy, R. Spatiotemporal Communication with Synchronized Optical Chaos. *Phys. Rev. Lett.* **86** (2001) 5204–5207.

[3] Murali, K. and Lakshmanan, M. Drive-response scenario of chaos synchronization in identical nonlinear systems. *Phys. Rev. E* **49** (1994) 4882–4885.

[4] Yang, T. and Chua, L. Impulsive Stabilization for Control and Synchronization of Chaotic Systems: Theory and Application to Secure Communication. *IEEE Trans. Circuits Syst., I: Fundam. Theory Appl.* **44** (1997) 976–988.

[5] Chitra, R.N. and Kuriakose, V.C. Phase synchronization in an array of driven Josephson junctions. *Chaos* **18** (2008) 013125.

[6] Bowong, S. Stability analysis for the synchronization of chaotic systems with different order: application to secure communications. *Phys. Lett. A* **326** (2004) 102–113.

[7] López-Mancilla, D. and Cruz-Hernandez, C. Output synchronization of chaotic systems: Model-matching approach with application to secure communication. *Nonlinear Dynamics & Systems Theory* **5** (2005) 141–156.

[8] Chen, G. and Dong, X. *From Chaos to Order: Methodologies, Perspectives and Applications.* Singapore, World Scientific, 1998.

[9] Pikovsky, A.S., Rosenblum, M.G. and Kurths, J. *Synchronization - A Unified Approach to Nonlinear Science.* Cambridge University Press, Cambridge, 2001.

[10] Lakshmanan, M. and Murali, K. *Chaos in Nonlinear Oscillators: Controlling and Synchronization*. World Scientific, Singapore, 1996.

[11] Heagy, J.F., Carroll, T.L. and Pecora L.M. Experimental and Numerical Evidence for Riddled Basins in Coupled Chaotic Systems. *Phys. Rev. Lett.* **73** (1994) 3528–3531.

[12] Fang, J.Q., Hong, Y. and Chen, G.R. Switching manifold approach to chaos synchronization, *Phys. Rev. E* **59** (1999) R2523–R2526.

[13] Tanaka, K., Ikeda T. and Wang, H.O. A unified approach to controlling chaos via an LMI-based fuzzy control system design. *IEEE Trans. Circuits Syst., I: Fundam. Theory Appl.* **45** (1998) 1021–1040.

[14] Li, C.D., Liao X.F. and Zhang, X.Y. Impulsive synchronization of chaotic systems. *Chaos* **15** (2005) 023104.

[15] Ucar, A., Lonngren, K.E. and Bai, E.W. Synchronization of chaotic behaviour in nonlinear Bloch equations. *Phys. Lett. A* **314** (2003) 96–101.

[16] Arecchi, F.T. and Boccaletti, S. Adaptive strategies for recognition, noise filtering, control, synchronization and targeting of chaos. *Chaos* **7** (1997) 621-635.

[17] Wang, X.F. Slower speed and stronger coupling: Adaptive mechanisms of chaos synchronization. *Phys. Rev. E* **65** (2002) 067202.

[18] Vincent, U.E. Synchronization of Rikitake chaotic attractor using active control. *Phys. Lett. A* **343** (2005) 133–138.

[19] Vincent, U.E. Controlling directed transport via adaptive backstepping control. *Acta Phys Pol B* **38** (2007) 2459–2469.

[20] Cao, J. and Lu, J. Adaptive synchronization of neural networks with or without time-varying delay. *Chaos* **16** (2006) 013133.

[21] Boukabou, A. On Nonlinear Control and Synchronization Design for Autonomous Chaotic Systems, *Nonlinear Dynamics and Systems Theory* **8** (2008) 151–167.

[22] Filali, R.L., Hammami, S., Benrejeb, M. and Borne, P. On Synchronization, Anti-synchronization and Hybrid Synchronization of 3D Discrete Generalized Henon Map. *Nonlinear Dynamics and Systems Theory* **12** (2012) 81–95.

[23] dos Santos, A. M., Sergio, S.R., Lopes, R., Ricardo, R.L. and Viana, L. Rhythm synchronization and chaotic modulation of coupled Van der Pol oscillators in a model for the heartbeat, *Physica A* **338** (2004) 335–355.

[24] Moukam Kakmeni, F. M., Bowong, S., Tchawoua, C. and Kaptouom, E. Chaos control and synchronization of a ϕ^6 -Van der Pol oscillator. *Phys. Lett. A* **322** (2004) 305–323.

[25] Enjieu Kadji, H. G. Yamapi, R. General synchronization dynamics of coupled Van der Pol - Duffing oscillators. *Physica A* **370** (2006) 316–328.

[26] Zhou, J., Cheng, X., Xiang, L. and Zhang, Y. Impulsive control and synchronization of chaotic systems consisting of Van der Pol oscillators coupled to linear oscillators. *Chaos, Solitons* & *Fractals*. **33** (2007) 607–616.

[27] Yamapi, R. and Filatrella, G. Strange attractors and synchronization dynamics of coupled Van der PolDuffing oscillators. *Comm. Nonl. Sci. Numer. Simulat.* **13** (2008) 1121–1130.

[28] Njah, A.N. and Vincent, U.E. Chaos synchronization between single and double wells Duffing Van der Pol oscillators using active control. *Chaos, Solitons* & *Fractals* **37** (2008) 1356–1361.

[29] Njah, A.N. Synchronization via active control of identical and non-identical ϕ^6 chaotic oscillators with external excitation. *J. Sound and Vibration* **327** (2009) 322–332.

[30] Njah, A.N. Synchronization via active control of parametrically and externally excited ϕ^6 Van der Pol and Duffing oscillators and application to secure communications. *J. Vibrat. Control* **17** (2010) 493–504.

[31] Ucar, A., Lonngren, K.E. and Bai, E.-W. Synchronization of chaotic behavior in nonlinear Bloch equations. *Phys. Lett. A* **314** (2003) 96–101.

[32] Moukam Kakmeni, F.M., Nguenang, J.P. and Kofane, T.C. Chaos synchronization in bi-axial magnets modeled by Bloch equations. *Chaos, Solitons* & *Fractals* **30** (2006) 690–699.

[33] Park, J.H. Chaos synchronization of nonlinar Bloch equations. *Chaos, Solitons* & *Fractals* **27** (2006) 357–361.

[34] Bindu, V. and Nandakumaran, V. M. Numerical studies on bi-directionally coupled directly modulated semiconductor lasers. *Phys. Lett. A* **277** (2000) 345–351.

[35] Parvathi, M.R., Bindu, M., Rajesh, S., John, M.P. and Nandakumaran, V. M. Synchronization and control of chaos in coupled chaotic multimode Nd:YAG Lasers, *Phys. Lett. A* **373** (2008) 96–101.

[36] Ucar, A., Lonngren, K.E. and Bai, E.W., Chaos synchronization in RCL-shunted Josephson junction via active control. *Chaos Solitons & Fractals* **31** (2007) 105–111.

[37] Vincent, U.E., Ucar, A., Laoye, J.A. and Kareem, S.O. Control and Synchronization of chaos in RCL-shunted Josephson junction using backstepping design *Physica C* **468** (2008) 374–382.

[38] Guo, R., Vincent, U.E. and Idowu, B.A. Synchronization of chaos in RCL-shunted Josephson junction using a simple adaptive controller. *Physica Scripta* **79** (2009) 035801.

[39] Tchoukuegno, R. and Woafo, P. Dynamics and active control of motion of a particle in a ϕ^6 potential with a parametric forcing. *Physica D* **167** (2002) 86–100.

[40] Tchoukuegno, R., Nana Nbendjo, B. R. and Woafo, P. Resonant oscillations and fractal basin boundaries of a particle in a ϕ^6 potential. *Physica A* **304** (2002) 362–378.

[41] Tchoukuegno, R., Nana Nbendjo, B. R. and Woafo, P. Linear feedback and parametric controls of vibrations and chaotic escape in a ϕ^6 potential. *Int. J. Non-Linear Mech.* **38** (2003) 531–541.

[42] Siewe Siewe, M., Moukam Kakmeni, F. M. and Tchawoua, C. Resonant oscillation and homoclinic bifurcation in a ϕ^6-Van der Pol oscillator. *Chaos, Solitons* & *Fractals* **21** (2004) 841–853.

[43] Siewe Siewe, M., Moukam Kakmeni, F.M., Tchawoua, C. and Woafo, P. Bifurcations and chaos in the triple-well ϕ^6-Van der Pol oscillator driven by external and parametric excitations. *Physica A* **357** (2005) 383–396.

[44] Yang, X., Xu, W., Sun, Z. and Fang, T. Effect of bounded noise on chaotic motion of a triple-well potential system. *Chaos, Solitons* & *Fractals* **25** (2005) 415–424.

[45] Yang, X., Xu, W. and Sun, Z. Effect of bounded noise on the chaotic motion of a Duffing Van der pol oscillator in a ϕ^6 potential. *Chaos, Solitons* & *Fractals* **27** (2006) 778–788.

[46] Huang, D. Synchronization-based estimation of all parameters of chaotic systems from time series. *Phys. Rev. E.* **69** (2004) 067201.

[47] Corron N. J., Pethel, S. D. and Hopper, B.A. Controlling chaos with simple limiters. *Phys. Rev. Lett.* **84** (2000) 3835–3838.

[48] Guo, R. W. A simple adaptive controller for chaos and hyperchaos synchronization. *Phys. Lett. A* **372** (2008) 5593–5597.

[49] Vincent, U.E. and Guo, R.W. A simple adaptive control for full and reduced-order synchronization of uncertain time-varying chaotic systems. *Comm. Nonl. Sc. Num. Simulat.* **14** (2009) 3925–3932.

[50] Guo, R. and Vincent, U.E. Control of a unified chaotic system via single variable feedback. *Chin. Phys. Lett.* **26** (2009) 090506.

[51] Yu, W. Stabilization of three-dimensional chaotic systems via single state feedback controller. *Phys. Lett. A* **374** (2010) 1488–1492.